LASER AND ULTRASOUND RADIATION PRETREATMENT OF CELLULOSE IN DISSOLVING WOOD PULP

by

Atsile Rosy Ocwelwang

Submitted in fulfilment of the academic requirements for the degree of Doctor of Philosophy in Chemical Engineering, at the School of Engineering, College of Agriculture, Engineering, and Science, University of KwaZulu-Natal

Durban, South Africa

Supervisor: Prof. Bruce B. Sithole

Co-supervisors: Prof. Deresh Ramjugernath, Dr. Viren Chunilall

December 2017

PREFACE

The research contained in this thesis was completed by the candidate for a doctoral degree while based in the Discipline of Chemical Engineering, School of Engineering, of the College of Agriculture, Engineering and Science, University of KwaZulu-Natal, Howard College Campus, South Africa.

The contents of this work have not been submitted in any form to another university for a degree, and except where the work of others is acknowledged in the text, the results reported are due to investigations by the candidate.

As the candidate's supervisor, I approve this thesis for submission.

_____ _____

Signed: Prof. B. Sithole (Supervisor) Date:

DECLARATION

I, Atsile Rosy Ocwelwang, declare that:

(i) This thesis, except where otherwise indicated is my original work.

(ii) The contents of this research have not been submitted in any form to another university for any degree or examination.

(iii) This thesis does not contain other person's data, pictures, graphs or other information unless specifically acknowledged as being sourced from other persons.

(iv) This thesis does not contain other person's writing unless specifically acknowledged as being sourced from other researchers. Where other written sources have been quoted, then:

a) Their words have been re-written, but the general information attributed to them has been referenced;

b) Where their exact words have been used, their writing has been placed inside quotation marks and referenced.

(v) This thesis does not contain text, graphics or tables copied and pasted from the internet, unless specifically acknowledged, and the source being detailed in the thesis and the References section.

_____ _____

Signed: A.R. Ocwelwang (candidate) Date:

ABSTRACT

Dissolving wood pulp (DWP) refers to wood extracted, chemically refined bleached pulp that comprises more than 90% pure cellulose. This type of pulp is mainly utilised for the production of various cellulose derivatives such as rayon, cellophane, cellulose ethers and cellulose esters. Production of these valuable products is achieved by dissolution of DWP in chemical solvents such as sodium hydroxide (NaOH) and carbon disulphide (CS_2). However, cellulose dissolution is not easily achievable due to the strong hydrogen bond interactions that give this biopolymer its highly ordered crystalline structure. High cellulose crystallinity limits the accessibility and chemical reactivity of this biopolymer. Various forms of pretreatment techniques have been developed to solve this problem. The primary aim of the pretreatment is to disrupt the rigid crystalline structure of cellulose, and this increases its structural accessibility and chemical reactivity. However, most pretreatment techniques have drawbacks such as being energy intensive, costly, corrosive, posing risks to personnel operating them, and not being readily accessible. For example, gamma ray irradiation has been shown to be an effective pretreatment technique for cellulose and other lignocellulosic materials, but it is a costly technology. For this reason, research into environmentally friendly and profitable pretreatment techniques is ongoing.

This study aimed to evaluate the effect of two procedures, namely, ultrasound and laser irradiation, as possible pretreatment techniques for cellulose activation. Ultrasound irradiation is a conventional method that has been used for pretreatment of a wide range of polymeric materials, whereas the use of laser irradiation as a pretreatment technique for cellulose activation has never been reported. Therefore, using lasers as a pretreatment for activation of DWP with the aim of modifying the cellulose structure to improve its chemical reactivity is a novel aspect of this thesis. The effects of these two pretreatment techniques on the structure of cellulose were studied and compared.

The effects of the two techniques were investigated separately in two parts. The first part focused on the effect of ultrasound irradiation on the structure of cellulose, and the dissolution behaviour of the ultrasonicated pulp samples in aqueous NaOH solution. The second part evaluated the effect of laser irradiation on the structure of cellulose, and the

chemical reactivity of the pretreated cellulose pulp samples was measured using the Fock test method.

A range of analytical techniques was employed to characterise the pretreated samples to evaluate the structural modifications that resulted from the pretreatments. Size exclusion chromatography with multi-angle light scattering (SEC-MALS) analysis was used to study the molecular structural properties of cellulose. X-ray diffraction (XRD), and Solid-state CP/MAS ^{13}C-NMR were used to investigate the crystalline structure of cellulose and to measure its degree of crystallinity (CrI). Ultrastructural and morphological properties of cellulose were also studied by atomic force microscopy (AFM), scanning electron microscopy (SEM), and morphological fibre analyser (MorFi). Untreated DWP samples were used as control samples for all procedures and analysis conducted in the study.

In the first part of this study, DWP samples were pretreated with ultrasound irradiation and subsequently dissolved in aqueous NaOH solution. SEC-MALS results showed a shift in average molar weight (Mw) from high to lower region after ultrasonication. Broadening of the molecular weight distribution (MWD) was displayed by increase in polydispersity index (PDI). A decrease in Mw was also observed with increasing pretreatment time; this confirmed the effect of the ultrasonic pretreatment on the molecular structure of cellulose. SEC-MALS analysis of the ultrasonicated and alkali treated samples displayed different dissolution behaviour compared to the control, and the changes in the MWD data did not follow any trend relative to treatment time.

XRD results indicated that ultrasound irradiation had minor or no effect on the degree of cellulose crystallinity (CrI). However, treatment of the ultrasonicated pulp samples with aqueous NaOH significantly decreased the CrI. This reduction in CrI indicates that alkali treatment transformed natural cellulose to regenerated cellulose. A CrI decrease of more than 50% was also observed for the samples treated for 60 minutes (alkcell-UT60 min).

AFM ultrastructural results revealed that ultrasonication did not induce visible changes on the surface of the S2 layer. An overall decrease of lateral fibril aggregate dimensions (LFAD) was observed after ultrasound irradiation, but the reduction did not show a linear relationship with increasing treatment time. Fibre distribution and dimensions results

from the MorFi analyser showed that with prolonged treatment time, the number of fibres in solution increased, average fibre length decreased, while the average fibre width did not display significant changes. SEM surface morphology results showed that after ultrasonication the surface of the fibres became smooth, and there was less or no fibrillation. SEM analysis revealed that after alkali treatment the surface of the fibres displayed folds and trenches which ran parallel to the length of the fibres. This is an indication of an increase in the surface area of the fibres due to the treatment with an alkali solution. Moreover, the fibres appeared compact and agglomerated.

In the second part of this study, laser radiation was used for pretreatment of DWP samples. The pretreatment caused visible morphological and molecular changes in the structure of cellulose. SEC-MALS results demonstrated that laser irradiation decreased the average Mw of the cellulose polymer and caused noticeable modifications on the molecular structure of this biopolymer. The PDI also showed increase; this rise in PDI is indicative of the size distribution of the Mw and the heterogeneity of the cellulose chain lengths as a result of the pretreatment. XRD results demonstrated that laser irradiation disrupted the crystalline structure of cellulose; an overall significant decrease in CrI was noticed for all the laser irradiated samples. NMR characterization of the irradiated samples also displayed a decline in CrI.

SEM characterization results illustrated that laser pretreatment disrupted the morphology of the cellulose fibres and created porous cavities on the fibre surfaces. AFM images for laser irradiated samples also displayed similar features. The S2 layer within the cross-sections of the samples irradiated with Nd:YAG laser at 266 nm and 355 nm also had small pores and dark areas between the fibril aggregates which represent the less stiff or potential accessible regions. Calculated LFAD results also confirmed these observations in that the data displayed a noticeable decline in LFAD after laser irradiation. Finally, the Fock test results showed that the laser pretreatment caused a linear increase in cellulose reactivity with increasing irradiation time.

From the results and observations presented in this study, it can be concluded that laser radiation pretreatment caused noticeable structural disruptions on the structure of cellulose compared to ultrasound irradiation. It disrupted and damaged the surface morphology of cellulose and further caused a significant degradation of the molecular

structure. Moreover, increase in cellulose reactivity as measured by the Fock test method was observed in all samples pretreated with lasers. The highest reactivity increase of more than 35% was obtained in samples irradiated with the Nd:YAG laser at a wavelength of 266 nm compared to Nd:YAG and CO_2 lasers at 355 nm, and 10.6 µm respectively. This observation showed that laser wavelength was influential in cellulose modification compared to laser power. Furthermore, the increase confirmed that laser radiation pretreatment reduced the cellulose Mw and disturbed its crystalline structure thus enhancing its accessibility and reactivity to chemical solvents. Therefore, the novel aspect of the thesis is that: Pretreatment of DWP with laser radiation modified the structural features of cellulose, and this led to an overall cellulose reactivity increase of about 20%. Consequently, this should result in a reduction of dosages of chemical reagents used for induction of cellulose reactivity and processing. The use of lasers for cellulose pretreatment could be a more affordable option compared to the conventional high energy radiation sources because they are less expensive and readily accessible.

ACKNOWLEDGEMENTS

All glory and honour to God all mighty, for His faithfulness, infinite mercies and grace throughout my journey, *Ebenezer*!

I would like to express my sincere appreciation to my supervisor and co-supervisors:

- Professor B.B. Sithole for his endless support, constructive criticism, and guidance throughout this project. Thank you for your patience, encouragement, and for believing in me and my work.
- Professor D. Ramjugernath, thank you for your genuine interest in my project, for asking the difficult questions, and for always giving valuable advice.
- Dr V. Chunilall, thank you for all your guidance, close supervision and technical training during this study. I am grateful to you for believing in my work, and for always sharing your insight on the subject.

My greatest gratitude goes to the National Research Foundation (NRF), Council for Scientific, Industrial Research (CSIR) – Professional Development Program (PDP), and the University of KwaZulu-Natal (UKZN) College of Agriculture, Engineering, and Science (CAES) for financial support. I would also like to thank the CSIR (NRE – Biorefinery Industry Development Facility (BIDF), the National Laser Centre (NLC) of South Africa), and UKZN for providing laboratory space and equipment for me to carry out my experimental work.

I would also like to acknowledge and thank the staff at NLC and BIDF, SAPPI Saiccor, the University of Stellenbosch (NMR unit), University of Fort Hare (XRD unit), and UKZN (NMR, XRD, and EM unit) for providing logistical and technical assistance, training and support for me to accomplish the aims and objectives of this study. A special mention to the following individuals who assisted me from day one: Mrs G. Andrews, Dr P. Lekha, Mr N. Gounden, Mrs E. Sibande, Mr P. Seemela, and Dr B. Masina, I am grateful for all your advice and help.

To my colleagues and friends at CSIR, especially members of my research group, thank you all for your words of encouragement, support and friendship. Finally, I would like to express my heartfelt gratitude to my family, especially my siblings for their relentless support and unconditional love throughout this journey. Many thanks go to my friends

and acquired family, thank you for your prayers, love, encouragement, and emotional support.

DEDICATION

To the loving memory of my late parents

Moeng and Abueng Ocwelwang

"If I have seen further in life, it is by standing on the shoulders of Giants."

—Sir Isaac Newton

LIST OF CONFERENCES AND PUBLICATIONS

The findings reported in this thesis were presented at the following local and international conferences:

- Ocwelwang, A.R., Sithole, B.B., Ramjugernath, D., Chunilall, V., "Ultrasonic Activation of Dissolving Wood Pulp as Pretreatment to Alkali Dissolution", Technical Association of the Pulp and Paper Industry of Southern Africa (TAPPSA) Conference and Exhibition 2016, UKZN, Durban, South Africa, 21st – 22nd September 2016. [Full manuscript, peer reviewed].
- Ocwelwang, A.R., Sithole, B.B., Ramjugernath, D., "Structural and morphological characterization of cellulose pulp pretreated with ultrasound irradiation", Proceedings of the 18th International Symposium on Wood, Fibre and Pulping Chemistry(ISWFPC), BOKU, Vienna, Austria, 09th – 11th September 2015. [Conference Proceedings, peer reviewed].
- Ocwelwang, A.R., Sithole, B.B., Ramjugernath, D., "Irradiation Treatment of Dissolving Chemical Pulps produced in South Africa", Proceedings of the International Conference on Chemical Thermodynamics/South African Institute of Chemical Engineers (ICCT/SAIChE 2014), Durban, South Africa, 27th July – 01st August 2014. [Abstract, peer reviewed].

The following manuscripts emanating from the contents of this thesis have been prepared for publication in peer-reviewed journals:

- Ocwelwang, A.R., Sithole, B.B., Ramjugernath, D., Chunilall, V., Gounden, N., "Structural Characterization of Dissolving Wood Pulp (DWP) after Ultrasound Irradiation Pretreatment". [Manuscript in preparation for submission to "Journal of Wood Chemistry and Technology"].
- Ocwelwang, A.R., Sithole, B.B., Ramjugernath, D., Chunilall, V., Gounden, N., "Effect of Laser Irradiation Pretreatment on the Structure of Dissolving Wood Pulp Cellulose characterised by AFM, CP/MAS ^{13}C NMR, XRD and SEC-MALS". [Manuscript in preparation for submission to "Cellulose Chemistry and Technology"].

TABLE OF CONTENTS

TABLE OF FIGURES

LIST OF TABLES

LIST OF ABBREVIATIONS AND SYMBOLS

α – Alpha

AFM – Atomic Force Microscopy

AGU – Anhydroglucose unit

Alkcell – Alkali cellulose

β – Beta

CO_2 – Carbon dioxide

CP/MAS ^{13}C-NMR – Cross Polarization / Magic Angle Spinning Nuclear Magnetic Resonance

CrI – Crystallinity Index

CS_2 – Carbon disulphide

DP – Degree of Polymerization

DWP – Dissolving Wood Pulp

EB – Electron beam

γ – Gamma

[η] – Intrinsic viscosity

LASER – Light Amplification by Stimulated Emission of Radiation

LFAD – Lateral Fibril Aggregate Dimensions

Min – Minutes

Mn – Number average molar mass

Mw – Weight average molar mass

MorFi analyser – Morphological fibre analyser

MWD – Molecular weight distribution

NaOH – Sodium Hydroxide

Nd:YAG – Neodymium Yttrium Garnet

nm – nanometer

PDI – Polydispersity Index

PHK – Pre-hydrolysis Kraft

rpm – Revolutions per minute

SEC-MALS – Size Exclusion Chromatography with Multi-Angle Light Scattering

SEM – Scanning Electron Microscopy

S1 – Outer layer of the secondary plant cell wall

S2 – Middle layer of the secondary plant cell wall

S3 – Inner layer of the secondary plant cell wall

SSA – Specific Surface Area

Θ – Theta

μm – micrometre

UT – Ultrasound Treated

XRD – X-Ray Diffraction

CHAPTER 1 – INTRODUCTION

1 Introduction

The global market for dissolving wood pulp (DWP) continues to grow exponentially due to the high demand for high-value end products that are derived from this natural resource (Sixta *et al.*, 2013; ReportLinker, 2014). DWP refers to chemically refined pulp that contains more than 90% cellulose content and low hemicelluloses and lignin content. This type of pulp is used as raw material for the production of cellulose based products such as viscose rayon, cellophane, cellulose ethers, cellulose esters and films (Chunilall *et al.*, 2006; Liu *et al.*, 2016). Cellulose derivatives and products find application in various industries including pharmaceuticals, automobile, food, textiles and clothing, paints, packaging, as well as in many household uses (Durbak, 1993; Azeredo, 2009; Jahan & Rahman, 2012; Shokri & Adibkia, 2013).

For decades, cellulose has been a subject of interest and extensive research because of its complex structure that limits its industrial application. The main hindrance of cellulose reactivity is its highly ordered crystalline structure that has crystallinity that varies between 60 and 70% depending on the source (Kollman & Côté, 1968; Weightman *et al.*, 2007). The high crystallinity in the cellulose structure results from the strong inter- and intramolecular hydrogen bond interactions formed between the molecular chains of this polymer (Kong & Eichhorn, 2005; Hu *et al.*, 2014). As a consequence, the accessibility and reactivity of cellulose are limited, and the full potential of this valuable macromolecule is severely limited (Engstrom *et al.*, 2006; Ioelovich, 2009; Hu *et al.*, 2014).

Extensive research has been carried out on various pretreatment methods with the aim of increasing cellulose accessibility and reactivity. This phenomenon is known as cellulose activation. Cellulose activation relates to the treatment of raw cellulose materials to disrupt the high crystalline structure of cellulose, thus making more hydroxyl (-OH) groups available for chemical reactivity. Conventional techniques used for cellulose activation are either physical, mechanical or chemical (Takacs *et al.*, 2001; Hu *et al.*, 2014). Cellulose activation alters the crystal structure of cellulose and increases the porosity of the polymer thus increasing specific surface area and chemical accessibility (Kunze & Fink, 2005; Takacs *et al.*, 2001).

There is limited research on the application of ultrasound and laser irradiation as possible pretreatment methods for cellulose activation. Hence, this study investigated the effect of laser radiation on the structure of cellulose, and this was compared to the effect of the conventional ultrasound radiation pretreatment. The study investigated and compared the effect of both techniques on cellulose structure. Furthermore, an analysis of how laser irradiation affects cellulose reactivity and how ultrasound irradiation influences dissolution of cellulose in alkali were carried out. These assessments were performed to determine the potential of these pretreatment technologies as auxiliary steps into cellulose derivatization and dissolution process.

1.1 Motivation for the study

The cellulose processing industry is currently experiencing environmental and economic challenges due to the use of large amounts of chemical reagents in cellulose derivatization processes. Production of viscose rayon with the viscose process requires concentrated sodium hydroxide and carbon disulphide (CS_2) to break down the highly crystalline structure of cellulose for production of viscose rayon fibres (Shen *et al.*, 2010). This process is still one of the principal methods for production of cellulose derivatives, but it is plagued by many weaknesses. The viscose process produces harmful environmental and atmospheric by-products that are costly and challenging to recover, and contribute to the emission of greenhouse gases (GHG) (Szabó *et al.*, 2009; Shen *et al.*, 2010). Complete elimination of these conventional cellulose processing methods is still not possible because application of most environmentally benign methods is still at research level. Until alternative, environmentally friendly, and economically viable cellulose processing techniques are fully developed and industrialised, continuous research in this field is essential.

The concept of incorporating cellulose biomass pretreatment with derivatization processes is a subject that has been under extensive research for decades. One of the pretreatment techniques that has been widely reported is the use of high-energy radiation sources for cellulose activation. Some of the radiation techniques that have been used include gamma, X-rays, electron beam, microwave, and ultrasound (Imamura *et al.*, 1972; Takács *et al.*, 1999; Cleland *et al.*, 2003; Kaczmarek *et al.*, 2005; Byun *et al.*, 2008). However, these technologies use energy intensive, expensive equipment that is

not readily available. For this reason, no commercial applications are using them. Very few studies have investigated the use of low-energy radiation sources for pretreatment of this polymer with the intention of producing cellulose derivatives. Hence, in this study, the effect of ultrasound and laser irradiation on the structure of cellulose was investigated. Ultrasound and laser irradiation techniques are classified as non-ionising radiation sources; they are relatively low energy radiation sources compared to conventional ionising radiation sources.

The novelty of this study lies in the application of laser radiation technology for pretreatment of cellulose with interest to explore its potential as an auxiliary pretreatment step to cellulose derivatization. There is currently no research on laser irradiation pretreatment of dissolving wood pulp, with the aim of disrupting the structure of cellulose for production of valuable cellulose derivatives. Ultrasound irradiation, on the other hand, is a well-established conventional non-ionising radiation technique that has been explored broadly for polymer degradation including cellulosic materials. Ultrasound irradiation makes use of acoustic sound waves with a frequency range 20 – 100 kHz medium to generate ultrasound power.

To the best of our knowledge, a contrast of the efficiency of laser and ultrasound irradiation pretreatment of DWP has not yet been reported. This study has the potential to develop into the "green chemistry" concept for cellulose activation since these two pretreatment techniques are environmentally clean and they do not require the use of chemicals. Furthermore, results obtained from the overall study will add new information to the knowledge base of the science community.

1.2 Research question

This project is an exploratory study that compares the effect of two physical pretreatment techniques, the laser and ultrasound irradiation on the structure of cellulose. Experimental tests were carried out on the particular pretreatment methods in a quest to answer the research questions below:

- What is the effect of ultrasound irradiation on the structure of cellulose (in comparison to laser radiation), and what is the impact of this pretreatment on alkali dissolution of cellulose?

- Can laser irradiation pretreatment of dissolving wood pulp impact the structural properties of cellulose, and help improve its accessibility and reactivity?

1.3 Aim and objectives

The primary focus of this project was to investigate the impact of ultrasound and laser radiation pretreatment on the structure of cellulose I and to further determine the effect of both the pretreatment techniques on the accessibility and reactivity of cellulose to chemical solvents by alkali dissolution test and Fock test method respectively.

Objectives of study:

- To determine and compare the effect of ultrasound (benchmark technique) and laser irradiation on the structural properties of cellulose in DWP;
- To analyse, and evaluate, the effect of neodymium yttrium garnet (Nd:YAG) and carbon dioxide (CO_2) lasers on the structure of cellulose;
- To determine the effect of laser irradiation pretreatment on the reactivity of cellulose (Fock reactivity test);
- To evaluate the effect of ultrasound irradiation pretreatment on the solubility of cellulose in sodium hydroxide (Alkali dissolution tests).

1.4 Thesis outline

This research study is composed of six chapters. Chapter one gives a brief background, motivation, research question, as well as the main aim and objectives of this study.

Chapter two presents a literature review of this study. An extensive review of cellulose, its sources, structure, and applications is given. Furthermore, discussions on the conventional viscose process and alkali dissolution method used for derivatization of cellulose I to cellulose II are presented. The chapter also outlines a background of the different types of pretreatment methods that are used for cellulose, the benefits and weaknesses of the methods are defined. Chapter two is concluded by a discussion of the techniques that were employed for structural characterization of cellulose in this study.

Chapter three describes the experimental protocols used in this study. This chapter details a list of materials that were utilised in the study, and it gives details of the pretreatment methods as well as the characterization techniques that were employed. Furthermore, a description of cellulose reactivity and dissolution test methods is given, and the chapter concludes with a description of the characterization techniques that were used for structural analysis.

Chapters four and five respectively present discussions of results and observations that were attained in this study. Chapter four is a presentation of structural characterization results of DWP samples after pretreatment with ultrasound irradiation and dissolution in aqueous NaOH solution. Chapter five is divided into two sections, the first section is a presentation of structural characterization results after laser irradiation and the second section presents the cellulose reactivity results.

Chapter six gives a summary of the main findings and results obtained from this study, as well as conclusions. Furthermore, recommendations for future work are outlined. A reference list of all the literature consulted in this study is provided at the end of the thesis.

CHAPTER 2 – LITERATURE REVIEW

2 Introduction

Woody plants are the primary source of the lignocellulosic biomass which mainly comprises of cellulose, hemicellulose, and lignin. Of these three biopolymers, cellulose is the main component that accounts for 40-55% of the plant cell wall and is wrapped in a matrix of hemicellulose and lignin which account for 20-35% and 5-30% respectively (Atalla, 1990; Jarvis, 2000; Harmsen *et al.*, 2010). Lignocellulosic materials, in particular, cellulose, find industrial applications in a variety of fields. Cellulose is first modified and converted to various cellulose derivatives and high-value end products (Ostberg *et al.*, 2012; Iqbal *et al.*, 2013).

However, the production of these valuable cellulose derivatives is hindered by the resistance of this biopolymer to different processing techniques. Moreover, this recalcitrant nature of cellulose restricts its commercial and large scale applications (Zhao *et al.*, 2007; Iqbal *et al.*, 2013). As a result, extensive research has been undertaken to evaluate the effect of various pretreatment technologies on the structure of lignocellulosic materials. The use of high-energy radiation sources for pretreatment of lignocellulosics has progressively developed over the years to the extent of being incorporated into the cellulose processing industry (Los Alamos Science, 1995; Takacs *et al.*, 2000; Cleland *et al.*, 2003; Weightman *et al.*, 2007; Byun *et al.*, 2008). A review by Rajgopal & Stepanik (1996) highlighted that electron processing technologies have the potential to alter the degree of polymerization of cellulose, improve the rate of cellulose derivatization, and ultimately save production costs. However, the efficiency of these pretreatment technologies is directly dependent on the energy input, and this is one of the major drawbacks of these techniques. For example, in a year, 50 000 tonnes of pulp would require an energy of 50 kiloWatts (kW) for processing (Rajagopal & Stepanik, 1996).

Various scholars have widely reviewed and contrasted the different types of high-energy radiation sources that are used in industry. However, low-energy radiation sources have not received much attention, and there are few reports on their application as pretreatment techniques for cellulose activation. Therefore, this chapter expands on the different high-energy radiation sources, previously reported benefits and shortcomings of these technologies. Furthermore, a review of the low-energy radiation sources is made, and the

focus is mainly on the evolution and application of ultrasound and laser radiation sources as pretreatment techniques for lignocellulosic materials. For the purpose of this study, the discussion is centred on the pretreatment of dissolving wood pulp (DWP).

An overview of current methods used for pretreatment of cellulosic biomass is provided together with conventional radiation techniques that have been used for pretreatment of this polymer. Structural changes that occur due to exposure of these materials to radiation pretreatment are discussed. Finally, the application of laser and ultrasound radiation pretreatment on cellulose is explored, as well as the current status and possible prospects of these technologies in the field of cellulose derivatization.

2.1 Dissolving Wood Pulp (DWP)

Dissolving pulp, also known as dissolving cellulose, refers to chemically refined bleached pulp that has more than 90% pure cellulose content (Chunilall *et al.*, 2006; Strunk, 2012; Bodhlyera *et al.*, 2015). Because of its high molecular weight cellulose content, and low hemicellulose content, dissolving pulp is also called alpha cellulose (α-cellulose) (Burton & Rasch, 1931; Weightman *et al.*, 2007). The α-cellulose content is measured by the insolubility of cellulosic materials in a mercerising caustic solution under certain fixed conditions (Burton & Rasch, 1931). Dissolving pulp can be produced from cotton linters, and wood, with the latter being the primary source (Wilkes, 2001). Over 80% of the dissolving pulp manufactured in the world is extracted from woody plants, softwood (e.g. pine and spruce) and hardwood (e.g. beech and eucalyptus) species (Sixta, 2006; Liu *et al.*, 2016). When the pulp is produced from wood, it is referred to as "dissolving wood pulp" (DWP).

DWP is extracted from wood by chemical pulping and subsequent bleaching processes. Chemical pulping entails treatment or cooking of wood chips in aqueous chemical solvents at high temperature and pressure to dissolve lignin that binds cellulose fibres together and to remove hemicellulose and extractives. The two main processes that are used for the production of this precious commodity are pre-hydrolysis Kraft (PHK) and acid bisulphite pulping processes (Jahan *et al.*, 2008; Gehmayr *et al.*, 2011; Bodhlyera *et al.*, 2015). The pulping process modifies the cellulose fibres by dissolving the majority of hemicellulose and lignin in preparation for the bleaching process. The main aim of

bleaching is to remove the residual lignin, to improve pulp brightness and purity. This is achieved by treating the pulp with oxidative bleaching agents which depolymerise lignin, remove hemicellulose, and decrease extractives (Durbak, 1993; Gümüskaya *et al.*, 2003; Jahan *et al.*, 2008; Bodhlyera *et al.*, 2015). Depending on the type of bleaching sequence followed during the refining process, DWP can be classified into different alpha grades which can vary between 90 and 96% (Durbak, 1993; Liu *et al.*, 2016).

The high purity, brightness and even molecular weight of dissolving cellulose are some of the attractive features of this precious resource that distinguish it from ordinary paper and paperboard pulps (Strunk, 2012; Bodhlyera *et al.*, 2015). Because of this reasons, dissolving cellulose is used as the primary raw material for a broad range of applications, and derivatization of various products as shown in Figure 2.1 (Azeredo, 2009; Ibarra *et al.*, 2010; Teras & Jokinen, 2010; Iqbal *et al.*, 2013).

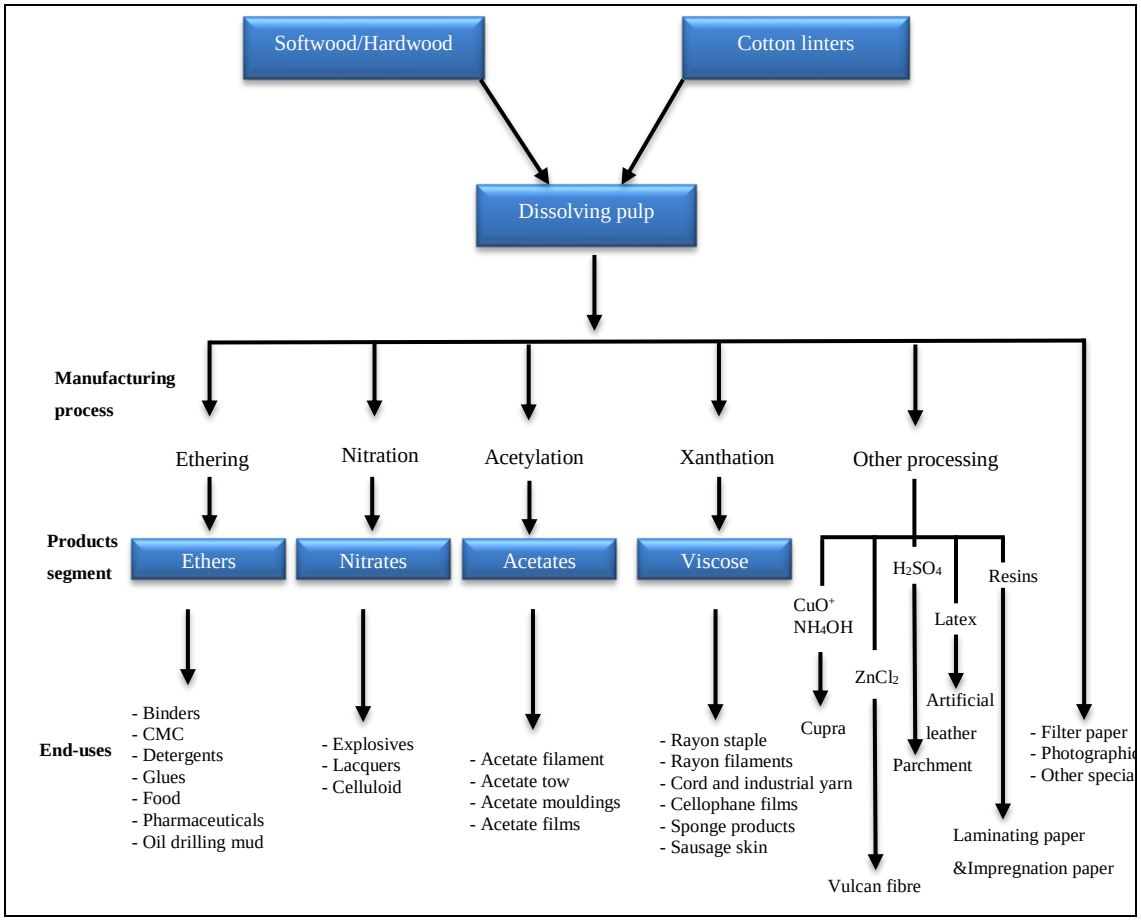

Figure 2.1: Dissolving wood pulp end-uses and end products, adapted from (Teras & Jokinen, 2010).

DWP undergoes a variety of manufacturing processes such as nitration, acetylation, xanthation which is also known as the viscose process, and other processes that are used for the production of various cellulose based end-products. These manufacturing processes are classified according to the different alpha grades used to produce these cellulose derivatives. For example, 90%, 92 -94% and 96% α-cellulose are respectively utilised for the production of microcrystalline cellulose (MCC), viscose, and cellulose acetate (Chunilall *et al.*, 2010; Liu *et al.*, 2016).

2.2 Structure of cellulose

Cellulose is one of the most abundant, biodegradable natural molecules found on Earth. This biopolymer is well known for its distinctive properties that make it attractive for conversion into useful cellulose derivatives (Engstrom *et al.*, 2006; Sixta *et al.*, 2013). Conversion of cellulose to these valuable materials is largely dependent on the accessibility and reactivity of this biopolymer. High cellulose accessibility and reactivity are essential for a homogeneous substitution of the hydroxyl (-OH) groups to produce high-quality products. Therefore, knowledge and understanding of the structural arrangement of cellulose are necessary. Naturally, cellulose has a complex structural arrangement that can be described in three fundamental levels; molecular, morphological and supramolecular (Atalla, 1990; Kopcke, 2010; Strunk, 2012). These levels are representative of a polymer with an entwined structural system. Thus, the description of each level demonstrates the link from one level to another.

2.2.1 Molecular structural level of cellulose

Cellulose was first discovered and isolated from plants by a French chemist called Anselme Payen in 1838 (Hon, 1994; Hallac & Ragauskas, 2011). In his research, Payen characterised cellulose into its chemical constituents and reported that it had the empirical formula $C_6H_{10}O_5$ (O'Sullivan, 1997; Klemm *et al.*, 2005). Cellulose is primarily sourced from plants as it is a fundamental constituent of the plant cell wall. It can also be extracted from algae, bacteria, fungi and other marine species such as tunicates (Klemm *et al.*, 2005; Esa *et al.*, 2014). Approximately 10^{11}-10^{12} tonnes of pure cellulose are produced by plants annually through the process of photosynthesis (O'Sullivan, 1997; Klemm *et al.*, 2005; Siquera *et al.*, 2010).

Cellulose is a fibrous polymer that is insoluble in water, dilute acidic and alkaline solutions at average temperature. Apart from being naturally abundant and affordable, cellulose is biocompatible, biodegradable, and renewable with excellent mechanical properties. For this reasons, cellulose is used in various industries such nanotechnology, pharmaceuticals, medicine, and in biorefinery for production of biofuels, biocomposites and other natural products (O'Sullivan, 1997; Czaja *et al.*, 2006; Azeredo, 2009; Shokri & Adibkia, 2013).

Cellulose is a linear homopolysaccharide formed by β-D-anhydroglucose units (AGU) that are covalently linked together by (1→4) glycosidic bonds between the equatorial -OH group at C4 and the C1 carbon atom. The basic building block of cellulose is made up of repetitive units of glucose monomers referred to as cellubiose; they form a linear cellulose chain as displayed in Figure 2.2. Each AGU is arranged in a chair conformation with three –OH groups in an axial position on carbon atoms C2, C3 and C6 of cellulose (O'Sullivan, 1997; Klemm *et al.*, 2005; Lavoine *et al.*, 2012; Peng *et al.*, 2013; Eriksson, 2014).

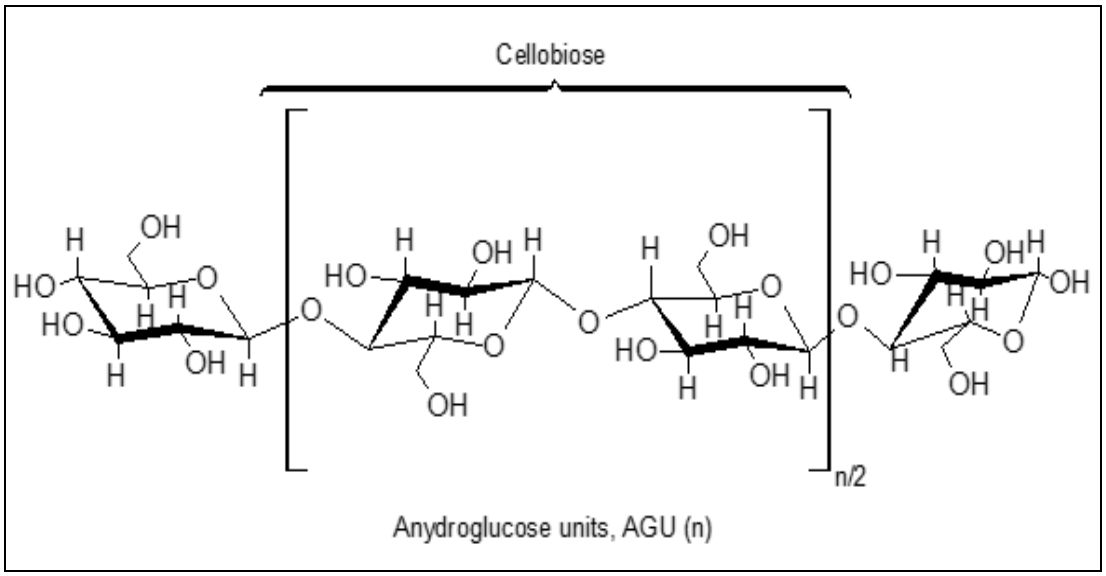

Figure 2.2: Molecular structure of cellulose, adapted from (Klemm *et al.*, 2005)**.**

The arrangement of the -OH groups in cellulose fibres is responsible for its crystalline fibrous structure. Native cellulose comprises of long straight monomer chains that are aligned parallel to each other, with a large number of -OH groups evenly distributed on both sides of the anhydroglucose units. The parallel alignment of the cellulose chains and

the distribution of the -OH groups on the polymer chains allow for the formation of strong intra- and inter-molecular hydrogen bonds. The intramolecular hydrogen bonds form between the -OH groups of the same cellulose chain, while intermolecular hydrogen bonds form between adjacent cellulose chains, thus creating a crystalline cellulose structure (Siqueira *et al.*, 2010; Harmsen *et al.*, 2010; Eriksson, 2014). In intramolecular hydrogen bonding, two bonds form per one glucose unit; the first one forms between the hydroxyl group on the C3 carbon and the ring oxygen atom of the neighbouring AGU (-O3-H--O5) and the second bond forms between the hydroxyl groups on C2 and C6 carbons atoms (-O6-H---O2-H). Concerning the intermolecular hydrogen bonding, only one bond exist per glucose unit. The bond occurs between the C6 –OH group of one and the C3 –OH group of the next cellulose chain (Gardner & Blackwell, 1974; Festucci-Buselli *et al.*, 2007).

Cellulose is not a chemically homogeneous polymer; each terminal of its molecular chains consists of two different glucose residues, the non-reducing and the reducing end groups (Figure 2.3). The non-reducing end comprises a closed ring structure with an alcoholic hydroxyl group on the C4 carbon. On the other end, at the C1 carbon atom, the reducing end group is comprised of an open chain aldehyde group. Aldehyde groups can form a pyranose ring, and this is in equilibrium with the cyclic hemiacetal form (Festucci-Buselli *et al.*, 2007; Kopcke, 2010).

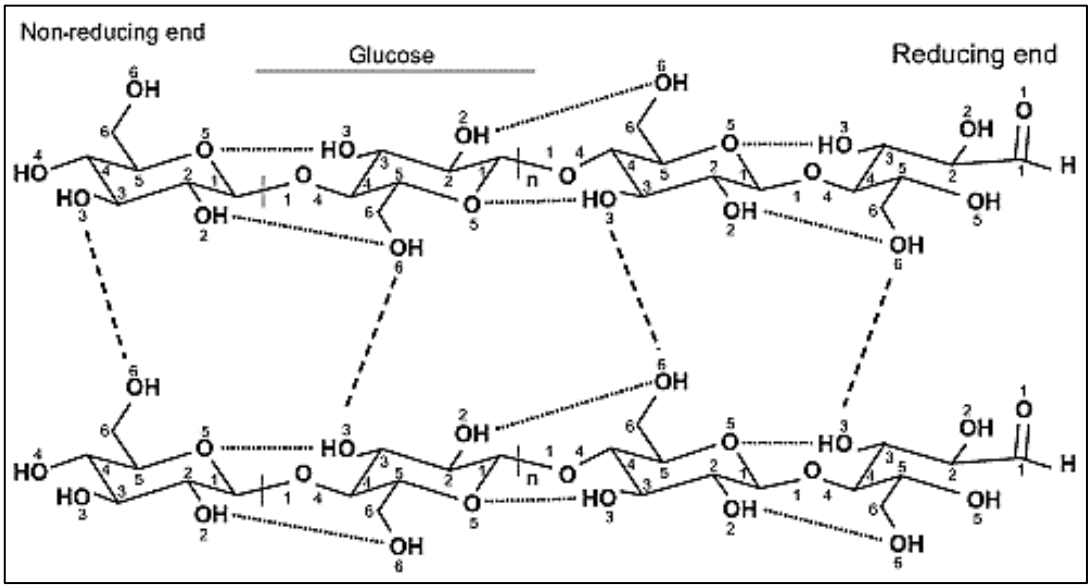

Figure 2.3: The structure of intra-(dotted lines) and inter-molecular (dashed lines) hydrogen bonds in natural cellulose, adapted from (Festucci-Buselli *et al.*, 2007)**.**

The structure of cellulose is characteristic of having high molecular weight (Mw) and degree of polymerization (DP). The DP is one of the most important features of cellulose that have a significant influence on the reactivity and derivatization of this biomolecule. It refers to the number of AGUs that make up the cellulose polymer chain; it is an expression of the polymer chain length (Klemm *et al.*, 2005; Harmsen *et al.*, 2010). The value of DP can vary considerably depending on the source of the polymer, for example, some scholars have reported that the DP value for bacterial cellulose ranges between 2000 to 8000 AGUs, and that plant and cotton celluloses have a DP of approximately 10000 and 15000 AGUs respectively. The DP has a significant influence on various properties of cellulose including the molecular weight distribution (O'Sullivan, 1997; Somerville, 2006; Lavoine *et al.*, 2012).

2.2.2 Morphological structure of cellulose

The morphological structure of cellulose primarily describes the arrangement of microfibrils into fibril aggregates to form fibre wall layers within this biopolymer. Cellulose is a relatively stable polymer; its structure consists of a network of microfibrils made from aggregated chains of cellulose molecules that are aligned parallel to each other and held together by strong hydrogen bonds (Klemm *et al.*, 2005; Carlmark *et al.*, 2012). Microfibrils are considered the smallest units in the morphology of plant cell wall; their diameter is approximately 3-4 nm. The microfibrils also agglomerate with each other to form large units referred to as macrofibrils or cellulose fibril aggregates which have a diameter of 20-25 nm (Figure 2.4).

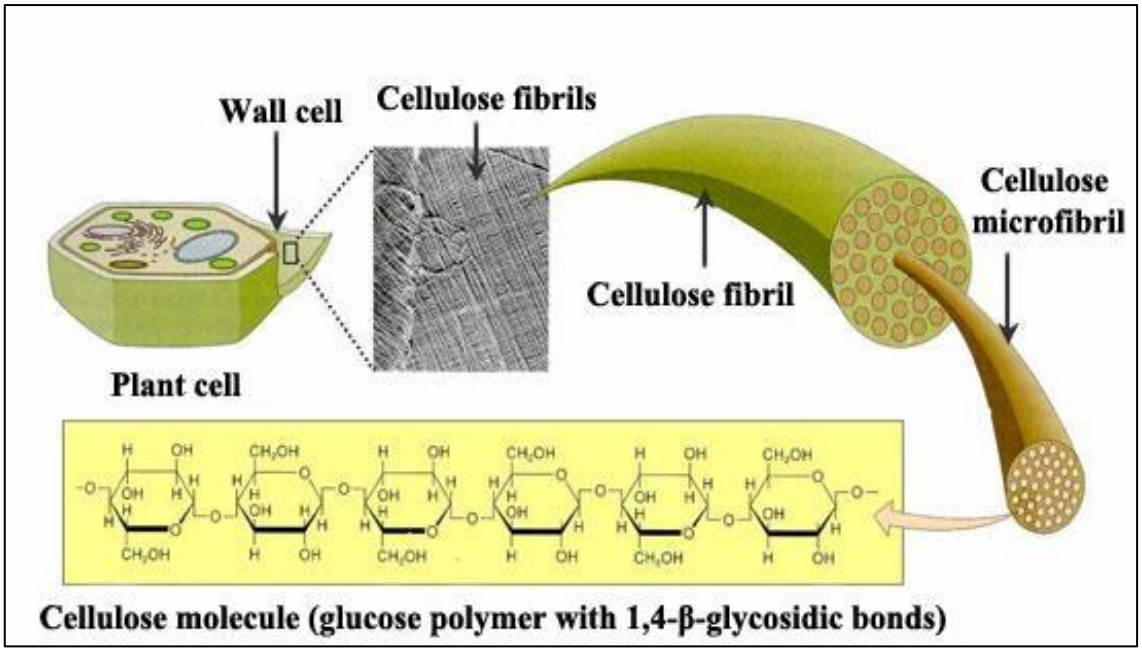

Figure 2.4: Arrangement of cellulose fibrils, microfibrils and cellulose molecules in the plant cell wall, adapted from (Funes, 2013)**.**

The cellulose fibril aggregates are tightly held together by intra- and intermolecular hydrogen bonds, dipole interactions and van der Waals interactions (Fahlén & Salmén, 2002; Fahlén & Salmén, 2005; Donaldson, 2007; Harmsen *et al.*, 2010). Thorough knowledge of the arrangement of cellulose chains within the molecule is essential for improving the reactivity and accessibility of cellulose, for the production of cellulose derivatives (Zuckerstatter *et al.*, 2009; Ostberg *et al.*, 2012).

The structure of the fibre cell wall consists of several distinct layers: primary cell wall (P), secondary cell wall (S), the lumen (L) as well as the middle lamella (ML) which serves as a binding agent between adjacent cells. The secondary cell wall can be divided further into three layers known as S1, S2, and S3. The three layers are differentiated from each other by the arrangement of the cellulose fibrils (Akerholm, 2003; Frone *et al.*, 2011; Chunilall *et al.*, 2012). The S2 layer is the most important structural component of the cell wall; it accounts for 40-90% of the total cell wall thickness. Moreover, it has a significant influence on the physical properties, and it gives plants their mechanical strength (Tabet & Aziz, 2013; Rafsanjani *et al.*, 2014). A schematic description of the fibre cell wall is shown in Figure 2.5.

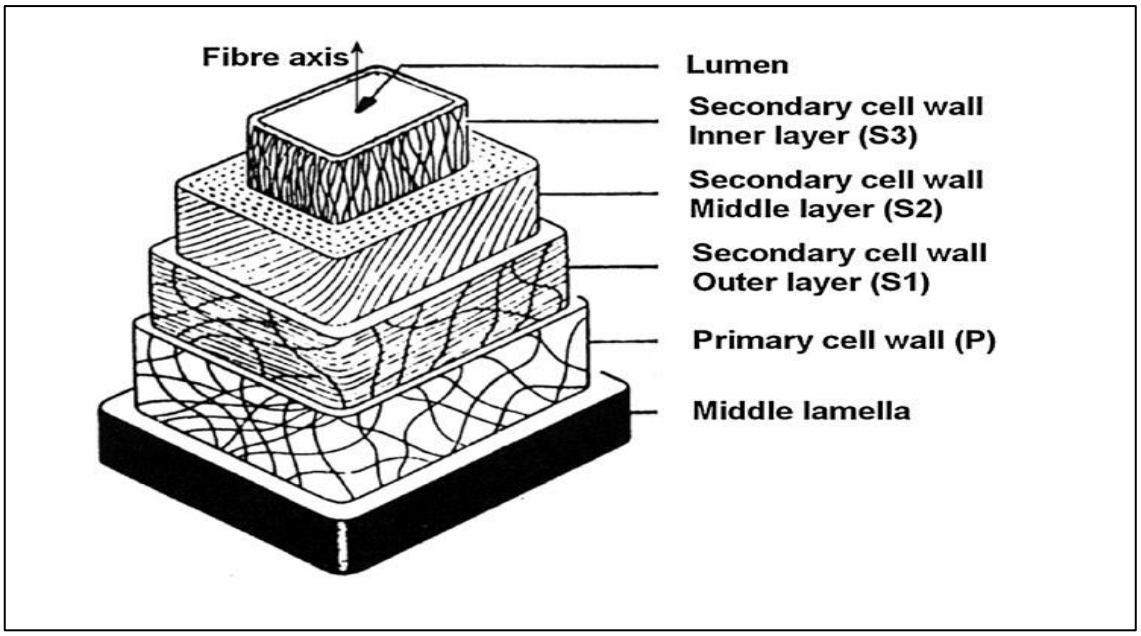

Figure 2.5: An illustration of the plant cell wall structure with the different cell wall layers, adapted from (Nieminen *et al.*, 2013).

2.2.3 Supramolecular structure of cellulose

The degree of cellulose crystallinity, in particular, surface area, and porosity are the main parameters that describe the supramolecular structure of cellulose. These properties of the cellulose structure have a significant influence on the mechanical properties of cellulose pulp as well as its reactivity and accessibility towards chemical processing (Josefsson *et al.*, 2001; Aldaeus *et al.*, 2015; Peciulyte *et al.*, 2015). The cellulose structure comprises of hydrogen bonded β-D-(1→4)-glucan units which are agglomerated together into microfibrils also referred to as "cellulose fibril aggregates." The cellulose fibril aggregates are what forms the cellulose fibres which are the building block of the plant cell walls. Cellulose fibrils are made up of crystalline regions with highly ordered cellulose chains as well as non-crystalline regions that are less ordered. The less ordered cellulose chains are also referred to as "amorphous regions" (Fahlén & Salmén, 2003; Fahlén & Salmén, 2005; Aldaeus *et al.*, 2015).

The ratio of crystalline to non-crystalline regions in cellulose is a major factor that affects the accessibility and reactivity of cellulose. The high crystalline regions of the cellulose act as a barrier rendering the polymer insoluble in conventional solvents and resistant to hydrolysis (O'Sullivan, 1997; Kontturi *et al.*, 2006; Carlmark *et al.*, 2012). The degree of crystallinity in the cellulosic material is usually described using the crystallinity index

(CrI). The crystallinity index of natural cellulose is reported to range from 40-95% with the remainder of the material being non-crystalline cellulose (Quiroz-Castañeda & Folch-Mallol, 2013).

Cellulose exists in six different crystalline domains labelled: cellulose I, II, III_I, III_{II}, IV_I, and IV_{II}. The polymorphic properties of cellulose have been widely studied with various spectroscopic and diffractometric techniques, such as X-ray diffraction (XRD), synchrotron X-ray, neutron fibre diffraction, and solid state ^{13}C nuclear magnetic resonance (NMR). Other characterization techniques that have been used include, the Fourier transform infrared (FTIR), and Raman spectroscopy (Atalla, 1990; O'Sullivan, 1997; Atalla & VanderHart, 1999; Nishiyama *et al.*, 2002; French & Cintrón, 2013).

Several research groups have reported that natural cellulose in higher plants exists in a crystalline form and that it is a composite of coexisting phases. Atalla *et al*. (1980) and Festucci-Buselli *et al*. (2007) indicated that native cellulose consists of two crystalline polymorphic forms which are cellulose Iα and Iβ. Other scholars have however argued that cellulose comprises of three crystalline forms including the para-crystalline cellulose which is a mixture of cellulose of Iα and Iβ. Compared cellulose Iα and Iβ, para-crystalline cellulose is said to have low crystalline order, but more ordered than amorphous cellulose (Hallac & Ragauskas, 2011; Quiroz-Castaneda & Folch-Mallol, 2013). The crystalline chain packing of cellulose Iα is described as having a triclinic unit cell with one chain, while cellulose Iβ has a monoclinic unit cell with two parallel chains (Figure 2.6) (Koyama *et al.*, 1997; Hallac & Ragauskas, 2011; Quiroz-Castaneda & Folch-Mallol, 2013). The triclinic Iα phase is metastable; it can readily convert into the more stable monoclinic Iβ phase by hydrothermal alkaline treatments and annealing (O'Sullivan, 1997; Poletto *et al.*, 2014).

The molecular chains of these two cellulose crystal forms have the same alignment, sheets of hydrogen bonded cellulose chains are stacked parallel on top of each other. However, the differentiating factor between their structures is the hydrogen bonding pattern, the chain conformation as well as the arrangement of the cellulose molecules within the unit cell. This distinction is mainly observed in the relative displacement of cellulose sheets that exist along the (110) lattice plane in the triclinic structure and the

(200) lattice plane in the monoclinic structure called “hydrogen-bonded” planes (Quiroz-Castaneda & Folch-Mallol, 2013; Poletto *et al.*, 2014). The quantity of each crystal form depends on the source of cellulose. For example, while higher plants synthesise both crystalline structures, the predominant phase is cellulose Iβ, whereas phase Iα is abundant in the cell wall of lower plants and bacterial celluloses (Brown, 1999; Atalla & VanderHart, 1999; Sun *et al.*, 2008; Peng *et al.*, 2013).

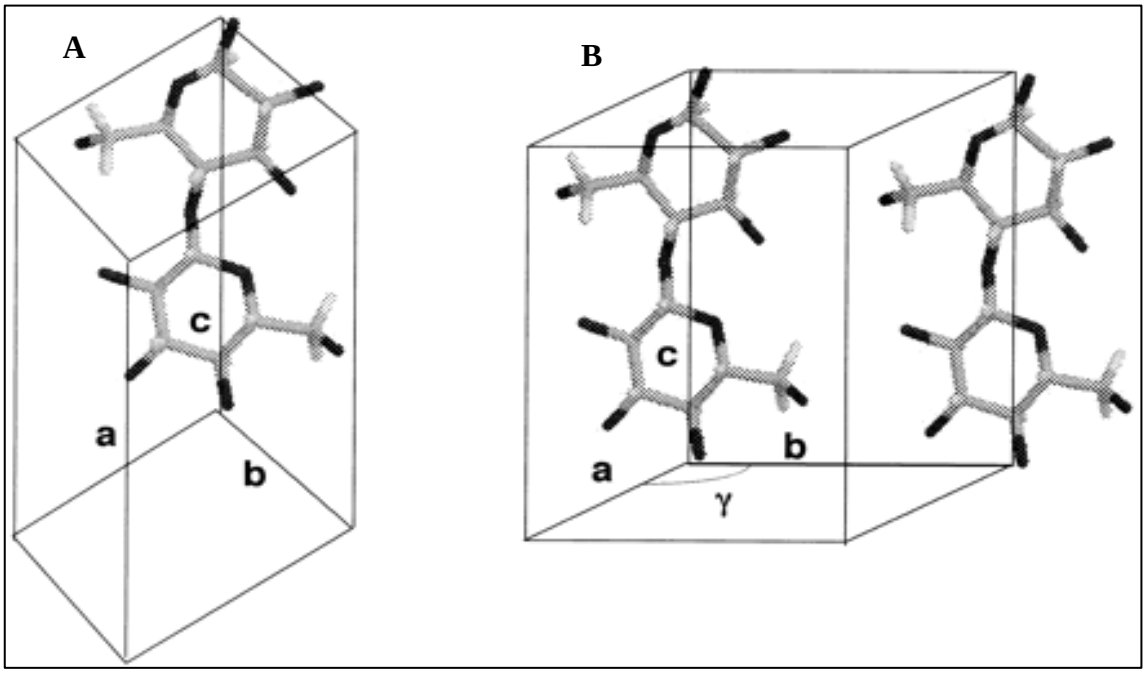

Figure 2.6: A schematic diagram of the mode of unit cell chain packing of the two crystalline polymorphs of cellulose I: (A) Triclinic unit cell (Iα) and (B) Monoclinic (Iβ), adapted from (Koyama *et al.*, 1997).

Cellulose I and II are the most studied crystalline forms of cellulose. Cellulose II is known to have more thermal stability than cellulose I; it is produced by treating cellulose I (natural cellulose) with an alkali solution by either mercerization or regeneration processes (Festucci-Buselli *et al.*, 2007; Wada *et al.*, 2008). These processes are irreversible; the cellulose microfibrils become swollen in a solvent, and this leads to a complete disruption of the highly ordered cellulose structure. The resulting cellulose II structure is made up of two monoclinic unit cells in which cellulose chains are stacked antiparallel to each other (O'Sullivan, 1997; Siqueira *et al.*, 2010; Frone *et al.*, 2011).

Figure 2.7 displays a schematic diagram of the interconversion processes of cellulose I into other cellulose polymorphs. Cellulose III_I and III_{II} form in reversible processes when celluloses I and II react with liquid ammonia (NH_3) or with organic amines (RNH_2) at lower temperatures in their reactions. Cellulose IV_I and IV_{II} polymorphs result when natural cellulose and regenerated cellulose react with glycerol at high temperatures (O'Sullivan, 1997; Rojas, 2013).

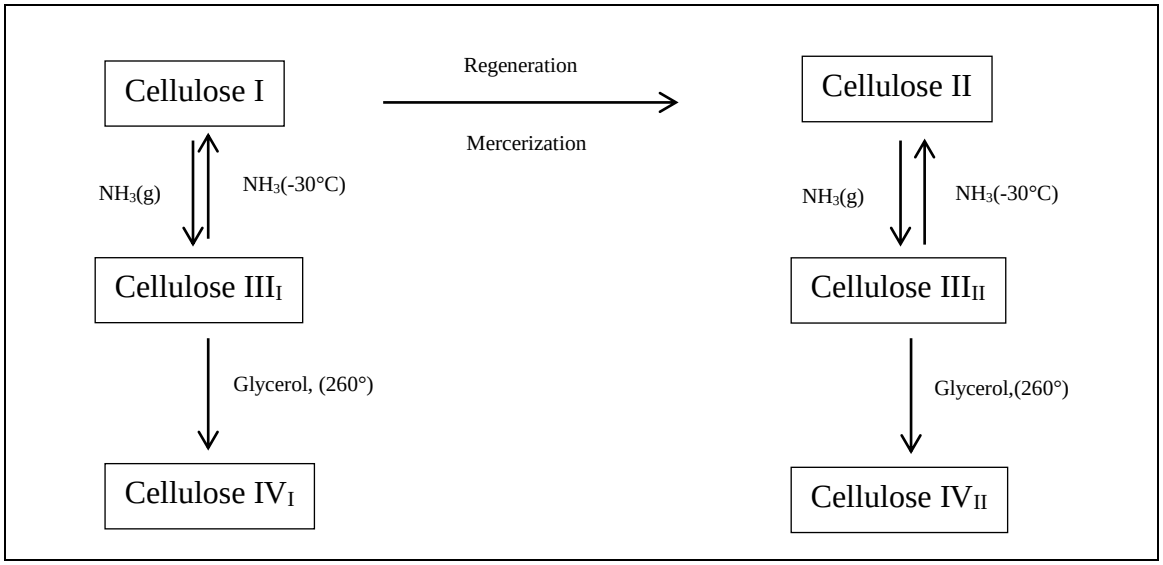

Figure 2.7: A schematic diagram of the formation of cellulose polymorphs, adapted from (Rojas, 2013).

2.3 Modification of cellulose I for production of cellulose derivatives

The global market for dissolving wood pulp and its output continues to rise with the growing demand for regenerated cellulose and natural cellulose based products (Liu *et al.*, 2016). This growth is motivated by the fact that cellulose possesses fundamental qualities that are not present in synthetic polymers such as biodegradability, renewability and natural abundance. The fibre and textile industry is still one of the major industries that use the dissolving wood pulp. Other industries where dissolving wood pulp finds application are pharmaceutical, food, painting, films, and more recently in the nanocrystalline and microcrystalline celluloses (NCC/MCC) industries (Stepanik *et al.*, 2000; Iller *et al.*, 2002; Ibarra *et al.*, 2010). According to a report by (Sappi, 2014), over 80% of the dissolving wood pulp produced globally is used for the production of regenerated cellulose which is also known as viscose rayon. The viscose manufacturing industry is documented as the second largest consumer of cellulose in the world after the

paper industry (Stepanik *et al.*, 1998; Cleland *et al.*, 1999). Various methods including Lyocell and Cuprammonium process have been developed for the production of regenerated cellulose, but the conventional viscose process is still the most common method used to manufacture this commodity.

2.3.1 Viscose process: Regenerated cellulose

The viscose process is a conventional viscose producing method that was discovered in 1892 by a British chemist Charles F. Cross, and two of his co-workers, Edward Bevan and Clayton Beadle (Dee Snell, 1926; Heinze & Koschella, 2005). They learned that sodium hydroxide (NaOH) and carbon disulphide (CS_2) could be used to dissolve wood derived cellulose fibres into a viscous solution that they referred to as "viscose". In 1893, these scientists were granted the first patent for their discovery (Wilkes, 2001; Shaikh *et al.*, 2012). The viscose process became very popular in the textile industry due to its ability to chemically manipulate cellulose pulp into versatile artificial fibres used to manufacture rayon (Dee Snell, 1926; Wilkes, 2001). Furthermore, the viscose process was economically feasible regarding the type of chemical reagents that were utilised. As a result, it is still the most important, and widely used method in the rayon manufacturing industry (Dee Snell, 1926; Heinze & Koschella, 2005; Shaikh *et al.*, 2012).

The main aim of the viscose process is to depolymerise cellulose and to adjust its molecular weight (Mw) to a level that is amenable for downstream processing (Stepanik *et al.*, 1998; Ostberg *et al.*, 2012). The viscose process involves a series of steps and chemical reactions. Figure 2.8 displays a schematic diagram of the viscose manufacturing process, and the main chemical reactions that occur during the process are illustrated below in equations (Eq. 2.1 to 2.4).

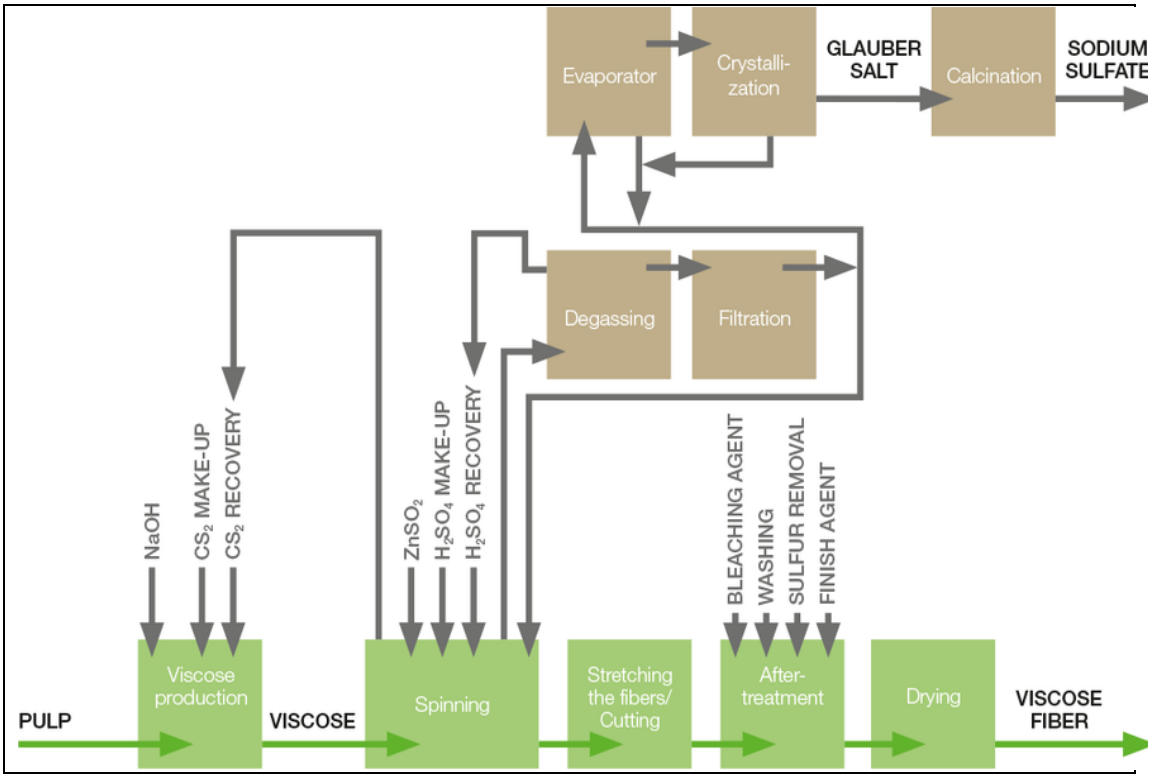

Figure 2.8: Viscose manufacturing process, adapted from (Lenzing, 2017).

In the first step, cellulose fibres are soaked in an aqueous solution of sodium hydroxide (NaOH), with a concentration ranging between 17-20% (w/v), this process is known as mercerization.

$$C_6H_9O_4OH + NaOH \rightarrow \underset{\text{(Sodium cellulosate)}}{C_6H_9O_4ONa} + H_2O \qquad 2.1$$

During mercerization, NaOH causes the cellulose fibres to swell up, separate, and finally dissolution of short cellulose chains and low molecular weight carbohydrates. Mercerization induces depolymerization and enhances the accessibility of cellulose fibres, and subsequently leads to increased rate of hydrolysis (Millert *et al.*, 1975; Engstrom *et al.*, 2006). Ultimately, mercerization converts cellulose I to sodium cellulosate which is commonly known as alkali cellulose or the white crumb (Eq. 2.1).

After mercerization, the swollen alkali cellulose (AC) mass is pressed to remove excess alkali solution to obtain a precise alkali to cellulose ratio, and shredded to increase the surface area of AC to ensure constant reactions in downstream viscose process steps. Subsequently, AC is aged or pre-ripened in a controlled environment for 8 to 12 hours at

40-50° C. During ageing, AC undergoes oxidation as it reacts with atmospheric oxygen. The oxidation step adjusts the viscosity of the solution, and further depolymerises the cellulose chain to the desired degree of polymerization (DP) before reaction with carbon disulphide (CS_2) (Morgan, 2005; Engstrom *et al.*, 2006).

Following depolymerization and shredding, the AC mass is reacted with CS_2 in the xanthation step (E.q. 2.2) to produce a thick yellow-orange compound of sodium cellulose xanthate also called the yellow crumb and by-product salts such as sodium trithiocarbamate (Na_2CS_3) which are responsible for the dark orange colour change.

$$C_6H_9O_4ONa + CS_2 \rightarrow C_6H_9O_4OCS_2Na \quad \text{(Sodium cellulose xanthate)} \qquad 2.2$$

The thick yellow-orange complex of sodium cellulose xanthate is dissolved in dilute aqueous NaOH to produce a homogenous viscous orange slurry called viscose (E.q. 2.3).

$$C_6H_9O_4OCS_2Na + NaOH \rightarrow \text{Viscose} \qquad 2.3$$

The formed viscose undergoes ripening and depolymerization for some time at a set temperature to improve the homogeneity of the degree of substitution (DS) (Weightman *et al.*, 2007). After ripening, the viscose is filtered, degassed to remove air bubbles from the slurry, and forced through tiny spinnerette holes into a sulphuric acid (H_2SO_4) bath. This extrusion process is referred to as spinning, the xanthate groups on the viscous solution are hydrolyzed as the viscose dope coagulates into fine cellulose filaments when it comes into contact with the acid (Eq. 2.4). The regenerated cellulose filaments are referred to as “rayon”.

$$C_6H_9O_4OCS_2Na + \tfrac{1}{2}H_2SO_4 \rightarrow C_6H_9O_4OH + CS_2 + \tfrac{1}{2}Na_2SO_4 \qquad 2.4$$

The rayon filaments are then stretched and strengthened in the drawing process. Finally, the fibres undergo a series of after-treatment steps; this entails bleaching of the fibres to enhance their brightness and purity and washing to remove impurities. Excess CS_2 is also recovered from the effluent and manufactured by-products such as hydrogen sulphide gas

(H_2S), and sodium sulphate (Na_2SO_4) are also recovered and collected (Stepanik *et al.*, 1998; Cleland *et al.*, 1999; Christoffersson, 2005; Ostberg *et al.*, 2012).

Disadvantages of the viscose process

The viscose process has proved to be successful in the production of viscose rayon for more than 100 years. However, this process is plagued by various challenges. The viscose process is widely known for its negative impact on the environment and toxic effect on human health. In the early 1940s, more than 100 cases of CS_2 poisoning were reported amongst factory employees in Piedmont within a two year period (Vigliani, 1954). In a similar study, Tiller *et al*. (1968) indicated that long-term exposure of workers to CS_2 at a viscose rayon factory was identified as the leading cause of coronary heart disease and subsequent death (Tiller *et al.*, 1968). Thus, further research and development of eco-friendly and profitable methods that will not compromise the quality of the end products are required.

2.3.2 Alkali dissolution of cellulose

The structural complexity and molecular composition of cellulose render it insoluble in most common solvents, thus limiting its application (Zhang *et al.*, 2002). The recalcitrance of the cellulose structure continues to be the driving force behind research to find environmentally friendly and non-degrading processes to dissolve this macromolecule. Direct dissolution of cellulosic biomass in an alkali solution is one method that has widely been studied. Alkali dissolution of cellulose is a longstanding method that has been used for cellulose modification. It is a process in which rigid inter- and intra-chain hydrogen bonding between the hydroxyl groups on the cellulose backbone are chemically broken down at a temperature below zero degrees. The aim of this process is to disrupt the crystal structure of cellulose to produce a clear solution of molecular cellulose (Wang, 2008; Olsson & Westman, 2013). The proposed mechanism for this disruption is that NaOH and water form a hydrate which breaks the inter- and intra-molecular hydrogen bonding network of this biopolymer (Medronho & Lindman, 2015).

Cellulose dissolution is different to mercerization because, in the latter process, the alkali solution interacts with the polymer as a swelling agent before xanthation occurs in the viscose process. In mercerization, the alkali solution works as a derivatizing solvent; it

reacts with one or all the –OH groups on the cellulose backbone to give an alkali-cellulose intermediate that is soluble in common solvents. This intermediate is the one that reacts with CS_2 as described in the viscose process (Olsson & Westman, 2013). Conversely, in cellulose dissolution, NaOH acts as a non-derivatizing solvent; it disrupts the forces that hold the cellulose molecules together without changing the chemical composition of the polymer (Isogai & Atalla, 1998; Olsson & Westman, 2013).

Complete dissolution of cellulose fibres in aqueous alkali solutions has been widely studied and reported by a variety of scholars. In their research, Zhang and co-workers have on separate studies indicated that their success in producing regenerated cellulose membranes and films by complete dissolution of cotton linters at low temperatures, with urea and thiourea as additives (Zhou & Zhang, 2000; Zhang *et al.*, 2002). A similar study by (Wang & Deng, 2009) displayed that complete cellulose dissolution is influenced by a variety of parameters including the concentration of NaOH, the temperature of the cooling system as well as the additive used. In their study, Wang and co-workers also observed that pretreated cellulose with shorter chain length and low DP were easier to dissolve in alkali compared to the reference samples (Wang *et al.*, 2014). Cellulose pretreatment which affected the DP and crystallinity also had a significant influence on the efficiency of the dissolution process.

The molecular weight (Mw) and degree of polymerization have been highlighted as the main influences on alkali cellulose dissolution. Isogai and Atalla noted that low Mw samples were able to fully dissolve in NaOH, unlike the higher plants cellulose samples (Isogai & Atalla, 1998). An inversely proportional relationship between alkali dissolution and the degree of polymerization has also been reported as a major role player in polymer reactions. Rahkamo and colleagues exposed dissolving pulp to enzymatic modification and dissolved the pulp in an aqueous NaOH solution (9 wt. %) at a temperature below freezing point. A significant increase in alkali dissolution by more than 20% was observed with a decrease in viscosity due to enzyme pretreatment (Rahkamo *et al.*, 1996).

2.4 Cellulose I reactivity and reactivity measurements

Conversion of cellulose pulp to its valuable derivatives such as cellulose esters, ethers, acetates and cellulose xanthate, is substantially dependent on the reactivity of this

polymer. Reactivity refers to the relative ease by which chemical reagents can access the three reactive cellulose hydroxyl groups. Furthermore, it is a measure of the ability of this polymer to take part in a variety of chemical reactions (Urquhart, 1958; Christoffersson *et al.*, 2002; Chunilall *et al.*, 2013). Cellulose reactivity is an important aspect of the dissolving wood pulp industry, and it is an important parameter for evaluating the quality of the pulp for manufacturing cellulose derivatives and regenerated cellulose. It is impractical to discuss cellulose reactivity apart from the molecular and supramolecular structural properties of this polymer. Some of the structural features of cellulose fibres such as morphology, crystallinity and the degree of polymerization (DP) have a significant influence on the reactivity and accessibility of this biopolymer (Christoffersson *et al.*, 2002; Park *et al.*, 2010; Duan *et al.*, 2016).

The correlation between cellulose structure and reactivity has long been a subject of interest because of the importance of this natural polymer for many industrial applications. As aforementioned, the cellulose polymer consists of a network of hydroxyl (-OH) groups. Each glucose unit that makes up the polymer chain has three -OH groups that can form hydrogen bonds with each other. It is the inter- and intramolecular hydrogen bonding system of the -OH groups within the polymer chain that is responsible for the high crystallinity structure of cellulose which results during linear packing of cellulose microfibrils (Atalla, 1990; O'Sullivan, 1997; Klemm *et al.*, 2005). Accessibility of these –OH groups towards chemical reagents during processing plays a key role in determining the reactivity of cellulose. Furthermore, cellulose accessibility cannot be discussed independently from cellulose structural features, mainly crystallinity (Nelson & Oliver, 1971; Ioelovich, 2009).

A study by Park and co-workers reported a high rate of enzyme digestibility for samples that had more amorphous regions compared to high crystalline cellulose. Similar results were obtained when Ioelovich observed that amorphous cellulose regions were more accessible to water molecules compared to the highly ordered crystalline regions. Furthermore, it was noted that water molecules had more fibre accessibility compared to organic solvents with lower polarity (Ioelovich, 2009; Park *et al.*, 2010).

Characterization of the cellulose structure was carried out by Aldaeus *et al*. (2015) to assess the impact of various structural factors on the extent of enzyme hydrolysability of

cellulose substrates. The structure of cellulose has displayed that it has an adverse influence on the throughput of enzymatic hydrolysis. Although a direct relationship between the actual conversion of the cellulose substrate and cellulose crystallinity has not yet been established, many structural and compositional factors influence cellulose hydrolysis for production of biofuels. Listed factors include cellulose particle size, supramolecular properties, specific surface area (SSA) and degree of polymerization (Puri, 1984; Park *et al.*, 2010; Peciulyte *et al.*, 2015; Aldaeus *et al.*, 2015).

2.4.1 Cellulose reactivity measurement: Fock method

Measurement of cellulose reactivity is an important parameter in the cellulose regeneration industry because it represents the processability of cellulose in downstream chemical reactions (Christoffersson, 2005; Tian *et al.*, 2014). The Fock test method is one of the conventional methods used for measuring the reactivity of cellulose at laboratory scale. Fock first described it in 1959; it is a micro-scale process that is similar to the conventional viscose process. Fock test procedure works in such a way that a small amount of cellulose pulp sample is mercerised in excess NaOH (9% w/w) and CS_2 to produce an orange cellulose xanthate solution. A quantity of the alkali activated cellulose is expected to react with CS_2. Subsequently, to regenerate cellulose, the cellulose xanthate complex is reacted with sulphuric acid (H_2SO_4). Finally, the amount of regenerated cellulose in solution is evaluated by oxidation with potassium dichromate ($K_2Cr_2O_7$) (Fock, 1959; Tian *et al.*, 2013). This method is preferred because it is a relatively direct and straightforward procedure that does not require specialised equipment. As a result, it can be carried out in a conventional wet chemistry laboratory under high safety measures due to the toxicity of CS_2. Moreover, the Fock test does not need a large quantity of the sample for analysis (Christoffersson, 2005; Kopcke, 2010; Tian *et al.*, 2013).

Using the Fock test method, Henriksson *et al*. (2005) reported an increase in cellulose reactivity after this macromolecule was pretreated with enzyme endoglucanase. In a similar study, Miao's research group tested the reactivity of hardwood pre-hydrolysis Kraft (PHK) pulp by the Fock test method. They observed an increase of more than 5% in reactivity of the PHK hardwood pulp when the pulp was first exposed to mechanical and enzymatic pretreatments (Henriksson *et al.*, 2005; Miao *et al.*, 2015). In essence, reactivity measurements are carried out to determine the extent to which the three –OH

groups on the glucose monomers are accessible for substitution and reaction with chemicals.

2.5 Pretreatment of cellulosic materials

Pretreatment of cellulosic biomass is primarily concerned with changing the structure and chemical properties of cellulose, and opening up the fibrillar structure of cellulose, to increase accessibility (Wertz & Bedue, 2013; Ogura *et al.*, 2013). Limited accessibility of the hydroxyl groups on cellulose monomer units causes inhomogeneity in the cellulose derivatives produced, and this affects the quality of the products (Henniges *et al.*, 2012). Pretreatment of cellulose is, however, expected to improve the accessibility of the material without damaging the carbohydrate. Furthermore, it must not form by-products that could, in turn, inhibit subsequent reaction processes, and it must be cost effective (Sun & Cheng, 2002; Wertz & Bedue, 2013; Chen, 2014). Figure 2.9 displays a schematic diagram for the overall goal of lignocellulosic biomass pretreatment.

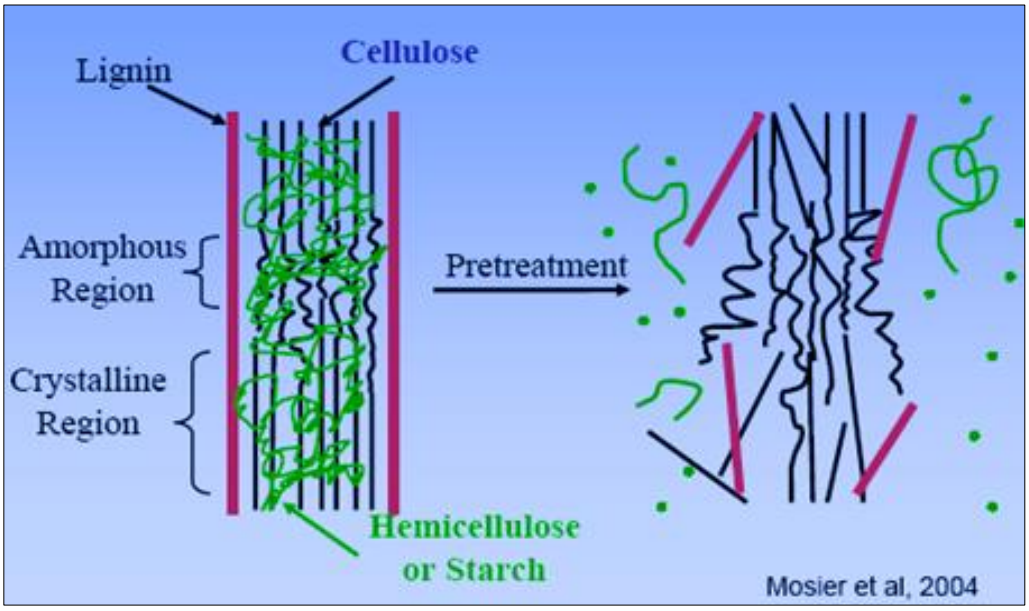

Figure 2.9: A schematic diagram showing the effect of lignocellulosic biomass pretreatment, adapted from (Harmsen *et al.*, 2010).

The primary purpose of all pretreatment techniques is to disrupt and alter the plant cell wall structure and to increase the ratio of cellulose non-crystalline regions to crystalline regions thus making it readily accessible for chemical reactivity (Mosier *et al.*, 2005; Kumar *et al.*, 2009; Brodeur *et al.*, 2011). Extensive research has been carried out on the

types of pretreatment methods used for cellulosic biomass. Table 2.1 presents some of the effects of various pretreatment techniques on the reactivity or digestibility of cellulosic materials found in the literature.

Table 2.1: Effect of various pretreatment techniques on the processability and reactivity of cellulosic biomass

Type of pretreatment	**Effect of pretreatment on cellulose reactivity**
Pretreatment of dissolving pulp with monocomponent endoglucanase at different enzyme dosages (ECU/g dry wt. pulp)	According to Fock method, the reactivity of the pretreated pulp increased from 75% to 100% with increasing enzyme dosage over different treatment times (0, 10, 30, and 90 min) (Engstrom *et al.*, 2006).
Enzymatic activation of hardwood and softwood dissolving-grade pulps with different commercial monocomponent endoglucanases	An increase of about 20% in Fock reactivity was achieved for both hardwood and softwood pulps relative to their respective reference samples (Ibarra *et al.*, 2010).
Pretreatment of sugarcane bagasse with 2% (v/v) H_2O_2 + 2% NaOH & 5% (v/v) H_2O_2 + 2% NaOH	Maximum saccharification of 57.4% and 63.3% were achieved respectively during enzyme hydrolysis of the pretreated samples (Irfan *et al.*, 2011).
Enzymatic pretreatment of pulp before viscose process stages	Reactivity of the enzyme pretreated pulp increased from 70% (reference sample) to about 85% after a relatively short treatment time (Ostberg *et al.*, 2012).
Wet oxidation pretreatment of wood pulp waste	The pretreatment caused signification modification on the structure of cellulose and improved enzymatic saccharification; this resulted in 76% glucose recovery (Ji *et al.*, 2015).

Depending on the desired end products, pretreatment techniques can be used individually or in combination to maximise their efficiency. Several pretreatment techniques can be used to achieve modification in the morphological, molecular or supramolecular

structure. Commonly used techniques can be divided into three classes: biological, chemical and physical pretreatments.

2.5.1 Biological pretreatment of cellulosic biomass

Biological pretreatment of cellulosic biomass for production of biofuels is one of the research areas that have gained much attention over the recent years. This technique refers to the use of cellulolytic and hemicellulolytic enzymes secreted by fungi and bacteria to disrupt the polymer chain and to create a porous cellulose substrate. The enzymes infiltrate the cellulose fibres and enhance their accessibility for hydrolysis. Commonly used enzymes include endoglucanases; endocellulases; and exocellulase (Christoffersson *et al.*, 2002; Taherzadeh & Karimi, 2008; Peciulyte *et al.*, 2015). Crucial steps in this pretreatment technique are hydrolysis of cellulose in the matrix to produce reducing sugars and fermentation of these sugars to give bioethanol (Hatakka, 1984; Sun & Cheng, 2002). Even though biological pretreatments do not cause harm to the environment, they are not favourable for the commercial and industrial application. Their disadvantage is that the microorganisms work at a slow pace and their treatment rate is also minimal (Maurya *et al.*, 2015).

2.5.2 Chemical pretreatment of cellulosic biomass

Chemical pretreatment methods involve the use of chemical solvents to hydrolyze hemicellulose and lignin in lignocellulosic biomass. The primary purpose of this form of pretreatment is to break down the crystalline structure of cellulose to improve its accessibility for downstream chemical and enzymatic reactions (Jiao & Xiong, 2014; SriBala *et al.*, 2016). These pretreatment methods are known to cause cellulose chain scission thus leading to depolymerization and transformation of the crystalline structure to amorphous structure. Subsequently, this enhances cellulose processability and enzymatic hydrolysis (Ye & Farriol, 2005; Badiei *et al.*, 2014).

Chemical pretreatment of cellulose is one of the most widely reviewed methods of cellulose activation. Some of the conventional methods that have been used in this technique include acid and alkaline hydrolysis, organosolv, ionic liquids and oxidative delignification where oxidising agents are used for disintegrating the lignin (Harmsen *et al.*, 2010; Chen, 2014; Sidiras & Salapa, 2015). Chemical pretreatment plays a significant

role in the production of pure cellulose from wood by pre-hydrolysis Kraft pulping and acid bisulphite pulping processes (Sixta *et al.*, 2004; Kumar *et al.*, 2009).

However, chemical pretreatment methods still encounter various disadvantages, some of the documented drawbacks include high costs, low product yield at long, laborious experiments. Moreover, they require specialised corrosion resistant reactors that can withstand toxic effluents that result (Maurya *et al.*, 2015). With the current stringency of environmental regulations, the use of chemicals and these techniques continues to be a liability for most pulp and paper industries, and industries that produce valuable cellulose end products.

2.5.3 Physical pretreatment of cellulosic biomass

Physical pretreatment is a method that alters the physical structure of the biomass. The primary goal of this is to reduce the particle size and crystallinity of lignocellulosic materials while increasing the surface area and reducing the degree of polymerization (Chen, 2014; Maurya *et al.*, 2015). There is a broad range of physical pretreatment methods that have been established for cellulosic biomass pretreatment. Mechanical pretreatments (e.g. grinding, crushing, milling, and chipping) are mostly used during the pulping stages. Other methods include pyrolysis, steam explosion, and radiation (Kumar *et al.*, 2009; Xiao *et al.*, 2010; Brodeur *et al.*, 2011; Tian *et al.*, 2011).

2.6 Radiation pretreatment of cellulose

Radiation processing of polymeric materials is a subject that has attracted considerable interest for a long time. It can be dated back to the early 1940s when most of the powerful nuclear radiation sources became popular and commercialised in the polymer industry (Chapiro, 2002; Chmielewski *et al.*, 2005). Over the years, radiation technology has progressively proved to be a useful tool for modifying polymers, and for enhancing their properties. With the increasing stringency of the environmental regulations towards pollution over the years, radiation processing has shown to be an effective alternative to conventional methods that have been used for polymer modification (Chmielewski & Haji-Saeid, 2004; Rao, 2009).

For many years, various industries, scientists, and scholars in the field of radiation chemistry have used this technology to process and manipulate the properties of both synthetic and natural polymers for different applications. Radiation chemistry is primarily concerned with the chemical effects that result in the material of interest due to its interaction with radiation energy (U.S.NRC, 2013; H.P.S., 2010; Meléndez-Ortiz *et al.*, 2015). Some of the earliest industrial applications of radiation technologies in the polymer industry include: crosslinking, grafting, and polymer chain scission, and polymer degradation. Additional uses of this technology include sterilization of disposable plastic medical devices; art conservation; food preservation, as well as bio-energy production from polysaccharides (Rosa *et al.*, 1983; Clough, 2001; Chmielewski *et al.*, 2005; H.P.S., 2010).

Radiation energy is one of the most abundant forms of energy that is available on earth. It naturally occurs in the form of light (solar energy), sound, and heat, and it can also be generated using modern technologies. It is emitted and transferred in the form of a magnetic wave or a particle (Dahlan, 2001). Radiation energy can be categorised according to the photon energy (eV) and wavelength (metres). Figure 2.10 below depicts the electromagnetic spectra of radiation energy from radio waves, through the visible light spectrum, up to X-rays and gamma rays (Bhattacharya, 2000; Kasaai, 2013).

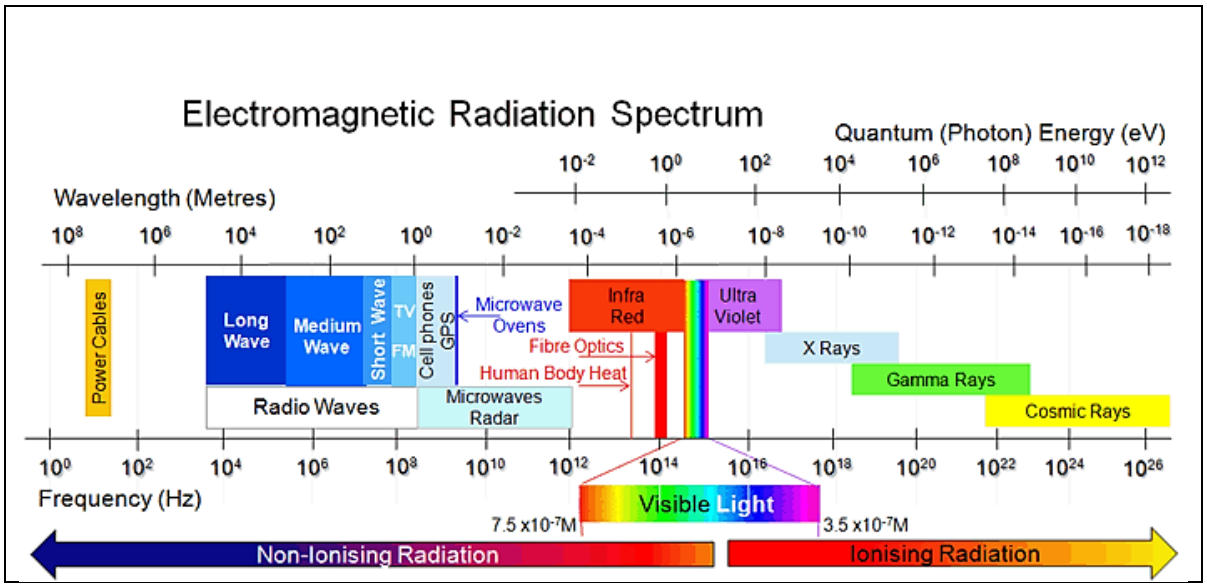

Figure 2.10: Electromagnetic spectrum of radiation energy, adapted from (Electropaedia, 2005).

As a form of physical pretreatment, radiation processing has many advantages compared to conventional processing methods like chemical and thermal treatments (Cleland, 2006; Chen, 2014). Radiation processing has higher throughput rates at less energy consumption relative to conventional methods, and it is environmentally benign since it does not use hazardous chemical reagents that result in toxic effluents. Moreover, radiation pretreatment gives higher quality products with desirable properties at shorter pretreatment times. Some of the radiation instruments are controllable, and relatively simple to operate (Cleland, 2006; Rao, 2009; Meléndez-Ortiz *et al.*, 2015).

Radiation energy can be classified into two types, ionising and non-ionising radiation depending on the quantity of energy that is produced by the source, and the impact of its interaction with an object during processing (EPA, 2012). Ionising radiation is the type of radiation that has sufficient energy to remove electrons from atoms and molecules, thus converting them into ions and free radicals (Wojnárovits, 2011). Absorption of radiation energy by the backbone of the polymeric material leads to the formation of free radicals, and subsequent initiation of chemical and biological reactions (Bhattacharya, 2000; Cleland *et al.*, 2003). On the other hand, non-ionising radiation does not have enough energy to produce ions when passing through matter, but the energy is sufficient to cause excitation of the molecules (Ng, 2003). Moreover, non-ionising radiation has the potential to cause biological effects, especially in human beings (Wilkening, 1991).

2.6.1 Ionising radiation pretreatment

Ionising radiation consists of high-energy particles and electromagnetic radiation in the short wavelength and high-frequency range of the electromagnetic spectrum (Kwiatkowska *et al.*, 2011). Some of the conventional radiation sources that have extensively been used to modify the structure of polymers and to improve their reactivity include gamma radiation (γ-radiation), X-ray, electron beam irradiation and pulsed electric field (Gueven, 2004; Kasaai, 2013; Meléndez-Ortiz *et al.*, 2015; Loow *et al.*, 2016). Ionising radiation can be produced from different sources, γ-radiation is emitted from radioactive nuclides; while X-ray and electron beam radiation are produced from high electron accelerators (Cleland, 2006; Henniges *et al.*, 2013).

Ionization processing of cellulosic biomass leads to the formation of radical reaction intermediates which undergo a series of chain reactions. These initiation reactions result

in the abstraction of the hydrogen atom from the cellulose molecule and the formation of new bonds (Gueven, 2004; Chmielewski *et al.*, 2005). Moreover, research has shown that exposure of cellulose fibre to ionising radiation causes cleavage of the long polymer chains into shorter chains and it can cause opening of the glucopyranose ring to give shorter sugar chains.

Several scholars have reported that structural modification of cellulose by ionization treatment increases cellulose accessibility to chemical reagents and this enhances the reactivity of the polymer (Kraft & Schelosky, 2000; Iller *et al.*, 2007). In their study, Khan and co-workers were able to show the impact of γ-radiation on the chemical and physical properties of jute biofibres which is one of the natural cellulose fibres that have been used in textiles for years (Khan *et al.*, 2006; Zhang, 2014). They argued that with increasing γ-radiation dose, the fibres displayed a significant decrease in tensile strength and chemical stability. Moreover, noticeable changes were observed in the thermal and mechanical properties of the biomolecule (Khan *et al.*, 2006). These observations are expected since various scholars have widely reported the efficiency of γ-radiation for cellulose modification. Research findings by (Ershov & Klimentov, 1984) attributed the degradation of cellulose and the reduction in the degree of polymerization (DP) to the breakage of the high crystalline structure of cellulose that is held together by the intermolecular hydrogen bonds. This phenomenon was also displayed in a study done by Takacs *et al*. (2000) where treatment of cotton cellulose, with γ-radiation, resulted in the transformation of the crystalline structure of cellulose from cellulose I to cellulose II, cellulose degradation was observed by a decrease in the DP.

Another form of ionising radiation that has also been widely evaluated for polymer processing, more especially cellulose, is electron beam irradiation. In the viscose manufacturing industry, various scholars argue that this technology has the potential to alter the structure of cellulose, thus making it amenable to chemical treatment (Rajagopal & Stepanik, 1996; Weightman *et al.*, 2007). Some of the observed benefits of cellulose pretreatment before the viscose process include possible reduction of the concentration of NaOH and CS_2 required for processing (Weightman *et al.*, 2007). Henniges *et al*. (2013) investigated the effect of electron beam radiation on the characteristics of microcrystalline cellulose (MCC). Their report displayed a linear relationship between radiation dose and the molar mass of MCC. After radiation treatment, the molar mass of

MCC decreased from 82 000 $gmol^{-1}$ to 5400 $gmol^{-1}$ when the radiation dosage was increased to 100 kilograys (kGy). According to this study, irradiation pretreatment ionises cellulose and disrupts its structure; this increases the accessibility and reactivity of this polymer to solvents. These observations are similar to what several scholars have reported using various ionising radiation techniques (Kraft & Schelosky, 2000; Clough, 2001; Dubey *et al.*, 2004; Alberti *et al.*, 2005).

Disadvantages of ionising radiation

Although radiation pretreatment of cellulosic biomass is a topic that has been broadly studied, the focus has mainly been on high energy radiation sources as mentioned above. The drawback to some of the high energy radiation sources is that they are energy intensive and costly. As a result, industrial or large-scale application of these techniques is limited and mostly at a level of research and development (Chen, 2014).

2.6.2 Non-ionising radiation pretreatment

Non-ionising radiation is located at the edge of the X-ray region to the opposite end of the electromagnetic spectrum, in the radio waves region. This portion of the electromagnetic spectrum is in the opposite direction from the ionising radiation range and towards low frequency ($3x10^2 \leq 3x10^{15}$ Hz) and long wavelengths (> 100 nm). Radiation energy which is known as Photon energy is directly proportional to the frequency of radiation and inversely proportional to the wavelength. In the non-ionising region, photon energy ranges between 1.77 electron volts (eV) to 12.4 eV. Hence, non-ionising radiation sources are classified as low energy radiation sources compared to the ionising radiation sources which have photon energy that ranges from 12.4 eV and 40 eV (Wilkening, 1991; Ng, 2003; Tee, 2003). There are two types of non-ionising radiation, optical radiation and radiofrequency. Optical radiation consists of the ultraviolet (UV), visible, infrared (IR) and lasers, whereas the latter covers the microwave, as well as the low and high-frequency radio wave which includes ultrasound irradiation (Oberhofer, 1984; Dahlan, 2001; Ng, 2003).

Non-ionising radiation energy does not have enough energy to knock out electrons from molecules instantly, however, depending on the wavelength and power density values, it can cause disruption to biological materials or human cells when exposed to it (Ng, 2003).

As a result, the effects of non-ionising radiation sources such as the ultrasound and laser have extensively been explored in various fields.

2.6.2.1 Ultrasound irradiation pretreatment

Ultrasound refers to longitudinal sound waves with a frequency more than 16 kHz that is emitted from the sound spectrum. The ultrasound frequency lies in the upper limit of the sound that is audible to the human ear, referred to as the sonic waves (20 Hz to 20 kHz). Based on its frequency, ultrasound can be divided into three categories, power or high-intensity ultrasound (16 - 100 kHz), high-frequency ultrasound (100 kHz-1 MHz) and diagnostic ultrasound (1-10 MHz) (Ma *et al.*, 2012; Martini, 2013; Loow *et al.*, 2016). The high-intensity ultrasound irradiation is widely applied in Sonochemistry; hence the application of ultrasound as pretreatment of materials is commonly referred to as sonication. The latter two categories are used for clinical and medical ultrasonography purposes (Kwiatkowska *et al.*, 2011; Ogutu *et al.*, 2015)

High-intensity ultrasound radiation is a process that has physical and chemical effects on the structure of cellulose. The driving force behind ultrasound irradiation is a process called acoustic cavitation. Acoustic cavitation is described as a process in which bubbles form, grow and implode in a liquid as a result of increased negative pressure from the applied sound energy (Suslick & Price, 1999; Karimi *et al.*, 2014). Cavitation refers to the formation, expansion, and collapse of microscopic gas bubbles when the suspended molecules absorb ultrasound energy. The volatile implosion of cavitation bubbles in solution generates a flow of explosive shock waves which create high pressure and temperature conditions in the system. Interaction of these rough shock waves with the polymer substrate leads to the formation of cavities; they induce disaggregation and breakdown of the biomass structure (Figure 2.11) (Suslick & Price, 1999; Wang & Cheng, 2009; Frone *et al.*, 2011). Some of the major factors that play an influential role in ultrasonication include frequency to transfer energy from the probe into the fluid; polymer concentration; the intensity of the sound waves; treatment time, and the system temperature (Mazzoccoli, 2010; Ofori-Boateng & Lee, 2014).

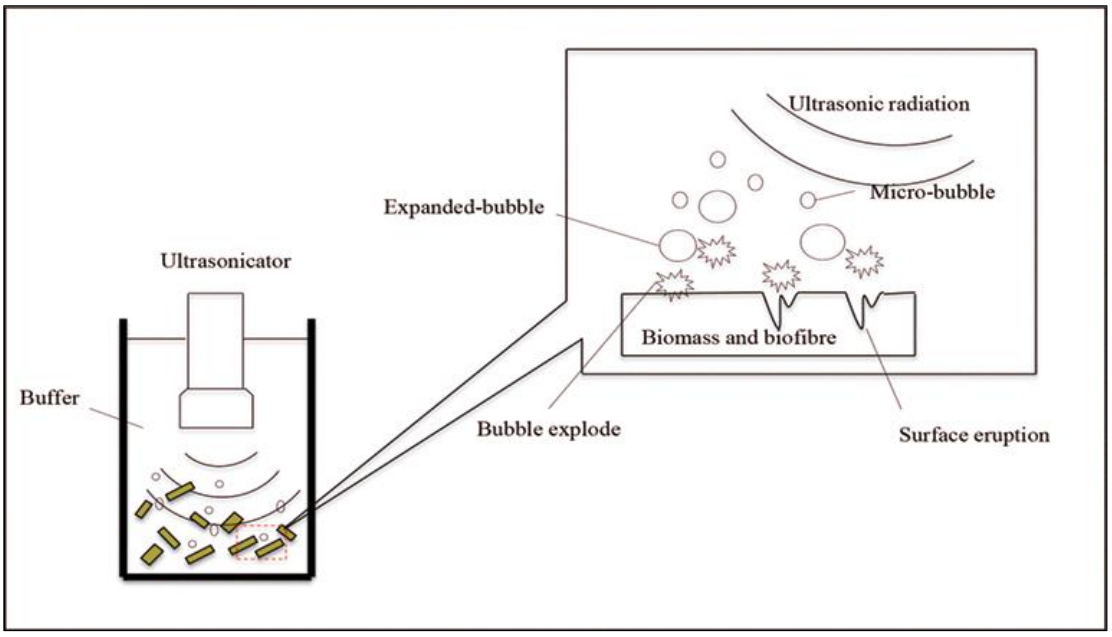

Figure 2.11: Mechanism of ultrasound irradiation of lignocellulosic biomass, adapted from (Kassim *et al.*, 2016).

Application of high-intensity ultrasound irradiation of a frequency range 20 kHz to 1 MHz for pretreatment of lignocellulosic biomass has widely been studied. It has shown that it has the potential to modify and disrupt the molecular structure of cellulose as pretreatment to downstream processing steps (Wang & Cheng, 2009; Cheng *et al.*, 2009; Rehman *et al.*, 2013). Various scholars have also observed that the interaction of cavitation bubbles and shock waves with the surface fibres results in different morphological and compositional modifications (Xing *et al.*, 2010). Moreover, this pretreatment technique has been documented for many years as the leading cause of cellulose depolymerization (Weissler, 1950; Garcia-Lopera *et al.*, 2005; Wong *et al.*, 2012).

In a study to increase the reactivity and accessibility of cellulose with sodium periodate, Aimin *et al.*, (2005) subjected cellulose fibres to ultrasound irradiation for different treatment times. Structural characterization results showed disruption of the primary cell wall layer, but the treatment did not have much of an effect on the crystallinity index (CrI) of the polymer. An increase in water retention values expressed an increase in accessible reaction sites and porosity. Structural observations made in this study are in agreement with what was observed by Oubani *et al.*, (2006) that ultrasonication caused

fibrillation of the cellulose fibre and increased surface area. Moreover, it was also noted that the degree of polymerization was reduced. However, contrasting observations were made on the crystallinity of the ultrasonicated samples; CrI decreased with increasing irradiation time. Sumari and co-workers reported similar results; they observed that with increasing pretreatment time, there was a reduction in particle size, crystallinity and sample crystallite sizes. The reaction temperature was varied between 40° and 60°C, but the results obtained did not show significant differences, implying that temperature changes did not have much influence in this experiment (Sumari *et al.*, 2013).

On the other hand, ultrasound irradiation has recently become popular in the nanotechnology field for isolation of cellulose fibrils with high crystallinity that is used as reinforcements for application in polymer nanocomposites (Cheng *et al.*, 2009; Wang & Cheng, 2009). Nanocomposites such as poly (vinyl alcohol) (PVA)/cellulose with high mechanical strength and excellent thermal properties is an example of such materials produced through ultrasound treatment (Frone *et al.*, 2011).

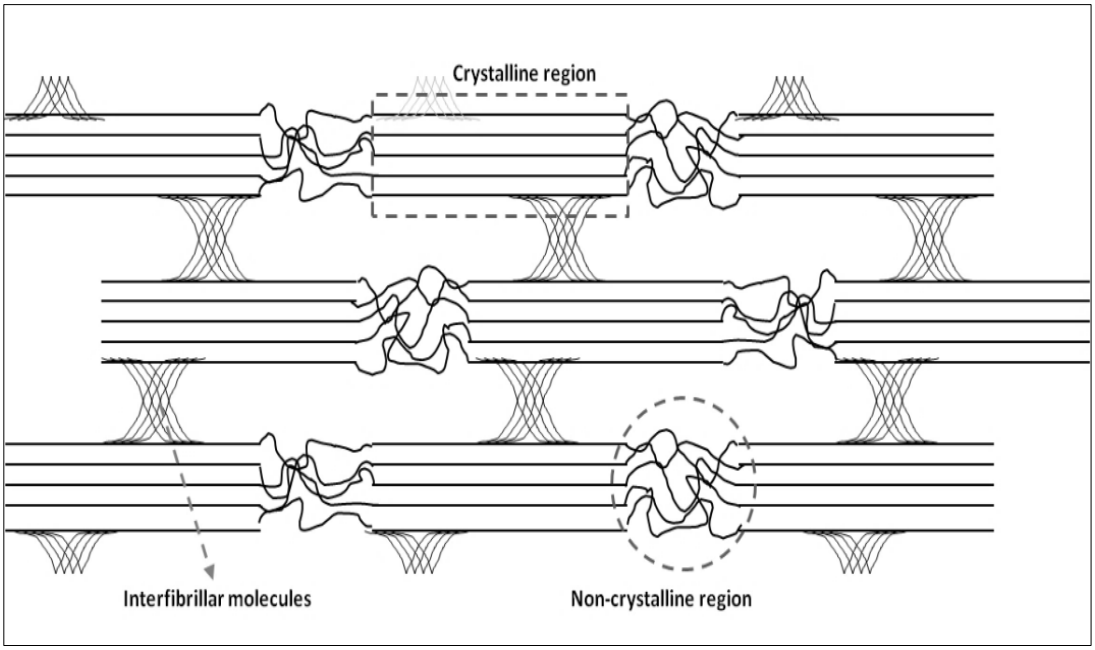

Figure 2.12: A schematic diagram of amorphous (accessible) and crystalline (inaccessible) region of cellulose, adapted from (Börjesson & Westman, 2015).

There is conflicting evidence when it comes to the degree of cellulose crystallinity and how it is affected by ultrasound irradiation. A proposed mechanism of ultrasound

pretreatment on cellulose is that the process attacks the easily accessible amorphous regions, thus leaving the highly ordered crystalline regions exposed (Figure 2.12). Moreover, ultrasound irradiated cellulose chains are prone to break at the centre point of the fibre; this suggests that degree of polymerization of the polymer is also an important factor that contributes to the efficiency of this technique. It has also been observed that ultrasonication is effective on long polymer chain than on the short and rigid ones. The commonly observed increase in crystallinity index after pretreatment of lignocellulosic biomass may be due to exposure of the crystalline region after ultrasonication (Mazzoccoli, 2010; Li *et al.*, 2015; SriBala *et al.*, 2016).

Interaction of lignocellulosic biomass with ultrasound irradiation is an interesting technique that can be used to achieve diverse objectives such as reduction of polymer molecular weight, thus controlling viscosity. Moreover, exposure of the biomass to Ultrasound irradiation can reduce particle sizes, cause surface erosion, disrupt the crystalline cellulose, isolate and extract valuable materials from biomass at reduced chemical compounds, adapted from (Mazzoccoli, 2010; Luo *et al.*, 2014).

Ultrasound irradiation demonstrates that it is an efficient and multipurpose technique that can be used in combination with biomass processing methods such as delignification, hydrolysis, and dissolution for process optimization. Over the years, high-intensity ultrasound irradiation has found use in wastewater treatment plants, biomass and bio-fibre for the production of biofuels (Harmsen *et al.*, 2010; Ma *et al.*, 2012; Luo *et al.*, 2014; Loow *et al.*, 2016). Ultrasonication of lignocellulosic biomass before hydrolysis for bioethanol production has shown that it can increase the rate of saccharification. Furthermore, enzyme hydrolysis has also demonstrated improved sugar recovery and yield after when ultrasound irradiation and NaOH were used together as pretreatment for lignocellulosic biomass. A combination of these two pretreatment techniques has shown that it can successfully break the intermolecular hydrogen bonds within the lignocellulosic biomass (Taherzadeh & Karimi, 2008; Kang *et al.*, 2013; Gabhane *et al.*, 2014).

There is extensive literature on ultrasound pretreatment usage in combination with chemical pretreatments for enzymatic hydrolysis for conversion of cellulose biomass to

bioethanol and other bio-based products (Taherzadeh & Karimi, 2008; Kumar *et al.*, 2009; Harmsen *et al.*, 2010).

2.6.2.2 Laser irradiation pretreatment

The term "LASER" is an acronym for "light amplification by stimulated emission of radiation". Lasers produce optical radiation from the mid-ultraviolet (UV) region, through to the visible region, and infrared region of the electromagnetic spectrum (Sliney, 2001; Dutta Majumdar & Manna, 2011). Laser technology comprises of three main elements: the amplifying medium, the means for exciting the medium to its amplifying state and an optical resonator. The amplifying medium determines the laser wavelength and the type of excitation that is required. Based on the amplifying medium, lasers can be categorized into four major classes, namely: gas lasers (e.g. carbon dioxide, helium-neon, excimer lasers); dye lasers; solid-state lasers (e.g. ruby, Nd:YAG lasers); and semiconductor lasers (Chow *et al.*, 2011; Singh *et al.*, 2012). Lasers are primarily operated in two modes, the continuous wave (CW) or the pulsed (modulated) mode (El-Dessouky, 2014).

The basis of laser theory was first presented by Albert Einstein in early 1917 using Planck's law of radiation. It was only in 1960 that Theodore Maiman built the first laser after years of extensive research by several scholars (Dutta Majumdar & Manna, 2011; Singh *et al.*, 2012). In his discovery, Maiman used a crystalline ruby rod to generate pulsed red laser radiation at a wavelength of 694 nm. This invention received positive reception and predictions that this new technology might change the global view of optical science (Baldacchini *et al.*, 2008; Singh *et al.*, 2012). Since then, research on the modification, operation and application of lasers gradually increased over the years. Advantages of using lasers are that they are a source of optical frequency radiation with high power and intensity that can be easily controlled to acquire desired results (Bass, 1983; Chow *et al.*, 2010). In summary, lasers are a source of light which is (1) nearly monochromatic; (2) nearly unidirectional; (3) has a spatial distribution imposed by the optical resonator; and (4) can be very energetic. It is because of these attractive properties that lasers are considered suitable for application in various industries (Bass, 1983; Sliney, 2001).

For many years, lasers have been used in sectors such as medicine, dentistry, cosmetics, steel cutting and manufacturing, cultural heritage, science and technology research, polymers and textile industries. In the medical field, they are used for diagnostics, cosmetic surgery, and for sterilization of equipment amongst other purposes (Boulnois, 1986; Pick & Colvard, 1993; Sasaki *et al.*, 2002). For historians and cultural heritage conservers, laser irradiation can be used as a safe alternative method for cleaning and to preserve old art materials and paper documents in archives (Rudolph *et al.*, 2004; Baldacchini *et al.*, 2008). In the polymer and textile industries, lasers have widely been used for modification of polymers, and research in this field continues to grow progressively (Said-Galiev & Nikitin, 1993; Kreutz *et al.*, 1995; Horn *et al.*, 1999; Kubovsky & Kacik, 2009).

Application of this technology in the polymer and textile industry has mainly been to change and enhance the structural properties of both natural and synthetic polymeric materials (Said-Galiev & Nikitin, 1993; Balakhnina *et al.*, 2013). The effect of laser pretreatment on various properties of textiles and fabric materials such as cotton, silk, polyester, nylon, linen has been studied on a broad scale (Kolar *et al.*, 2000; Chow *et al.*, 2010; Montazer *et al.*, 2012; Shahidi & Wiener, 2016). Treatment of these materials is mostly carried out using lasers that have wavelengths in the UV- and IR-spectral regions such as excimer, CO_2 and Nd:YAG lasers (Kolar *et al.*, 2000; Haller *et al.*, 2001; Kolar *et al.*, 2002; Kan, 2014; Montazer *et al.*, 2014). The mechanism of laser radiation processing involves deposition of energy onto the surface of a sample by excitation or de-excitation of electrons within a short period of time (Dutta Majumdar & Manna, 2011).

Chow *et al*. (2011) used different characterization techniques to study the effect of CO_2 laser pretreatment on cotton fabrics. Scanning Electron Microscopy (SEM) analysis showed that the pretreatment caused pores and cracks on the surface of the material, and Fourier Transform Infrared (FTIR) spectroscopic results displayed that the treatment modified the chemical structure of cellulose, and caused oxidation of the –OH groups to produce carbonyl/carboxyl groups. CO_2 laser treatment has shown it is an efficient alternative method that can be used to modify the surface and colour properties of fabrics like denim compared to the conventional environmentally harsh chemical methods (Kan *et al.*, 2010; Kan, 2014). In their study, Kan *et al*. (2010) used laser treatment to engrave

and modify the visual effect of the surface of the denim fabric instead of using the conventional dyeing methods. Furthermore, the treatment altered properties of the material such as surface morphology, crystallite size, bending rigidity, and wettability of fabric. In a similar study where natural polymer, raw, and unbleached cotton fabrics were pretreated with a CO_2 laser, improved morphological and reaction properties were observed. Irradiation of cotton fabrics resulted in yellowing of the sample surface, and this was suggested to be due to thermal effect and surface oxidation of the material, in which aldehyde groups form. This reaction is similar to the caramelization reaction usually observed in reducing sugars that have an aldehyde group (Montazer *et al.*, 2014).

To a great extent, the effect of laser treatment on polymers is influenced by the laser power. Montazer *et al.* (2012) observed that with increasing laser power, crystalline sizes of polyester decreased, the polymer melted, and its surface porosity was altered. Other scholars argue that the effect of laser radiation on polymer properties like crystallinity is relatively dependent on three main factors: radiation energy delivered per unit area of the polymer; laser power; as well as the energy absorbed by the polymer substrate at a given fluence (Said-Galiev & Nikitin, 1993; Hsu *et al.*, 2012). In their study, Hsu and co-workers reported that laser treatment of poly (L-lactic acid) (PLLA) caused a reduction of polymer crystallinity as a function of radiation fluence. In another study, a decrease in PLLA crystallinity was also reported when this biodegradable polymer was irradiated with Nd:YAG laser at varying fluence (Bhatla & Yao, 2008).

Laser pretreatment technique is used in various research fields as it is a procedure that is usually carried out in combination with downstream hydrolysis processes for the production of bio-based products. For example, Tian *et al*. (2012) pretreated corn stover chips with CO_2 laser radiation to break down the tight lignin bound structures of cellulose and hemicelluloses to expose them for enzymatic hydrolysis. SEM images obtained after the pretreatment demonstrated that the surface structure of corn stover samples had been disrupted. The FTIR results confirmed the structural disruption by showing an increase in the peak intensity of lignin due to the biomass degradation. The pretreatment was able to remove lignin and some of the hemicellulose, thus improving the rate of saccharification and hydrolysis of the test samples significantly.

The main advantage of using laser radiation pretreatment method over chemical methods is that chemical pretreatments cause environmental pollution, and require specialised equipment and reactors to carry out. From various literature studies, it can be concluded that lasers have an effect on the properties of polymeric materials and this can produce improvement in their reactivity.

2.7 Structural characterization of cellulose

The structure of cellulose has a great influence on how it behaves chemically. Therefore, a clear understanding of structural characteristics of this polymer is of utmost importance for improving current methods used for cellulose processing and derivatization (Schult *et al.*, 2002).

2.7.1 Size Exclusion Chromatography Multi-Angle Light Scattering (SEC-MALS)

Size-exclusion chromatography (SEC-MALS) is a useful technique for monitoring the molecular weight, molecular weight distribution (MWD) and the degree of polymerization (DP) of polymers during pretreatment and processing (Schult *et al.*, 2002; Hallac & Ragauskas, 2011; Sun & Sun, 2015). Moreover, it gives an indication of the quality of the biopolymer products that result as well as their polymerization properties (Sun & Sun, 2015). The SEC-MALS is extensively used in the paper and pulp industry to determine the DP of cellulose because it is one of the molecular features that influence the accessibility and reactivity of this biopolymer to solvents. The DP of cellulose plays a significant role in the properties and quality of the derived end products (Puri, 1984; Hallac & Ragauskas, 2011).

SEC-MALS, formerly known as gel permeation chromatography (GPC) was first introduced in the 1950s as an ideal method for determining the MWD of synthetic and natural polymers that have been dissolved in suitable solvents (Gaborieau & Castignolles, 2011). SEC-MALS is a separation technique; it separates molecules in an aqueous solution based on their molecular sizes; this is also referred to as separation by hydrodynamic volume (Trathnigg, 2000; Schult *et al.*, 2002). The molecules pass through a porous material with a broad distribution of pore sizes. When the sample is injected into the column, molecules can either diffuse into the pores of the packing material or exit the

column. Undissolved molecules and those that are too bulky to enter into the packed column pores are the first ones to be eluted from the column. Smaller polymer molecules, on the other hand, are eluted last since they are retained longer in the column because they can permeate into the column system (Silva, 1995; Trathnigg, 2000).

SEC-MALS is a non-adsorptive and non-destructive analytical method, it can provide detailed information about the polymer such as molecular weight average molar mass (Mw), molecular weight distribution (MWD), polydispersity index (PDI) and the intrinsic viscosity ([η]) (Silva, 1995; Garcia-Lopera *et al.*, 2005). The intrinsic viscosity is a function that is used to measure the molecular mass of the polymer; it is an expression of the polymer chain length or degree of polymerization (DP). The DP denotes the number of the repeating units of the polymer chain, and it can be calculated by dividing the molecular mass of cellulose by that of a single cellulose repeating unit which is 162 g/mol. The polydispersity expresses the ratio of Mw and Mn; where Mw and Mn represent the weight average molar mass and number average molar mass, respectively. PDI gives an indication of the broadness of the MWD of a polymer (Garcia-Lopera *et al.*, 2005; Sun & Sun, 2015; Oberlerchner *et al.*, 2015). Table 2.2 presents examples of typical Mw and PDI values of cellulose pulps of softwood and hardwood species that were pulped and bleached by different bleaching sequences.

Table 2.2: Typical ranges of Mw and PDI for different cellulose pulps, adapted from (Silva, 1995)

Characteristic of cellulose pulps	**Ave. Mw (g/mol)**	**PDI (Mw/Mn)**
Softwood, bleached (C-E-H), Kraft pulp	645745	3.773
Hardwood, semi-bleached, Kraft pulp	640995	4.912
Prehydrolyzed softwood Kraft pulp	419923	3.031
Softwood, bleached (D-O-E-D-P), Sulfite/Mg base pulp	465946	2.777
Softwood, bleached (Dc-Eo-P-D)	433517	3.391
Softwood Kraft pulp (91% α cellulose)	559243	5.378
Softwood Sulfite pulp (91% α cellulose)	379532	3.340
Commercial cellulose	211987	3.635
Cotton linters	360535	1.678
Rayon fibre	219128	1.784

2.7.2 X-Ray Diffraction (XRD)

Cellulose is known for its biphasic structure; it is comprised of crystalline and non-crystalline (amorphous) regions (Oubani *et al.*, 2006). Since its discovery in the 1800s, the structure of cellulose, particularly its crystallinity, has been extensively studied. This is because crystallinity plays a significant role in the mechanical, physical and chemical properties of this polymer (French & Cintrón, 2013; Ju *et al.*, 2015). Moreover, it is important to understand the crystallinity of cellulose because it is one of the main factors that affect the behaviour of cellulose during pretreatment and reactivity (Nelson & Oliver, 1971; Kumar *et al.*, 2009).

X-ray diffraction is one of most common techniques used for measuring the crystallinity of cellulose and other crystallographic features such as crystalline phase, crystallite sizes and the *d*-spacing between monomer chains. The degree of cellulose crystallinity is measurable based on the relative amount of the crystalline region within the total structure of cellulose, and it is referred to as crystallinity index (CrI) (Segal *et al.*, 1959; Park *et al.*, 2010). This observation is parallel to what has been reported that XRD crystallinity

measurements take into account the crystalline regions of cellulose more than the amorphous region fractions (Terinte *et al.*, 2011).

XRD is a versatile, non-destructive analytical method; its functioning is based on the interaction of monochromatic X-rays with the crystalline sample. X-rays are generated in the cathode ray tube and then filtered to produce monochromatic radiation which goes through a collimator to increase their intensity and finally directed onto the sample. Bombardment of the target sample with the incident X-ray beams leads to interaction of the crystalline atoms with the incident beam thus causing the X-rays to scatter from the sample in different directions. This reflection of the incident X-rays from the surface of the crystal lattice planes is referred to as X-ray diffraction. The diffracted beams are then detected, processed and converted into count rates and recorded provided the conditions of Bragg's law are satisfied. Figure 2.13 presents the Bragg's law reflection where: λ is the wavelength of X-rays, *d* is the spacing between the planes in the atomic lattice, and θ is the angle between the incident rays and the surface of the crystal lattice planes (Bragg, 1913; Henry *et al.*, 2012).

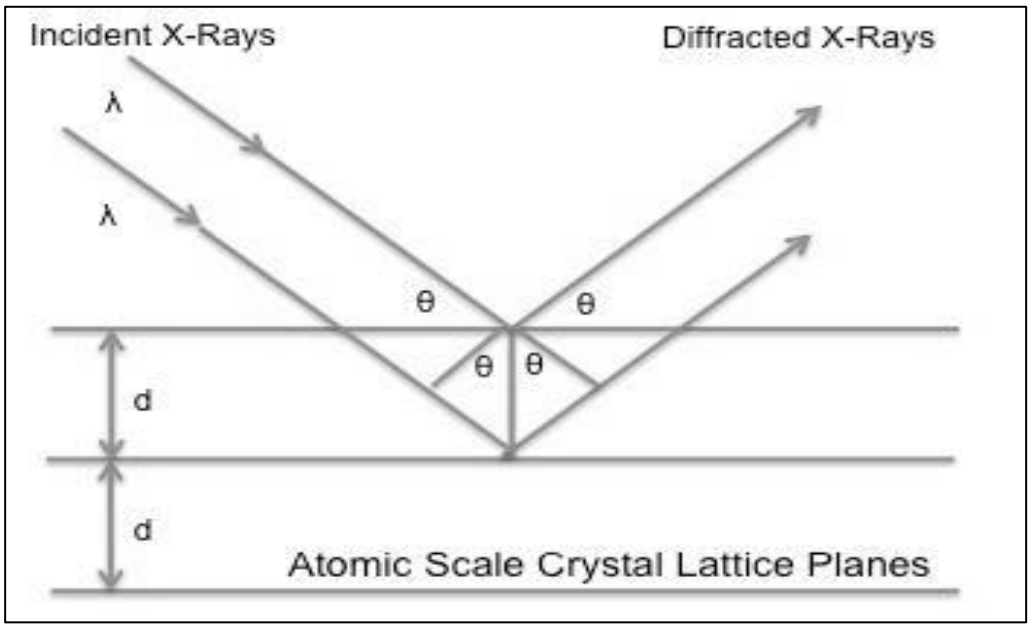

Figure 2.13: A schematic representation of the Bragg's Law reflection, adapted from (Bragg, 1913).

Park and co-workers have broadly expounded on the various methods that have been used to estimate the CrI values using NMR, FTIR, and XRD. They also outlined and compared

common methods that are used to compute CrI and how the value of CrI varies depending on the method of choice (Park *et al.*, 2010). Some of the well known XRD based methods include the peak height method that was developed by Segal and co-workers for estimation of CrI of natural cellulose, the peak deconvolution method and the amorphous subtraction method (Segal *et al.*, 1959; Park *et al.*, 2010). Various studies have successfully investigated the crystalline nature and computed the CrI status of cellulose and other lignocellulosic materials with this technique. In a study by Fang and co-workers, XRD analysis was conducted to study the effect of surfactant-assisted microwave pretreatment on the structure of peanut shells biomass. Research findings showed that the pretreatment increased the crystallinity degree of the pretreated samples compared to the untreated ones by 7.96% (Fang *et al.*, 2014). Similarly, Xing's research group used the XRD to evaluate the effect of ultrasound pretreatment on the crystalline structure of chemimechanical pulp. A slight decrease in crystallinity from 52% to about 49% was observed after ultrasonic pretreatment of unbleached pulp (Xing *et al.*, 2010). The crystallinity of cellulose can range 30% to over 90% depending on its original source and the acquisition process (Park *et al.*, 2010; Terinte *et al.*, 2011).

2.7.3 Cross-Polarization Magic Angle Spinning ^{13}C-NMR (CP/MAS ^{13}C-NMR)

CP/MAS ^{13}C-NMR also referred to as "solid state NMR" spectroscopy is a useful non-destructive analytical technique that has widely been used to study the ultrastructure and interactions of cellulose in its natural and processed form (Larsson *et al.*, 1997). Solid state NMR is sensitive to the magnetic non-equivalence in an environment of chemically equivalent nuclei. Over the years it has proved to be a valuable technique for determining the degree of cellulose crystallinity as well as its crystallite sizes (Evans *et al.*, 1995; Larsson *et al.*, 1997; Park *et al.*, 2010). Hence this technique has been applied in the characterization of cellulose structural and chemical properties for a long time.

However, this has not always been the case as in the past; this technique could not be used for structural determination due to line broadening caused by chemical shift anisotropy and static dipolar interactions between ^{13}C and ^{1}H. To overcome this problem, solid state NMR is coupled with high-resolution cross-polarization magic angle spinning (CP/MAS). The CP/MAS comprises of three techniques, the first being cross polarization (CP) which enhances the intensity of the ^{13}C signals. The second technique is the high-power proton decoupling which removes the strong dipolar interactions between ^{13}C and

neighbouring protons. Finally, the third method is the magic angle spinning (MAS) which eliminates chemical anisotropy by setting the sample to spin rapidly at an angle of 54.7° with respect to the external magnetic field (Atalla & Vanderhart, 1984; Foston *et al.*, 2011; Chunilall *et al.*, 2013). A combination of CP/MAS, high-power proton decoupling, and ^{13}C-NMR is a useful technique that produces high-resolution spectra with high ^{13}C nuclei sensitivity.

In the early 1980s, Atalla and Vanderhart, tested out their model using this method and they revealed that natural cellulose exists as a composite of two different crystalline forms, referred to as cellulose Iα and cellulose Iβ (Atalla *et al.*, 1980; Atalla & Vanderhart, 1984). The proportion of each polymorph is dependent on cellulose origin, for example, cellulose Iα is predominantly found in bacterial and algal cellulose, whereas cellulose Iβ is found in higher plants and tunicate cellulose (Atalla & Vanderhart, 1984; Larsson *et al.*, 1997).

Typical CP/MAS ^{13}C-NMR spectra of native cellulose consist of six anhydroglucose unit signals that are divided into fine structure clusters due to the supra-molecular structure of cellulose I fibril. Figure 2.14 presents a standard CP/MAS ^{13}C-NMR spectrum of cellulose I displaying the polymer's wide chemical shift ranging from 60 to 92 ppm (Larsson *et al.*, 1997; Wickholm *et al.*, 1998).

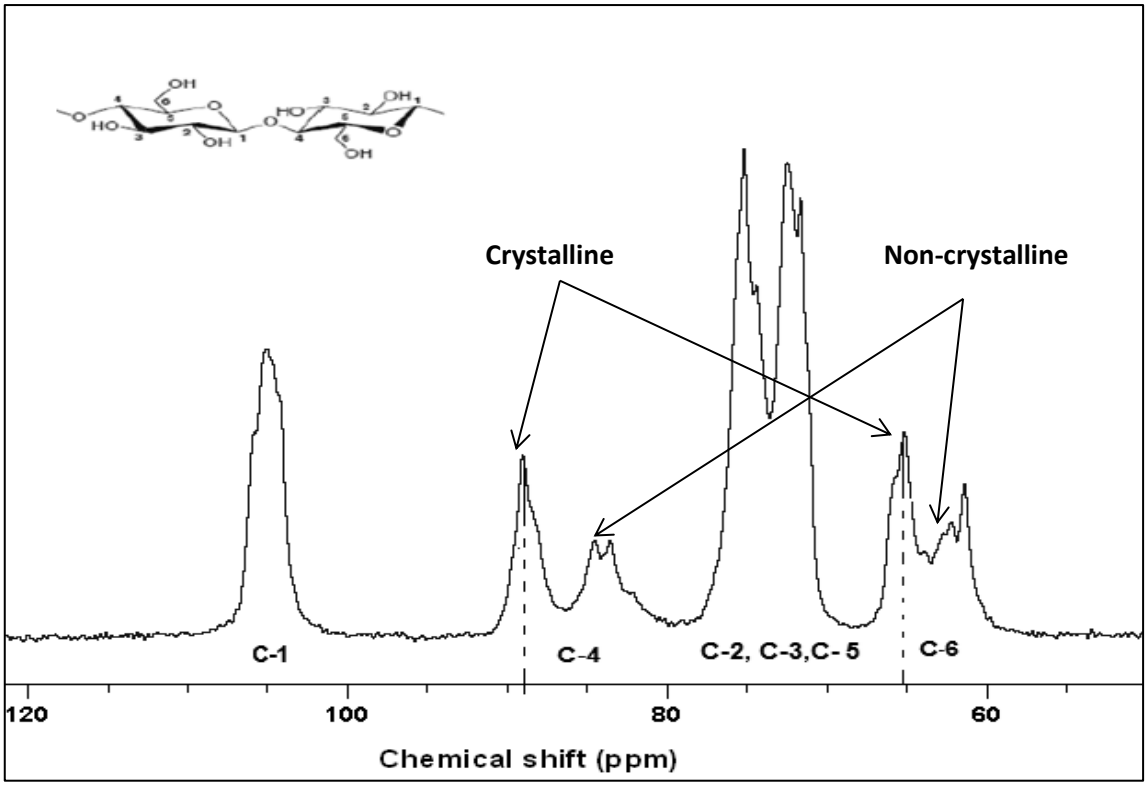

Figure 2.14: The overall CP/MAS ^{13}C-NMR spectrum of cellulose I showing the crystalline and non-crystalline regions and carbon atoms assignments on the AGU, adapted from (Larsson *et al.*, 1999).

From the lower to upper end of the spectrum, the region between 60 and 70 ppm is assigned to the C-6 carbon atom. Following the C-6 assignment is a resonance cluster between 70 and 81 ppm ascribed to the ring carbons C-2, C-3, and C-5. The region between 81 and 93 ppm represents the C-4 region, and the last carbon atom C1 is associated with the area between 102 and 108 ppm (Atalla & Vanderhart, 1984; Atalla & VanderHart, 1999). The ^{13}C-NMR spectrum of cellulose I is very informative; however, accessibility to this information is masked by the severe overlap between the spectral signals. To attain quantitative information on the supra-molecular structure of cellulose, the ^{13}C-NMR analysis is carried out in combination with spectral fitting (Larsson *et al.*, 1999; Chunilall *et al.*, 2012).

The most useful information on the ^{13}C-NMR spectra of native cellulose is found in the C4 region with a distribution from 80 to 92 ppm (Figure 2.15) (Wickholm *et al.*, 1998; Hult *et al.*, 2000). This region consists of sharp peaks in the range 86 to 92 ppm which corresponds to the crystalline cellulose domain, relatively broad peaks from 80 to 86 ppm

correspond to the non-crystalline sphere (Larsson *et al.*, 1999; Hult *et al.*, 2000). In their study, Larsson and his colleagues were able to quantify these regions by performing spectral fitting on the C-4 area of the ^{13}C-NMR cellulose I spectra. Their model revealed all the C-4 region crystalline domains as cellulose Iα, Iβ, I(α+β), para-crystalline cellulose, cellulose at accessible fibril surface (AFS) and cellulose at inaccessible fibril surfaces (IFS) (Larsson *et al.*, 1999). This model was in correspondence with what has previously been reported by Atalla and Vanderhart (Atalla & Vanderhart, 1984).

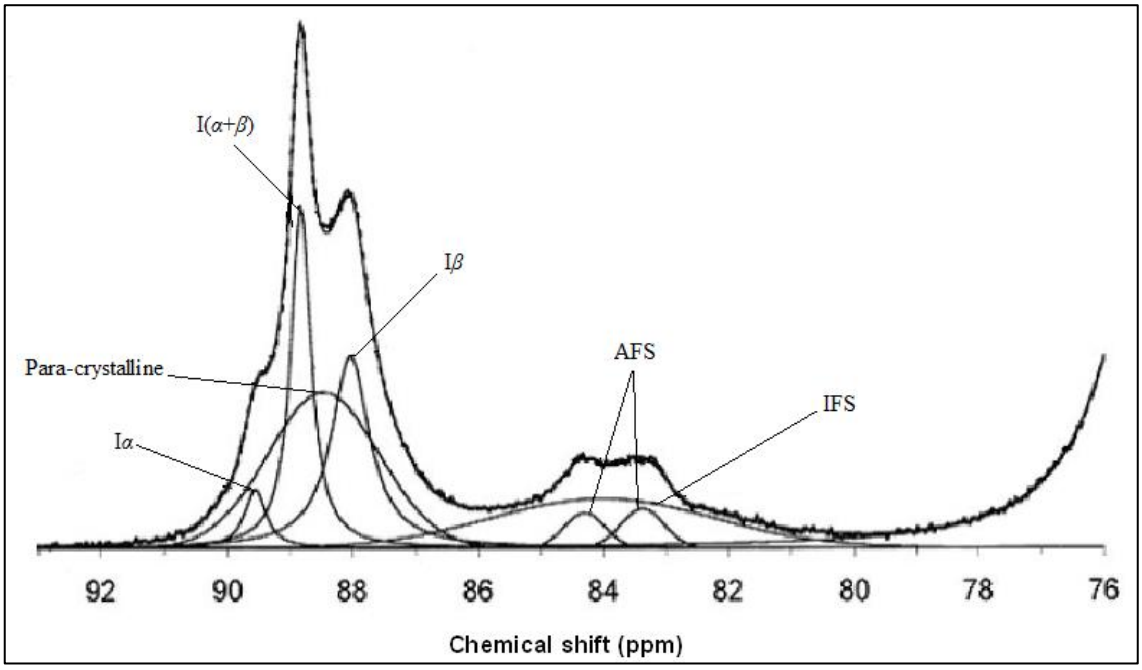

Figure 2.15: The C-4 region spectral fitting of quantitative cellulose I CP/MAS ^{13}C-NMR spectrum with the respective signal assignments, adapted from (Larsson *et al.*, 1999).

2.7.4 Atomic Force Microscopy (AFM)

Removal of hemicelluloses and lignin from cellulose during chemical processing has widely been reported as the leading cause of cellulose microfibril aggregation. This phenomenon has been documented as one of the factors that reduce the reactivity of cellulose and ultimately the quality of the cellulose derivatives in downstream processes (Pönni *et al.*, 2012; Chunilall *et al.*, 2012). Atomic force microscopy (AFM) is the most common subdivision of the scanning probe microscopy (SPM) family that is widely used to study the surface structure and topography of various materials including natural and synthetic polymers (Giessibl, 2003; Starostina & West, 2006). The AFM was first developed and commercialised by Binnig and his colleagues in 1986 at IBM Zurich

research laboratories in Switzerland (Giessibl, 2003; Safanama *et al.*, 2012). The invention of the AFM was achieved after extensive studies on the Scanning Tunnelling Microscope (STM) and realization of its limitations that it cannot analyse nonconductive materials (Binnig *et al.*, 1986; Copolovici & Sîrghie, 2013).

The AFM is a relatively novel analytical technique that is useful for visualising the surface of natural fibres as well as their ultrastructural properties at a high-resolution. It can also be used to study the molecular composition and mechanical properties of a broad range of polymers (Safanama *et al.*, 2012). The AFM provides three-dimensional (3D) image profiles of the topographic structure of molecules at the nanoscale. Hence, it finds application in a wide variety of disciplines of research such as surface science, material engineering, biochemistry, and biology.

Using the AFM in conjunction with image analysis, various research groups have studied the changes that occur in the transverse fibre wall of cellulose during mechanical and chemical treatment. They observed the degradation of lignin and hemicellulose matrix during chemical pulping leads to coalescence and enlargement of the cellulose microfibrils (Fahlén & Salmén, 2005; Chunilall *et al.*, 2006). Fahlen and Salmen combined the AFM with image analysis and computed the pore sizes and the cellulose microfibril aggregates after the removal of the matrix (Fahlén & Salmén, 2005). To confirm the results they obtained from the solid state NMR, Chunilall and co-workers also used this technique to measure the average diameter or the lateral fibril aggregate dimensions (LFAD) of the cellulose fibril aggregates within the S2 layer of the fibre wall (Chunilall, 2009; Chunilall *et al.*, 2013). Figure 2.16 illustrates a schematic diagram of how microfibrils are agglomerated to form cellulose fibril aggregates.

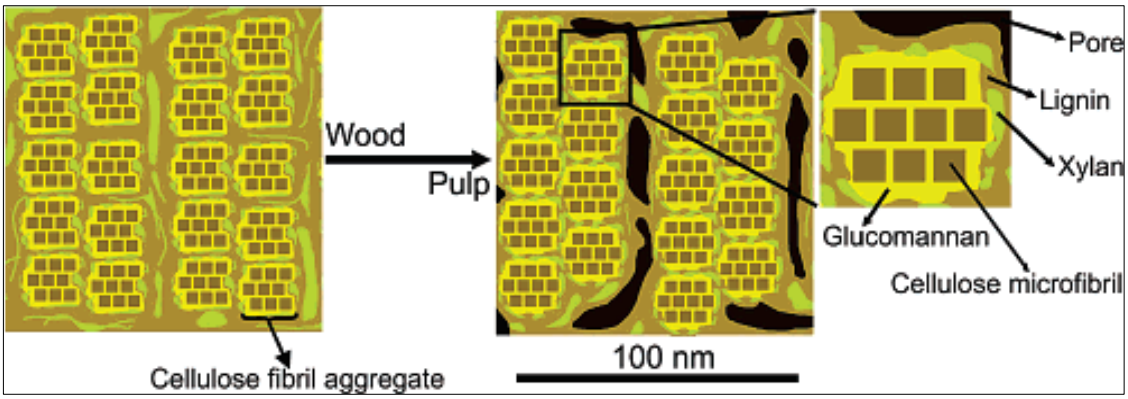

Figure 2.16: A schematic presentation of the transverse section of the S2 cell wall layer displaying the cellulose microfibrils and cellulose fibril aggregates, adapted from (Fahlén & Salmén, 2005).

The benefits of using the AFM lie in the fact that it is non-destructive and samples can be analysed in their native state. Moreover, this technique is particularly useful for characterization of nonconductive materials and biological samples because of its ability to analyse samples in a liquid medium. Some of the characterization properties that can be obtained from AFM analysis include particle surface, morphology, shape, and size (Starostina & West, 2006; Chang & Andersson, 2011).

The fundamental principle for AFM functionality is the measurement of the attractive and repulsive forces that are created between the sharp tip and the surface of the sample when they are close to each other (Figure 2.17) (Safanama *et al.*, 2012). The tip is a sharp probe that is fixed at the free end of a small flexible spring-like structure called the cantilever. The cantilever is usually made out of silicon or silicon nitride, and its backside is commonly coated with a thin layer of gold or metallic coating to enhance the reflectivity of the laser beam during scanning (Safanama *et al.*, 2012).

During analysis, the tip is gently lowered onto the surface of the sample on a glass slide mounted on a piezoelectric scanner. The piezoelectric scanner provides sub-Angstrom motions of the samples, and the tip gently scans across the sample. As the tip moves over the sample surface, a change in topography is detected, and this causes the cantilever to deflect towards and away from the surface. This vertical deflection of the cantilever is monitored by the laser beam which is focused on the back of the flexible cantilever. The incident laser beam is reflected off the back side of the cantilever, and its displacement is

detected and recorded on the position sensitive photodiode detector (Barattin & Voyer, 2008; Chunilall, 2009).

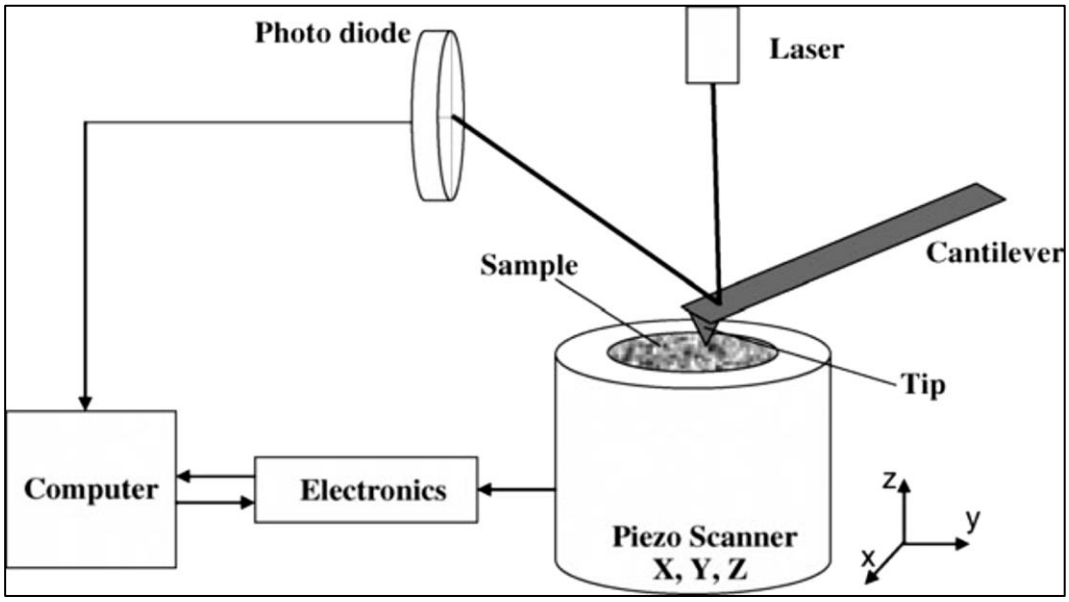

Figure 2.17: A schematic diagram of an AFM , adapted from (Barattin & Voyer, 2008).

The AFM can be operated in two primary imaging modes to obtain topographic images of the sample surface, the contact and Tapping mode. The difference between these AFM imaging modes is mainly on the interaction and movement of the tip on the sample surface. In the contact mode, the tip touches the sample surface, and they move together in a lateral x, *y*-plane. The force created between the tip and the sample surface is kept constant by the feedback loop while the piezoelectric scanner adjusts the height of the tip relative to the sample surface. In the Tapping mode, the tip does not have direct contact with the sample surface (Chunilall, 2009; Fahlén & Salmén, 2005). The cantilever oscillates below its normal resonance frequency so that direct interaction between the tip and the sample surface is minimal. This latter mode is the one preferred when analysing sensitive materials like biological samples because the shear force between the tip and the sample surface can rupture samples with a soft surface. The AFM features make it a useful technique for characterization of the fibre wall cross-section (Fahlén & Salmén, 2005).

2.7.5 Scanning Electron Microscopy (SEM)

Electron microscopy was first introduced in the mid-20th century. A scanning electron microscope is a powerful tool for structural analysis of wood from morphological level to ultrastructural level. The images yield information about the topography, morphology (size and shape), composition and crystallographic information of the sample. The SEM is commonly used to complement the AFM. Unlike the conventional light microscopes that use light waves to create their images, the SEM works by scanning the surface of a sample with a high-energy beam of electrons emitted from an electron source which is under the influence of an electric current. Nonconductive samples like natural fibres are coated with a conducting metal layer before analysis to prevent the sample from charging when exposed to the electron beam.

The electron gun is focussed on the sample, and when a beam of electrons from the gun hits the surface of the specimen, the electrons interact with the atoms of the sample to produce signals in the form of secondary electrons. Backscattered electrons and diffracted backscattered electrons are then used to determine the crystal structures and orientations of minerals. The secondary electrons from the surface of the sample are then detected by the secondary electron detector, which amplifies them and converts them into an electric signal. The SEM forms a three-dimensional (3D) image from the number of electrons that are emitted from the sample. The SEM produces micrographs of the sample surface, revealing details about the shape, width, and length of the sample.

2.7.6 Compact Morphological fibre (MorFi) Analyser

Pretreatment of cellulosic biomass can result in various forms of structural, morphological and molecular modifications such as depolymerization, chain scission, fibrillation, and bond breakage (SriBala *et al.*, 2016; Loow *et al.*, 2016). These induced modifications can have an influence on the behaviour of cellulose during chemical processing and ultimately the properties and quality of the derived end products (Chevalier-Billosta *et al.*, 2007). Thus, understanding of the structural properties of this biopolymer is essential. The MorFi analyser is one of the common techniques for studying the morphological features of cellulose fibres during processing. Fibre morphology encompasses five parameters, length, width, coarseness, kink, and curl. Fibre length and width are the commonly presented features (Hirn & Bauer, 2006).

MorFi analysis is based on the image analysis of fibres in a suspension acquired by use of a high-resolution camera. The benefit to using this technique is that it has a quick turnaround time and it provides reliable morphological features or dimensions (Chevalier-Billosta *et al.*, 2007; Besbes *et al.*, 2011). As a result, this technique has widely been used in the pulp and paper industry for years to monitor the quality of fibres at different stages of lignocellulose processing (Hirn & Bauer, 2006). More recently it has also proved to be a useful characterization technique in the nanoscience and nanotechnology research field (Hirn & Bauer, 2006). In their waste valorization study, Chen and co-workers measured the fibre length and width distribution of cellulose and nanocellulose fibres extracted from agro-waste (Chen *et al.*, 2014). Various authors have reported on the efficiency of this technique for characterization and evaluation of the morphological properties of nanofibres and nanocomposites isolated from cellulose (Sarrazin *et al.*, 2009; Besbes *et al.*, 2011; Nechyporchuk, 2015). Thus, the MorFi analyser has shown that it is useful for monitoring modifications induced by various pretreatment methods.

CHAPTER 3 – MATERIALS AND METHODS

3 Introduction

Chapter three lists equipment and reagents that were used in this study. It also describes the experimental procedures that were followed to achieve the aim and objectives of this study. An outline of the ultrasound and laser radiation pretreatment techniques that were used for cellulose structural modification is given; this is followed by a description of the Fock reactivity and alkali dissolution methods. Finally, an overview of the characterization techniques used for structural analysis of cellulose is presented.

3.1 Materials and methods

This section lists and describes the materials and chemical reagents that were used in this study. Furthermore, this section discusses the method followed to manufacture the cellulose pulp that was used as a raw material in this study.

3.1.1 Dissolving wood pulp

Dissolving wood pulp (DWP) was prepared from *Eucalyptus dunnii* (*E.dunnii*) on a batch-scale at the CSIR - Biorefinery Industry Development Facility (BIDF), Durban. *E.dunnii* is one of the clones of the plantation hardwood *Eucalyptus* species grown in South Africa. It is primarily grown for the production of pulp, paper, and other solid wood products. A 92α grade pulp was prepared from wood chips by acid bisulphite pulping process followed by a hypochlorite 4-stage bleaching sequence. The pulp was made into hand-sheets using a 'Rapid Köthen' hand-sheet former according to the TAPPI Standard Test Methods (T 205 sp-02) for laboratory determination of physical properties of pulp. The handsheets were air-dried for five days in a dark conditioned room with a temperature fixed at 23° C. This method of drying pulp has been reported to cause negligible coalescence of microfibrils compared to oven drying (Chunilall *et al.*, 2013). The prepared handsheets were used as the raw material and source of cellulose samples.

3.1.2 Chemical reagents

The chemical reagents employed in the study were: sodium hydroxide (NaOH) pellets, acetic acid (AA), carbon disulphide (CS_2), sulphuric acid (H_2SO_4), potassium dichromate ($K_2Cr_2O_7$), potassium iodide (KI), sodium thiosulphate ($Na_2S_2O_3$), and the starch

indicator. They were all of analytical grade (AR) and were used as received from the suppliers (Merck SA (Pty) Ltd).

3.2 Methodology

This section outlines the methods and procedures that were followed to achieve objectives of this study. A detailed description of the steps followed during pretreatment of cellulose pulp with ultrasound and laser irradiation is given below.

3.2.1 Pretreatment: Ultrasound irradiation

A UP400S-Ultrasound processor, with a tip of a diameter of 20 mm, a working frequency of 24 kHz, and a maximum power of 400 W (Hielscher Ultrasounds, Teltow, Germany) was used to perform the ultrasound irradiation experiments. Three grams (3 g) of cellulose pulp was first torn into smaller pieces and soaked overnight in 1000 mL of deionized water. Ultrasound pretreatment or sonication of the pulp samples was carried out in an ice bath to avoid overheating of the experimental set-up. The samples were ultrasonicated for 10, 20, 30, 45 and 60 minutes (with 1-minute breaks after every 5 minutes of ultrasonication to avoid overheating the system), to evaluate the effect of pretreatment time. An average power in the range 35 – 77 W was noted during pretreatment of every sample using a power meter connected to the ultrasound processor. After ultrasonication, the samples were filtered using a vacuum pump and air dried in a temperature controlled room. After drying, structural characterization of the samples was performed, and the untreated cellulose pulp sample (UT-t=0) was used as a control.

3.2.2 Pretreatment: Laser irradiation

Irradiation pretreatment was carried out using two types of lasers, the Quanta-Ray Pro series Neodymium–doped yttrium garnet (Nd:YAG) and carbon dioxide (CO_2) lasers accessed at the CSIR-National Laser Centre (NLC) in Pretoria, South Africa. The approach taken in this study was first to conduct a series of preliminary experiments with different lasers of varying wavelength to identify the lasers which favourably interacted with the cellulose material, and modified its structure without scorching it. Furthermore, the laser screening tests were useful in selecting optimum processing parameters. CO_2 and Nd:YAG lasers were chosen based on the interaction of the laser beam and the cellulose material.

Figure 3.1 displays a schematic diagram of the experimental setup of laser irradiation pretreatment of DWP samples. The schematic diagram shows the path length and direction of the laser beam from the laser. The helium-neon (He/Ne) laser light was used as a safety measure to assist in locating the position of the colourless beam from the laser. The three mirrors were used for redirecting and channelling the path of the laser beam through the collimator which was used for adjusting the laser power directed towards the pulp sample mounted on the computer (PC) controlled XYZ stage. The XYZ stage was used as a mobile sample holder for all experiments, and the temperature of the room was maintained at 23° C to ensure that the instruments were not overheated. Moreover, safety precautions were observed by wearing appropriate personal protective equipment (PPE) when operating the laser, i.e., safety goggles.

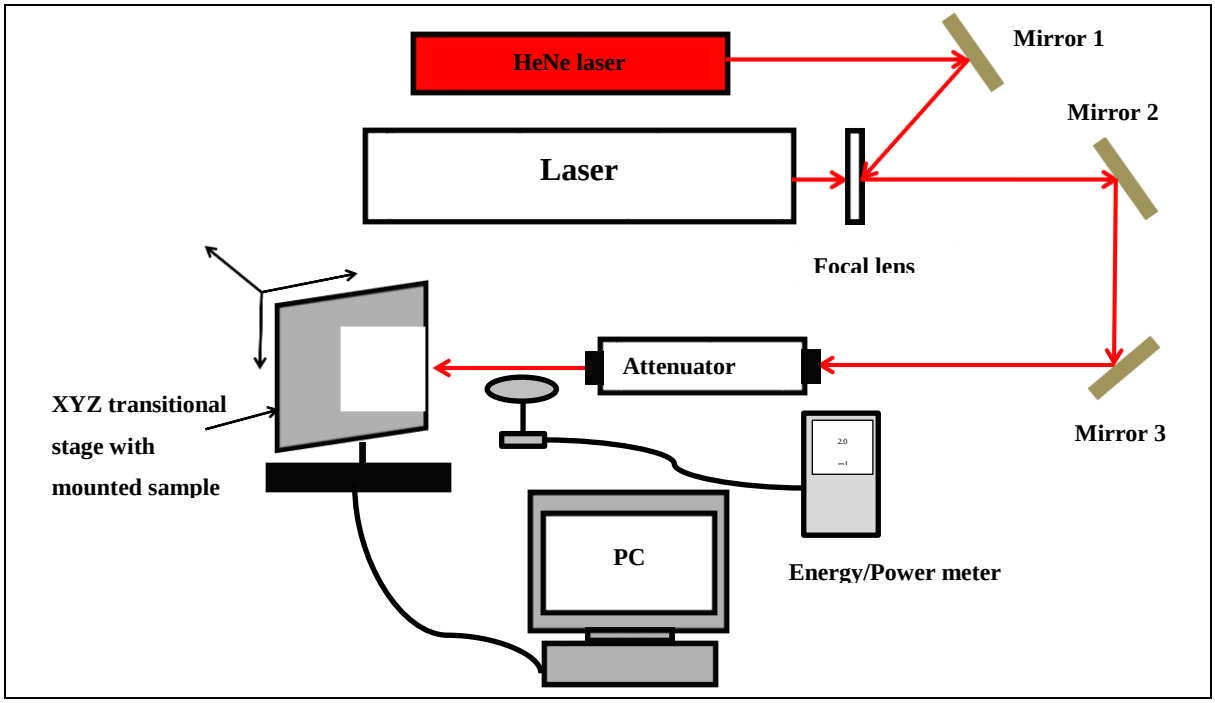

Figure 3.1: A schematic diagram of the experimental setup of laser irradiation of DWP samples

The Nd:YAG laser is a pulsed laser, that gives an output of energy milliJoules (mJ); its emission wavelength for this study was fixed at 266 nm and 355 nm which is located on the ultraviolet (UV) region on the electromagnetic (EM) spectrum. The CO_2 laser is a continuous wave (CW) laser that gives its output in power (Watts) and has an emission wavelength of 10.6 µm which is in the infrared (IR) region. Variables that were evaluated were: laser power density of the lasers for the two lasers at different wavelengths, and the

treatment time in minutes (15, 30 and 45 minutes). Laser power density, also known as laser fluence describes the laser energy delivered per unit area of material scanned (Savalani *et al.*, 2006; LIDARIS, 2016). Before calculating the power density of the Nd:YAG laser, the energy output was converted to power by calculating the peak power which is given in Watts (W) using equation [3.1]. Equation [3.2] was used to calculate power density of the lasers, and it is given in units of Watts per cm^2 (W/cm^2) (Savalani *et al.*, 2006; LIDARIS, 2016).

$$Peak\ power\ (W) = \frac{Laser\ pulse\ energy\ (J)}{Pulse\ duration\ (seconds)} \quad [3.1]$$

$$Intensity\ of\ Power\ Density\ (^{W}/_{cm^2}) = \frac{Laser\ Peak\ power\ (W)}{Effective\ focal\ spot\ area(cm^2)} \quad [3.2]$$

The average thickness of the hand-sheets after drying was 0.5 mm, and the sheets were cut into squares of dimension 5x5 cm^2. The pulp samples were mounted on the PC controlled mobile sample holder (XYZ stage) and directly placed in the direction of the laser radiation source. The distance between the pulp sample and laser source was fixed at 40 cm. The laser power output was measured before and after sample exposure using Coherent laser energy and power meters. The temperature output of the laser beam was also measured during irradiation to assess the effect of heat on the sample. The diameter of the laser beam spot size was 10 mm, and the repetition rate of the pulsed laser was 10 Hz. The power density delivered to the sample varied from 0.32 – 0.4 W/cm^2 in the Nd:YAG lasers for both wavelengths (266 & 355 nm) and 1.53-2.55 W/cm^2 for the CO_2 laser at 10.6 μm. The respective power density and settings of these two lasers were chosen as optimum conditions for this study after a series of preliminary laser screening tests.

After laser irradiation pretreatment, the samples were analysed and characterised to assess the effect of the pretreatment on the structural and molecular properties of cellulose. The characterization techniques that were used in this study are outlined below.

3.3 Cellulose reactivity and dissolution tests

The sections below discuss the wet chemistry treatments that were conducted on the pulp samples after pretreatment with ultrasound and laser radiation.

3.3.1 Alkali dissolution test

Dissolution of cellulose in aqueous NaOH or alkali solution is an essential step for conversion of cellulose to valuable products and derivatives. Therefore, after structural characterization of the ultrasonicated cellulose samples, the samples were dissolved in a solution of aqueous sodium hydroxide (NaOH) to convert cellulose I to alkali cellulose (alkcell) or cellulose II. The method followed was adapted from (Zhang *et al.*, 2002) and modified for this study.

One gram (1 g) of cellulose was dispersed in a reaction vessel with 100 mL of pre-cooled (-4 °C) prepared 18% (w/w) aqueous NaOH solution. The reaction was carried out for 30 minutes with continuous stirring, and the temperature was kept below 6 °C until a slurry formed. A milky viscous solution resulted, and it was placed in the freezer and kept for 2 hours at -5 °C to allow for complete dissolution. After 2 hours, the solution was thawed and stirred vigorously for 15 minutes until a semi-clear solution resulted. The solution was centrifuged for 30 minutes at 9000 rpm using a centrifuge (Universal 320 LR Centrifuge, Hettich Instruments, Germany). A clear solution with a gel-like residue resulted. It was then filtered and neutralised with 150 mL of 10% acetic acid (AA). The resultant white material was washed thoroughly with deionized water, filtered, and then oven dried overnight at 55 °C. Structural characterization of the samples was then carried out, and the alkali cellulose sample (alkcell – UT-t=0) that was not ultrasonicated was used as the control sample.

3.3.2 Fock reactivity test

Cellulose reactivity of the laser pretreated DWP samples was measured according to Fock test method with slight modifications as adapted from Fock (1959) and Tian *et al*. (2013). The method was used to measure the reactivity of pulp samples in a system of NaOH and CS_2 after pretreatment with two lasers at three different wavelengths (i.e. Nd:YAG laser at 266 & 355 nm, and CO_2 laser at 10.6 µm). This method is suitable for giving an estimate of the pulp reactivity; it is, however, not an absolute method for determining

how pulp reacts in a viscose plant. It was chosen for this study because it is a straightforward and quick method that does not require a large sample. The Fock reactivity is a two-part experiment that is conducted over two days. Due to the project time limit and budget, the samples were run in sets of three replicates to determine the repeatability.

Step 1: Xanthation and regeneration of cellulose

A 0.5 gram mass of oven dried pulp was measured and added to a 100 mL Erlenmeyer flask with a stopcock. A 50 mL volume of aqueous sodium hydroxide (NaOH) (9% w/w) and 1.3 mL of carbon disulphide (CS_2) were measured and added to the flask. The mixture was stirred for 4 hours with a magnetic stirrer at room temperature. After 4 hours of stirring, distilled water was added to the sample to give a total weight of 100 g. The reaction flask was shaken vigorously until the sample was thoroughly mixed. This step was followed by centrifugation of the sample for 15 min at 5000 rpm. Then 10 mL of the upper liquid phase was pipetted into a 100 mL beaker and neutralised with ca. 3 mL sulphuric acid (H_2SO_4) (20% w/w) added dropwise with a medicine dropper. The mixture was then transferred into a tube with a stopper and set overnight for 15-20 hours in a fume cupboard. During this time, cellulose was regenerated and the solution degassed to remove CS_2.

Step 2: Potassium dichromate ($K_2Cr_2O_7$) oxidation reaction

The amount of regenerated cellulose was measured by adding 20 mL of H_2SO_4 (68% w/w) into a 100 mL flask with the regenerated cellulose solution. Using a magnetic stirrer, the solution was stirred for 1 hour to acidify the regenerated cellulose sample. The acidified sample mixture was transferred carefully into a reaction vessel, after which, 10 mL of 0.17 M potassium dichromate ($K_2Cr_2O_7$) solution was added. The mixture was then refluxed for 1 hour and during this time oxidation occurred. Once the hour elapsed, the oxidised sample was allowed to cool down to ambient temperature, and it was then transferred to a 100 mL volumetric flask and filled to the mark with distilled water. Exactly 40 mL of the liquid was then pipetted out and transferred into a 100 mL Erlenmeyer flask, 5 mL of potassium iodide (KI) (10% w/v) was added to react with the solution. The iodine produced was titrated with 0.1 N sodium thiosulphate ($Na_2S_2O_4$). Starch was used as an indicator to give a sharp endpoint colour. The titration was carried out until the colour of the solution changed from a dark blue-black to a light blue colour.

The volume of the titrant ($Na_2S_2O_4$) was recorded and used for pulp reactivity calculations as described below.

The Fock reactivity calculation is based on the amount of unreduced Cr^{6+} that remains after the oxidative reaction between potassium dichromate and cellulose. Chemical equations below (3.1 – 3.4) display reduction-oxidation reactions that occurred during the cellulose titration:

$$4\ Cr_2O_7^{2-} + 32\ H^+ + C_6H_{10}O_5 \rightarrow 8\ Cr^{3+} + 6\ CO_2 + 21\ H_2O \qquad 3.1$$

The unreduced Cr^{6+} in reaction (3.1) is reduced by iodide to Cr^{3+}:

$$14\ H+ + 6\ I - + Cr_2O_7^{2-} \rightarrow 2\ Cr^{3+} + 3\ I_2 + 7\ H_2O \qquad 3.2$$

and the iodine is then titrated with sodium thiosulphate:

$$6\ S_2O_3^{2-} + 3\ I_2 \rightarrow 3\ S_4O_6^{2-} + 6\ I^- \qquad 3.3$$

Finally, the addition of reactions (3.2) and (3.3) gives:

$$14\ H^+ + Cr_2O_7^{2-} + 6\ S_2O_3^{2-} \rightarrow 2Cr^{3+} + 3\ S_4O_6^{2-} + 7\ H_2O \qquad 3.4$$

Step 3: Fock reactivity (%) calculations

The percentage (%) reactivity of the dissolved cellulose that reacted with carbon disulphide was calculated using the equation [3.3]:

$$Dissolved\ cellulose\ (\%) = \frac{\left(\left\{V1C1 - \left(V2C2\ x\frac{100}{40}\right)x\left(\frac{1}{6}\right)\right\}x\ M\ x\frac{1}{4}\ x\frac{100}{10.4}\right)}{m}x\ 100 \qquad [3.3]$$

Where, *V1* is the volume of the $K_2Cr_2O_7$ added (L), *C1* is the concentration of the $K_2Cr_2O_7$ 0.17 M, *V2* is the volume of titrated $Na_2S_2O_4$ (L), *C2* is the concentration of $Na_2S_2O_4$ (0.1 N); *M* is the molecular weight of the glucose unit (162 g/mol), and *m* represents the weight of the oven dried pulp sample. The figure $(100/40)$ refers to the dilution of the sample in the volumetric flask (100 mL) and the amount taken out and titrated (40 mL).

The number $(1/6)$ indicates that each dichromate ion consumes 6 thiosulphate ions (Eq. 3.4) and the term $(1/4)$ denotes that cellulose consumes 4 dichromate ions (Eq. 3.1). The last term, $(100/10.4)$ designates the first dilution to 100 g and that a 10 mL sample (equivalent to 10.4 g) that was pipetted out and acidified with *ca*. 3 mL H_2SO_4.

3.4 Characterization techniques

Outlined below are some of the characterization techniques that were employed in this study to evaluate and identify the changes that took place in the cellulose structure as a result of laser and ultrasound irradiation pretreatment. Untreated pulp samples were used as references for all techniques.

3.4.1 Size Exclusion Chromatography Multi-Angle Light Scattering (SEC-MALS)

SEC-MALS was used to evaluate the molecular weight (Mw) and the molecular weight distribution (MWD) of the pretreated samples. It is essential to study these properties of cellulose because they assist with monitoring the chemical behaviour and physiochemical characteristics of this biomolecule when it is exposed to various treatments (Sun & Sun, 2015). The SEC-MALS used in this study was fitted with two detectors, the DAWN EOS light scattering detector and the differential refractive index (RI) detector by Wyatt Technologies.

Sample preparation

To prepare the pulp sample for the SEC-MALS analysis, the first step was to prepare nitration acid that was used to convert natural cellulose to its soluble derivative. Nitration acid was prepared by adding 76 grams of phosphorus pentoxide (P_2O_5) to 40 mL of phosphoric acid (H_3PO_4) (84% w/v). The reaction mixture was stirred vigorously and then allowed to cool down in an ice bath for 3 hours with intermittent stirring. A measured amount of fuming nitric acid (61 mL) was added to the acid mixture with constant stirring. The nitration acid was then stored at 0 °C overnight.

About 150 mg of the pulp sample was pre-cooled in an ice bath for an hour after which, 15 mL of the prepared nitration acid was added to the pulp and mixed. The mixture was cooled down to 0 °C and kept on ice for 3 hours with occasional shaking to mix the

contents. Excess nitration acid was pressed out and filtered from the formed cellulose nitrate using a sintered glass crucible. The sample was neutralised by a stepwise addition of 150 mL of 2% (w/v) aqueous sodium carbonate (Na_2CO_3) solution without suction. The sample was washed with 800 mL of deionized water without suction. After washing the sample a few times, the water that was covering the sample was removed by suction using a vacuum line, and for 2 hours the sample was stabilised by covering it with methanol at room temperature. After 2 hours, the methanol was removed by suction, and the cellulose nitrate sample was dried over P_2O_5 for 15 hours at 20 ℃. Approximately 0.009 mg of cellulose nitrate was weighed out and dissolved in 10 mL tetrahydrofuran (THF). The mixture was stirred in a shaker for 4 hours to ensure that the sample was dissolved completely. Two (2 mL) of the sample was injected into a syringe attached to a 0.45 μm glass fibre filter. Data was acquired and processed using the ASTRA Software for Windows (version 4.72.03) Wyatt technologies.

3.4.2 X-Ray Diffraction (XRD)

XRD analysis was carried out on the ultrasound and laser irradiated pulp samples to study the changes in the crystalline structure of cellulose. A D8 Bruker AXS Advance XRD, fitted with a LynxEye detector, using a Cu Kα X-ray radiation source with a wavelength of 1.54 Å was utilised in this study. The operating power of the instrument was 300 W (voltage, 30 kV, and a current of 10 mA) with a scanning rate of 0.01°. The XRD Bragg angle was set to scan from 2θ = 5° to 35°, and the data was processed using a DIFFRAC SUITE software package. The crystallinity index (CrI) for all samples was calculated using the peak height method developed by Segal *et al*. (1959) and described by Park *et al*. (2010) according to equation [3.4]:

$$CrI = \left(\frac{Imax - Imin}{Imax}\right) \text{ x } 100\% \qquad [3.4]$$

Where, I_{max} refers to the diffraction intensity at (002) peak position when 2θ =22.5° and I_{min} is the minimum intensity above the baseline between 2θ= 18° and 19° corresponding to crystalline and non-crystalline cellulose regions, respectively.

Sample preparation

The dry cellulose specimen was fixed onto a 20 mm disc and mounted on an aluminium sample holder. The samples were irradiated by X-ray beam with the described specifications. The data was exported as Microsoft Excel format and used to plot diffractograms.

3.4.3 Cross Polarization Magic Angle Spinning ^{13}C-NMR (CP/MAS ^{13}C-NMR)

The CP/MAS ^{13}C-NMR is a powerful tool that can provide valuable information about the molecular and supramolecular structure of polymer molecules. In this study, CP/MAS ^{13}C-NMR technique was primarily used to examine the changes in the crystalline structure of cellulose samples after pretreatment with laser and ultrasound irradiation. Spectra were recorded on the Bruker Advance III 600 MHz instrument operating at a magnetic field strength of 7.04 *T* and an ambient temperature (298±1 °K). The magic angle spinning (MAS) spinning rate was of 5 kHz. A double air-bearing probe was used. The acquisition was performed with a Contact Pulse (CP) sequence using a 4.3 μs proton 90° pulse, 800 μs ramped (100 - 50%) falling contact pulse and a 2.5 s delay between repetitions. The TPPM15 pulse sequence was used for ^{1}H decoupling. Glycine was utilised for the Hartmann-Hahn matching procedure, as well as an external standard for calibration of the chemical shift scale relative to tetramethylsilane ($(CH_3)_4Si$). The data point of maximum intensity in glycine carbonyl was assigned a chemical shift of 176.03 ppm. The NMR data was processed using the built-in Topspin software (version 2.1). The crystallinity index (CrI) was evaluated by deconvolution of peaks in the C-4 region of the cellulose I NMR spectra into crystalline and amorphous peaks. The signal at 86-92 ppm corresponds to the highly ordered crystalline area of cellulose, and the signal at 79-86 ppm corresponds with the non-crystalline cellulose or less ordered cellulose chains. The area of the crystalline peak (86 to 92 ppm) was divided by the total area assigned to the C-4 peak (80 to 92 ppm).

Sample preparation

After pretreatment, all pulp samples were first wet with deionized water (40 – 60% moisture), uniformly packed in a zirconium oxide rotor and analysed. Untreated pulp samples were used as a control. After analysis, data was retrieved and processed using the Topspin software (version 2.1).

3.4.4 Atomic Force Microscopy (AFM)

Cellulose processing and manipulation cause structural alteration of the fibres on the ultrastructural level. Therefore, to understand the effect of laser and ultrasound irradiation on the structure of cellulose, AFM analysis of the ultrastructure of the cellulose fibres, particularly the S2 layer within the secondary cell wall was conducted. The analysis was carried out by the NT-MDT manufactured Solver P47H base with a SMENA head. The AFM tip used was of the following specifications: SuperSharpSilicon SPM-Sensors (SSS_NCLR, Nanosensors) with a resonance frequency of 146-236 kHz, Force constant of 21-98 N/, a tip radius of 2 nm. The data obtained was then used to compute the lateral fibril aggregate dimensions (LFAD).

Sample preparation

Samples for AFM analysis were prepared with caution to minimise alteration of the cell wall structure and preserve the ultrastructure of the fibre cell wall. The pulp samples were first strung out into strands of fibres using tweezers and aligned on the prepared pieces of aluminium foil. The piece of foil with fibre threads was then rapidly dipped in liquid nitrogen slush; after that, the piece of foil was placed in the freeze drying equipment for about 24 hours. The freeze-drier stage was pre-cooled to -70 °C before insertion of the samples and the system was kept under vacuum by a connected vacuum pump. On the second day, the pulp fibres were then embedded in the prepared epoxy resin and placed in the oven fixed at 70 °C for 8 hours. This was to allow the resin to polymerise and harden. After this procedure, the next step was to transversely section a 1.0 μm thick cross-section on the ultramicrotome (EM UC7, Leica Microsystems, Germany) using the lab-prepared glass knives. The cross-sections of the samples were then picked and placed on a glass slide, dried and scanned on the AFM.

AFM sample scanning

The pulp fibre cross-sections of the pretreated samples and an untreated control were studied on the AFM. The AFM can be operated in three basic imaging modes, the contact, non-contact and the Tapping mode. In the contact mode, the sample is in direct touch with the sample, and this is applicable to studies of hard surfaces. In the case of non-contact mode, the AFM tip scans the sample by vibrating on top of the sample surface, and this is useful for analysis of soft specimens. The Tapping mode, on the other hand, is

an extension of the non-contact mode but the tip vibrates at a higher altitude on top of the sample surface. For the purpose of this study, the latter mode was selected because the tip has less direct contact with the sample. This mode of scanning has less potential of damaging the structure of the fibre wall, and it also keeps the fibre wall in its native structure. The samples were scanned in ambient conditions at a room temperature of 25 °C. The area of interest was the S2 layer of the cellulose fibre wall. At first, an area of 13x13 μm of the entire fibre was scanned; this was reduced progressively to 8x8 μm, 4x4 μm and finally, a 1x1 μm area was scanned. The images were taken in both height and phase mode. In the height mode, deflection of the cantilever is directly used to measure the *z* position, while in the phase mode; the lateral movements of the cantilever measure the surface properties of the material.

AFM image analysis

Image analysis of the acquired 1x1 μm scans was conducted to determine the change in LFAD due to the pretreatments. The Image-Pro Plus (Version 6.0) software was used to analyse AFM scans and to obtain images in phase mode. Phase imaging is useful for assessing fine surface features such as aggregation and elasticity. Firstly, a grayscale photograph of the phase mode scan was obtained, and then a watershed segmentation filter was applied. Then the image was masked to reveal possible fibril aggregate areas and the mean of the aggregate diameter was measured in nanometres (nm). The image analysis data was compiled and presented in Microsoft Excel format.

3.4.5 Scanning Electron Microscopy (SEM)

In this study, SEM micrographs of the pretreated pulp samples were acquired by analysis with ZEISS EVO LS15 scanning electron microscope fitted with a secondary electron detector. The SEM was equipped with the Energy dispersive X-ray spectroscopy (EDX) analyser. The accelerating voltage used was between 5 kV at different magnifications. The purpose of using the SEM was to assess morphological changes on the surface of cellulose pulp samples as a result of the laser and ultrasound radiation pretreatment.

Sample preparation

The pretreated dry pulp samples were mounted onto metal stubs using a carbon double sided tape with the side to be examined facing upwards. Before exposure to the SEM, the

samples were sputter coated with a gold layer (gold and palladium ratio of 80:20) using an EIKO IB3 Ion coater to create a conductive metallic layer that inhibits charging and improves sample imaging. After sputter coating, the samples were ready for analysis on the SEM. Image analysis was conducted on the Soft Imaging Software (SIS).

3.4.6 Compact Morphological Fibre (MorFi) analyser

Further morphological analysis of the ultrasound irradiated pulp samples was carried out using the Compact MorFi analyser (TechPap, France). The fibre analyser was used to characterise the average fibre distribution (length and width) and the change in the number of fibres after the pretreatment in comparison to the untreated control samples.

Sample preparation

The moisture of the ultrasonicated samples and control sample was measured on the moisture analyser and recorded on the MorFi sample spreadsheet. Moisture content measurements were used to calculate the mass of the pulp required to achieve a consistency of 30 mg/L. The samples were weighed according to the values given by the spreadsheet and the actual mass weighed was recorded into the worksheet. The weighed samples were transferred to their respectively labelled 100 mL beakers and wet by adding water into the beaker until the sample was submerged. The weighed sample was then washed into the disintegrator holder with 700 mL tap water and placed into the disintegrator instrument. The samples were fragmented in the disintegrator for three (3) minutes. Once the disintegration was complete, the disintegrator blades were washed into the holder with approximately 50 mL of tap water to ensure that there was no sample left behind on the blades. The sample was then transferred to a 1000 mL volumetric flask using a funnel to make sure that nothing was spilt over. The funnel was rinsed with approximately 200 mL aliquots of tap water and the 1000 mL volumetric flask was then filled to the mark. The flask was closed using a stopper and shaken to ensure a homogeneous mixture. The contents were then rapidly transferred into a 1000 mL plastic beaker and taken for measurement of fibre dimensions using a fibre analysis apparatus.

Sample analysis

The study was carried out in duplicate, and the results were recorded on the application software and exported to Microsoft (MS) Excel for data analysis.

CHAPTER 4: RESULTS AND DISCUSSIONS – ULTRASOUND IRRADIATION

4 Introduction

Chapter 4 presents characterization results for dissolving pulp samples after ultrasound irradiation and treatment with aqueous sodium hydroxide (NaOH) solution.

4.1 Ultrasound irradiation of cellulose

Ultrasound irradiation is a powerful and environmentally benign pretreatment technique that can be used to depolymerise and disrupt the cell wall structure of cellulose (Wong *et al.*, 2009; Karimi *et al.*, 2014). This method is widely known for its ability to cause polymer degradation by breaking the cellulose fibre chains into smaller units. The chain breakage is due to the mechanical stress that results during cavitation (Antti *et al.*, 2008; Frone *et al.*, 2011; Wong *et al.*, 2012).

This part of the study investigated the effect of ultrasound irradiation on the structure of cellulose. Furthermore, the impact of this pretreatment technique on the dissolution behaviour of cellulose in an aqueous sodium hydroxide (NaOH) solution was also studied. The samples were ultrasonicated for 10, 20, 30, 45, and 60 minutes and subsequently reacted with 18% (w/w) NaOH solution. Untreated pulp samples were used as experimental control. Structural characterization of the pretreated samples was conducted, and the results are outlined below.

4.1.1 Size Exclusion Chromatography with Multi-Angle Light Scattering (SEC-MALS) results

SEC-MALS is a standard technique that is used in research laboratories and industrial institutions to determine the average weight molar mass (Mw) and molecular weight distribution (MWD) of both synthetic and natural polymers including cellulose (Conner, 1995; Trathnigg, 2000). The Mw and MWD play a major role in polymer characterization because these parameters can directly influence properties and behaviour of the polymer, especially during reactivity and dissolution (Rogošić *et al.*, 1996). In this study, the Mw and MWD were analysed by SEC-MALS after pretreatment of the pulp samples with ultrasound radiation and dissolution in aqueous NaOH.

Figure 4.1 displays SEC-MALS chromatograms of cellulose obtained after ultrasound irradiation. The chromatograms of the pretreated samples show a slight shift in average Mw from a high to lower value compared to the untreated control sample. Moreover, an increase in the width of the MWD curves is also observed, and this is more pronounced after 60 minutes of ultrasonication. The UT-60 min curve shows that this sample has a relatively broad MWD and a high fraction of the low Mw polysacharrides as shown by the long tail-end bump towards the low molecular weight side. These observations are in agreement with the average MWD data shown in Table 4.1. With increasing treatment time (10, 20, 30, 45 and 60 minutes), the weight average molar mass (Mw) displays a significant decrease of 6.4%, 8.5%, 8.7%, 10.2%, and 12.0% respectively. The decrease in Mw is an indication of cellulose depolymerization which can be attributed to cleavage of the long cellulose chains due to the cavitation bubbles that are generated in solution during ultrasound irradiation (Wong *et al.*, 2009; Wong *et al.*, 2012).

Changes in the Polydispersity index (PDI) was also observed after the pretreatment. PDI is a ratio of the molecular weight averages (Mw/Mn), it is an indication of the broadness of the MWD of a polymer. Samples that were ultrasonicated for 10 and 20 minutes display minor declines in PDI, but the latter three samples that were irradiated for 30, 45 and 60 minutes show an increase in PDI. Compared to the control sample, a PDI % increase of 86.5% was observed when the sample was exposed to ultrasound irradiation for 60 minutes. These observations correspond to earlier findings which have displayed that the length of ultrasound treatment time also plays a significant role in determining the extent of polymer degradation (Antti *et al.*, 2008; Goodwin *et al.*, 2011; Wong *et al.*, 2012).

On the other hand, minor declines in the intrinsic viscosity were observed in samples after exposure to ultrasound irradiation. The intrinsic viscosity has widely been documented as a function of the average Mw of a polymer, and it is used for estimating the viscosity-average degree of polymerization (DP) (Weissler, 1950; Liu *et al.*, 2006). However, a different conclusion can be drawn from the observed results because no parallel decreasing trend was realised between the Mw and molecular weight average intrinsic viscosity ([η]w).

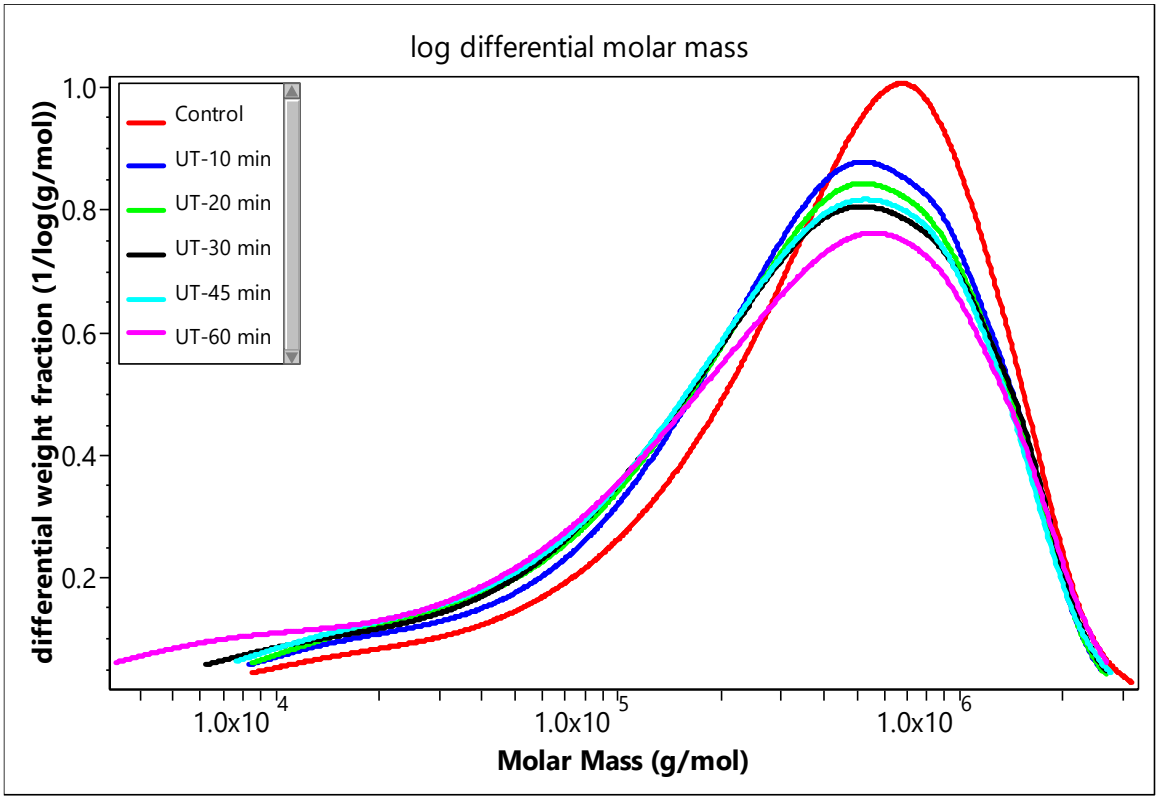

Figure 4.1: SEC-MALS chromatograms of dissolving pulp samples ultrasonicated for 10, 20, 30, 45 and 60 minutes compared to the control sample.

Table 4.1: Average molecular weight distribution (MWD) results after ultrasound irradiation

Sample ID	***Mw (x10^5 g/mol)**	***[η]w (mL/g)**	***PDI (Mw/Mn)**
Cellulose I control	5.78±0.3	1218.0±24.4	4.28±0.4
UT - 10 min	5.41±0.1	1194.11±2.15	4.107±1.0
UT - 20 min	5.29±0.2	1212.74±9.9	4.253±1.2
UT –30 min	5.28±0.3	1207.57±6.6	5.001±2.4
UT - 45 min	5.19±0.0	1217.86±7.5	4.847±0.4
UT - 60 min	5.09±0.3	1191.99±8.7	7.981±2.6

*Mean calculated from a total of three experimental trials (n = 3)

Since ultrasound irradiation has been reported to cause cellulose depolymerization and alteration in MWD, it can be resolved that ultrasound irradiation can improve cellulose dissolution (Xing *et al.*, 2010; Sumari *et al.*, 2013). Low Mw polymers react much faster, and they require less driving force for dissolution compared to the high Mw polymers (Sumari *et al.*, 2013). Figure 4.2 presents the SEC-MALS chromatograms with average

modifications that occurred in the molecular structure of cellulose pulp samples after ultrasound irradiation and dissolution in aqueous NaOH solution. Compared to the native cellulose control, the alkcell control and all UT-alkcell samples displayed slight shifts from high to lower average Mw. However, in comparison to the alkcell control, the test samples exhibited different behaviour, the curves for alkcell-UT samples ultrasonicated for 10, 30 and 60 minutes display a shift to high Mw. In contrast, the alkcell-UT-20 and 45 minutes shifted to the low Mw. The shift was more pronounced on alkcell-UT45 minutes sample, and this was accompanied by broadening of the peak. These peak shifts correspond to the results as shown in Table 4.2.

The Mw of alkcell-UT 45 min peak displayed a significant decline in average Mw from $4.75x10^5$ g/mol to $4.06x10^5$ g/mol. The decrease in average Mw for this sample reveals an inversely proportional relationship with the corresponding PDI ratio. The PDI increased from 2.763 to 4.171 to show that after ultrasonication and NaOH treatment, the distribution of the Mw widened. Furthermore, a directly proportional relationship is observed between the Mw and intrinsic viscosity to this sample, a noticeable intrinsic viscosity decrease from 1178.18 mL/g to 1113.50 mL/g was achieved. These observations agree with earlier suggestions made about Mw and intrinsic viscosity. Some scholars have been able to determine the average Mw of cellulose from the intrinsic viscosity (Weissler, 1950; Kulicke *et al.*, 2005). However, from the observed cellulose modifications, after the ultrasound irradiation and alkali dissolution, no apparent trend could be established in comparison to pretreatment time. This lack of change or minimal changes in cellulose Mw and its distributions may be due to cross-linking within the cellulose molecules as a result of the pretreatments (Yacob *et al.*, 2013; Saini *et al.*, 2015).

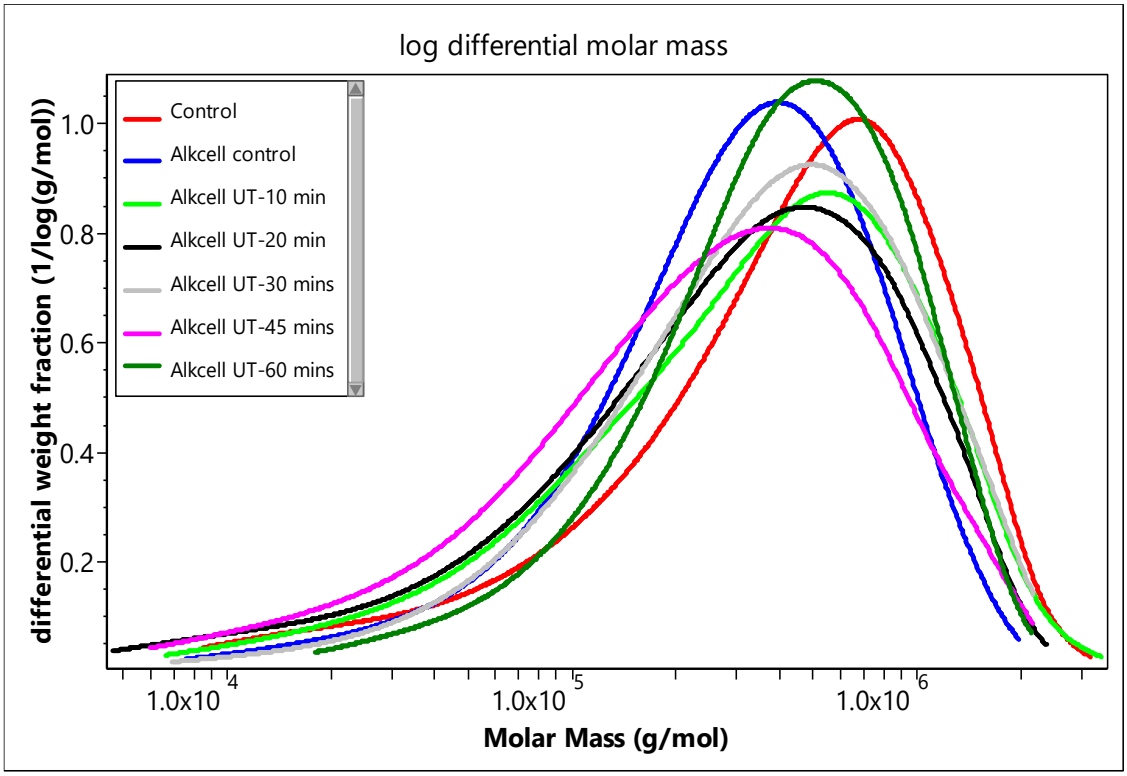

Figure 4.2: SEC-MALS chromatograms of the ultrasound irradiated-alkali cellulose samples (cellulose II) compared to cellulose I-control and alkcell control.

Table 4.2: Average MWD results after ultrasound irradiation and alkali dissolution treatment

Sample ID	*Mw (x10^5 g/mol)	* [η]w (mL/g)	*PDI (Mw/Mn)
Cellulose I control	5.57±0.4	1358.89±10.0	4.549±0.2
Alkcell control	4.75±07	1178.18±3.6	2.763±0.9
Alkcell-UT10 min	5.36±0.2	1248.87±3.7	3.916±0.4
Alkcell-UT20 min	4.65±0.4	1151.68±16.1	4.619±0.2
Alkcell-UT30 min	5.19±0.3	1262.56±6.9	3.031±0.6
Alkcell-UT45 min	4.06±0.9	1113.50±16.9	4.171±0.3
Alkcell-UT60 min	5.30±0.2	1337.01±7.6	2.263±1.1

*Mean calculated from a total of three experimental trials (n = 3)

4.1.2 X-Ray Diffractions (XRD) results

High cellulose crystallinity is a consequence of the strong intra and intermolecular hydrogen bonds that hold the cellulose molecules together (Wong *et al.*, 2012). Cellulose crystallinity is one of the most important parameters that significantly influence the

mechanical, physical and chemical properties of this biopolymer. Pretreatment of cellulose with ultrasound radiation induces changes in the physical structure of cellulose by isolating the cellulose surface fibres, this has various chemical effects on the structure, and may ultimately lead to improved cellulose reactivity (Suslick & Price, 1999; Cheng *et al.*, 2010). XRD is a well-established technique that is used for characterising the crystallinity of a wide range of crystalline materials. In this study, XRD analysis was performed to examine the crystalline structure of cellulose after ultrasound irradiation, and the degree of crystallinity (CrI) was calculated by the peak height method that was developed by Segal *et al*. (1959). Figure 4.3 depicts superimposed XRD patterns of the samples after ultrasound irradiation for 10, 20, 30, 45 and 60 minutes and the untreated pulp sample used as a control. The diffraction patterns display characteristic natural cellulose peaks with different intensities and width. The first peak is located at approximately $2\theta = 16°$; this peak is broad because it is an overlap of two peaks located at $2\theta = 15.5°, 16.4°$. The third peak is an intense sharp peak located at $2\theta = 23.2°$. These 2θ reflections correspond to (101), (1-01), and (002) crystallographic planes; and they confirm the native cellulose crystalline structure (Borysiak & Doczekalska, 2005; Park *et al.*, 2010).

After ultrasound irradiation, the peak intensities of the pretreated samples display a slight decrease and a shift in 2θ to higher values compared to the untreated control sample. However, the shape of the peaks did not change after ultrasonication; this shows that the treatment did not have much of an effect on the crystalline structure of cellulose. These observations are in agreement with what has been shown in the literature (Xing *et al.*, 2010). Estimated CrI results shown in Table 4.3 also confirmed these observations, with increasing treatment time cellulose crystallinity was slightly decreased from 62.2% (control) to 60.8%, 56.7%, 59.6%, 60.9% and 57.1% in samples ultrasonicated for 10, 20, 30, 45, and 60 minutes, respectively.

Ultrasound irradiation has been reported to have a significant effect on various structural properties of cellulose. However, observations made in this study suggest that the pretreatment did not cause visible changes in the degree of cellulose crystallinity. Xing *et al*. (2010) also recorded minor modifications on the crystallinity of cellulose after ultrasound irradiation which was suggested to be due to the damage induced by the acoustic cavitation process. Ultrasound irradiation does not have much effect on the

crystalline structure of cellulose; however, it has shown that it removes the amorphous regions and the upper layer of cellulose fibres thus exposing the crystalline regions. As a result, various studies have reported that ultrasound irradiation can cause the cellulose crystallinity to either increase or remain unchanged (Aimin *et al.*, 2005; Cheng *et al.*, 2010; Frone *et al.*, 2011).

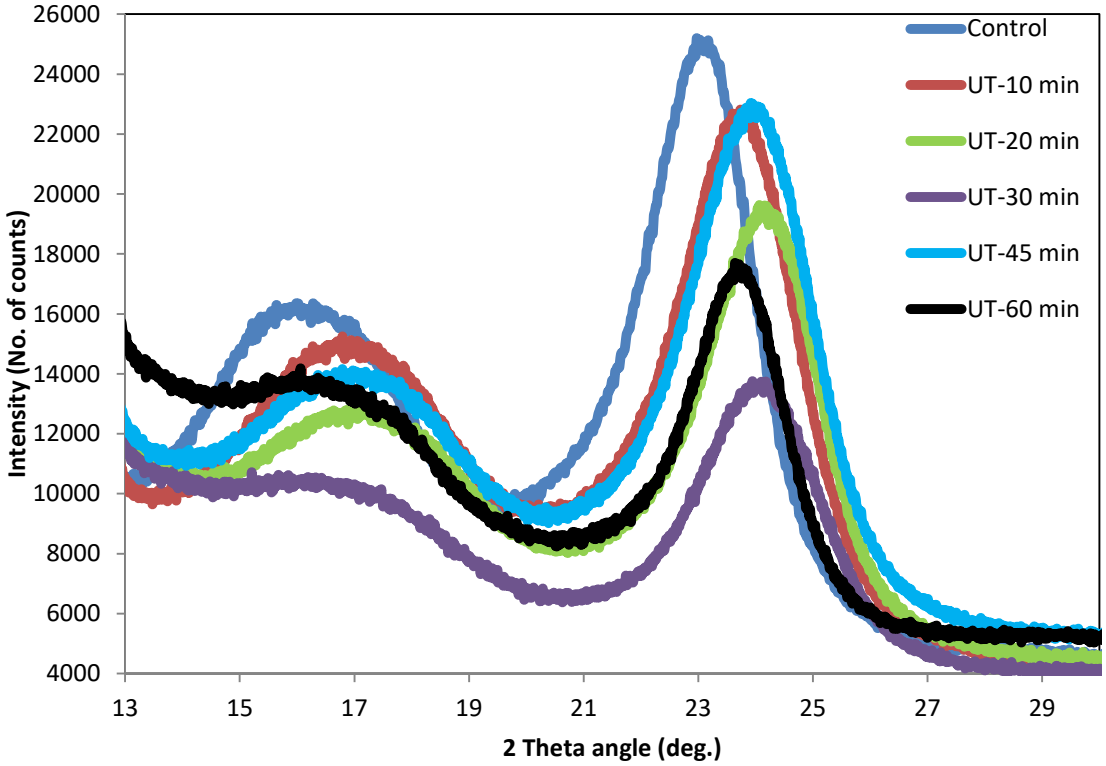

Figure 4.3: Superimposed XRD pattern for dissolving pulp samples after ultrasound irradiation compared to the control sample

Table 4.3: Average crystallinity index (CrI) results after ultrasound irradiation

Sample ID	**Treatment time/min**	***CrI - XRD (%)**
Control	0	62.2±2.2
UT-10 min	10	60.8±1.9
UT- 20 min	20	56.7±2.5
UT-30 min	30	59.6±3.3
UT-45 min	45	60.9±1.5
UT-60 min	60	57.1±1.6

*Mean calculated from a total of three experimental trials (n = 3)

Figure 4.4 presents X-ray diffraction patterns of cellulose pulp samples after ultrasonication and treatment with aqueous NaOH solution (alkali treatment) compared to the untreated natural cellulose (cellulose I control). After the samples were treated with aqueous NaOH solution, all diffractograms display a shift to lower 2θ values and characteristic cellulose II peaks. The peaks shifted to approximately 2θ = 12.7°, 20.6° and 22.2° which respectively correspond to (110), (10$\bar{1}$) and (002) crystallographic plane reflections (Oudiani *et al.*, 2011). From the results, the conversion of cellulose I to cellulose II is observed after treatment with aqueous NaOH solution. This transition is proven by the disappearance or reduction of all the peaks that correspond to Bragg's angle at 2θ = 16° and 23° in native cellulose. The high ordered crystalline structure of cellulose I was transformed to the amorphous structure of cellulose II (alkcell); this conversion can be attributed to the reduction of the existing inter- and intramolecular hydrogen bonds that tightly bind the cellulose molecules together (Ciolacu *et al.*, 2011).

Table 4.4 displays the change in crystallinity index after ultrasonication and alkali treatment. A CrI decline of 55% was achieved for the alkcell-UT 60 min sample in comparison to the alkcell-control sample. Other alkcell-UT samples also displayed noticeable changes in CrI after alkali treatment. These observations agree with what has been reported about the ability of aqueous NaOH solution to infiltrate and break the crystalline regions of cellulose (Medronho & Lindman, 2015). Ultrasound treatment alone was unable to disrupt the cellulose crystalline structure, but when it was used in combination with alkali treatment, noticeable changes in cellulose crystallinity were noticed.

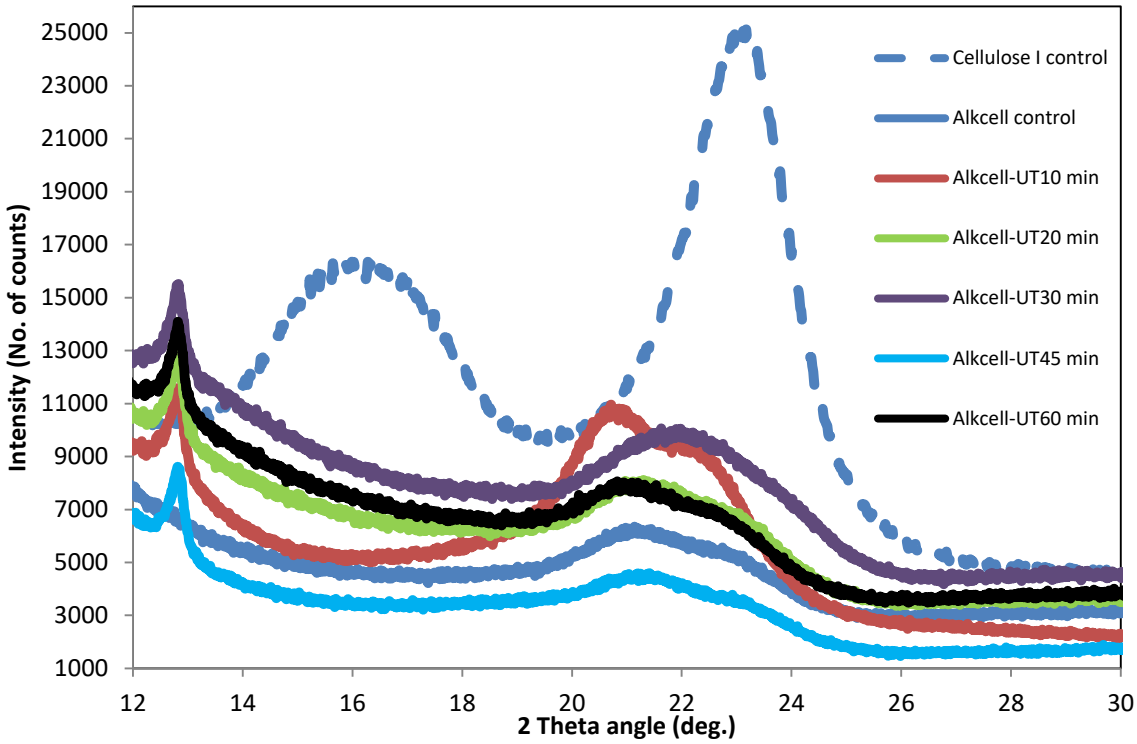

Figure 4.4: Superimposed XRD patterns of dissolving pulp samples after ultrasound irradiation and treatment with aqueous NaOH solution

Table 4.4: Average CrI results after ultrasound irradiation and alkali treatment

Sample ID	**Treatment time/min**	***CrI - XRD (%)**
Alkcell-control	0	30.7±0.9
Alkcell-UT 10 min	10	22.8±1.0
Alkcell-UT 20 min	20	23.4±2.6
Alkcell-UT 30 min	30	20.2±0.3
Alkcell-UT 45 min	45	23.4±2.5
Alkcell-UT 60 min	60	13.9±0.0

*Mean calculated from a total of three experimental trials (n = 3)

Moreover, the transformation of cellulose chains from the crystalline structure of native cellulose to the thermodynamically stable cellulose II phase was achieved. Although the relationship between the effect of increasing treatment time and the pretreatment is not pronounced, the samples that were ultrasonicated for 10 and 30 minutes displayed a complete conversion to amorphous cellulose while other test samples were a combination of both phases. These observations are attributable to the proposed mechanism of alkali

treatment of cellulose which suggests that NaOH molecules can enter the crystalline regions of the cellulose, cause them to swell and ultimately break the hydrogen bonds within the network structure. These structural modifications ultimately lead to the overall decrease in cellulose crystallinity, increased accessibility and reactivity (John & Anandjiwala, 2008; Öztürk *et al.*, 2009; Olsson & Westman, 2013). The above observations are in agreement with what has been reported in various studies that ultrasound irradiation combined with alkali treatment can alter the morphology and crystalline structure of cellulose (Wong *et al.*, 2012; SriBala *et al.*, 2016).

4.1.3 Atomic Force Microscopy (AFM) results

Surface topography and roughness modifications after pretreatment with ultrasound radiation were determined with the AFM with the aim of finding the correlation between the pretreatment and morphological alterations. Figure 4.5 displays 1x1 μm phase images of the secondary cell wall (S2 layer) of the ultrasonicated samples as well as the untreated control sample. No obvious changes were observed on the micrographs of the cross-sections after ultrasonication when compared to the control sample; there are no visible pores that formed due to the pretreatment. The tightly bound regions on the fibril aggregates are more pronounced after ultrasonication compared to the dark areas which represent the less stiff regions. Table 4.5 presents the average LFAD obtained after ultrasound irradiation of the cellulose pulp samples in comparison to the control sample. LFAD is a measure of the diameter of the lateral fibril aggregates, and it has a significant influence on the availability of the surface area for chemical processing (Chunilall *et al.*, 2006; Pönni *et al.*, 2012).

After ultrasound irradiation, a slight decrease in LFAD was observed. The LFAD value for the control sample decreased from 31.98 nm to 28.4 nm, 29.3 nm, 23.0 nm, 29.7 nm and 25.6 nm after ultrasonication for 10, 20, 30, 45 and 60 minutes, respectively. Even though the decrease does not show a trend with increasing treatment time, it can be seen that to some extent; ultrasound irradiation had an effect on the ultrastructure of cellulose fibres. Earlier studies have established that there is an inversely proportional relationship that exists between the LFAD and specific surface area (Chunilall *et al.*, 2010). Therefore the slight decrease in LFAD suggests that there is an increase in available surface area for reactions.

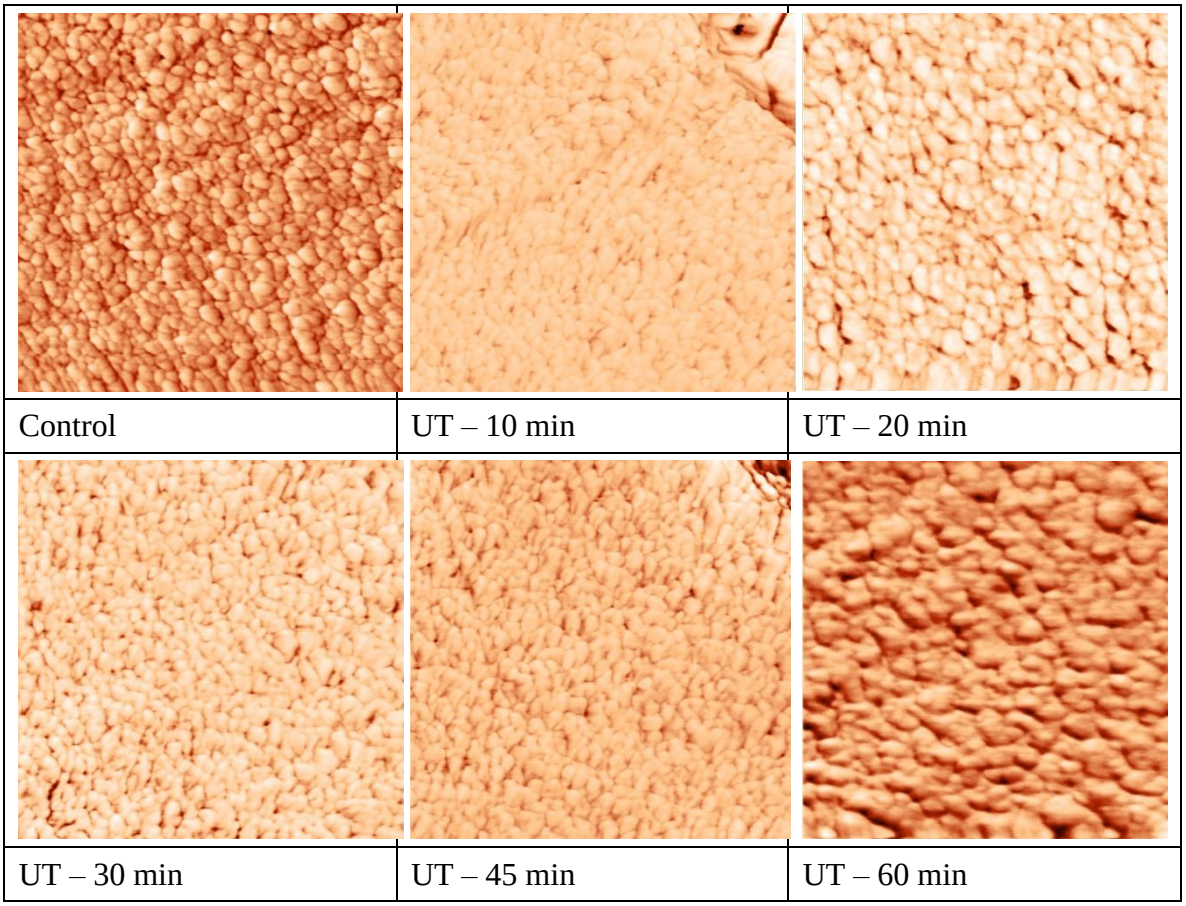

Figure 4.5: AFM 1x1 μm phase images of the cross-section of secondary cell wall (S2) layer for the ultrasound irradiated pulp samples compared to the control.

Table 4.5: Average LFAD results for ultrasound irradiated pulp samples

Sample ID	**Time/mins**	***LFAD/nm**
Control	0	31.98±2.7
UT -10 min	10	28.4±2.8
UT -20 min	20	29.3±2.1
UT -30 min	30	23.0±1.6
UT -45 min	45	29.7±2.9
UT -60 min	60	25.6±1.5

*Mean calculated from a total of three experimental trials (n = 3)

4.1.4 Scanning Electron Microscopy (SEM) results

Pretreatment is a paramount step in cellulose processing because it helps to overcome the recalcitrant nature of this polymer by inducing various physical and chemical

modifications to its ultrastructure (Brodeur *et al.*, 2011). Acoustic cavitation is a phenomenon of ultrasound irradiation that is known as the driving force behind the morphological changes that occur on the surface of materials during application of this pretreatment technique. The generated microbubbles collide and collapse to produce high energy shockwaves which damage the surface of cellulose fibres and causes bond breakage (Suslick & Price, 1999).

Figure 4.6(a) to (f) presents SEM micrographs for the control sample (untreated natural cellulose) and ultrasonicated cellulose samples. Before ultrasonication, the surface of the control sample displayed "scaly" irregular folds which may be due to the S1 cell wall layer. With increasing ultrasonication time, cavitation of microbubbles led to the dislocation and erosion of the S1 cell wall layer until the surface of the fibres became smooth as shown in the fibre obtained after treatment for 60 minutes. Ultrasound irradiation efficiently induced noticeable morphological changes on the surface of the cellulose fibres. These observations are in agreement with earlier findings that displayed that by acoustic cavitation, ultrasound irradiation can disrupt both the primary and secondary cellulose cell wall. Modification of cellulose surface morphology leads to increased surface area and improved chemical accessibility and processing (Wong *et al.*, 2012; Karimi *et al.*, 2014).

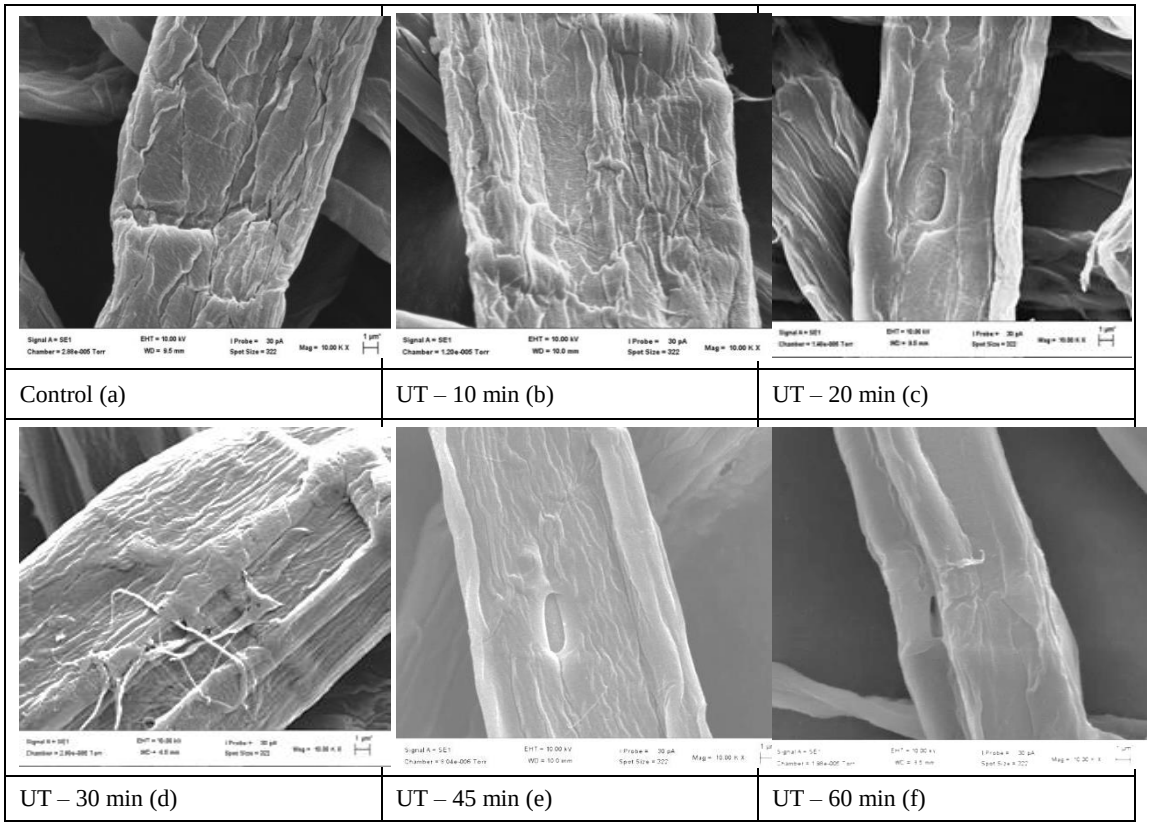

Control (a)	UT – 10 min (b)	UT – 20 min (c)
UT – 30 min (d)	UT – 45 min (e)	UT – 60 min (f)

Figure 4.6: SEM images of pulp samples after ultrasound irradiation (10, 20, 30, 45 and 60 minutes) compared to the control.

Figure 4.7(a) presents the SEM micrograph of the surface of cellulose fibres after alkali treatment only (alkcell control sample), and Figure 4.7(b-f) presents images of cellulose fibres that were exposed to ultrasound irradiation and alkali treatment respectively. The images demonstrate noticeable changes on the surface of all the test samples and the alkcell control sample. After the treatments the samples became compact and agglomerate; the surface of the fibres was rough with wrinkles and grooves. These observations were more apparent on samples UT+alkali (c) to (f). Treatment of cellulose fibres with NaOH solution at low temperature is known for its ability to penetrate the crystalline regions of cellulose and for breaking the hydrogen bonds within the complex network structure of this polymer (Olsson & Westman, 2013; Medronho & Lindman, 2015).

The combination of alkali treatment of cellulose with ultrasound irradiation has also shown that it can disintegrate and break the surface of fibre walls. Therefore, the cracks and roughness noticed on the surface of the cellulose fibres after the treatments are an indication of a possible increase in exposure and accessibility of new reaction sites.

Increased surface area is known to enhance reactivity because the substrate is more accessible to reagents (Xing *et al.*, 2010; Kang *et al.*, 2013). These modifications are attributable to the localised shockwaves of ultrasound caused by the cavitation process.

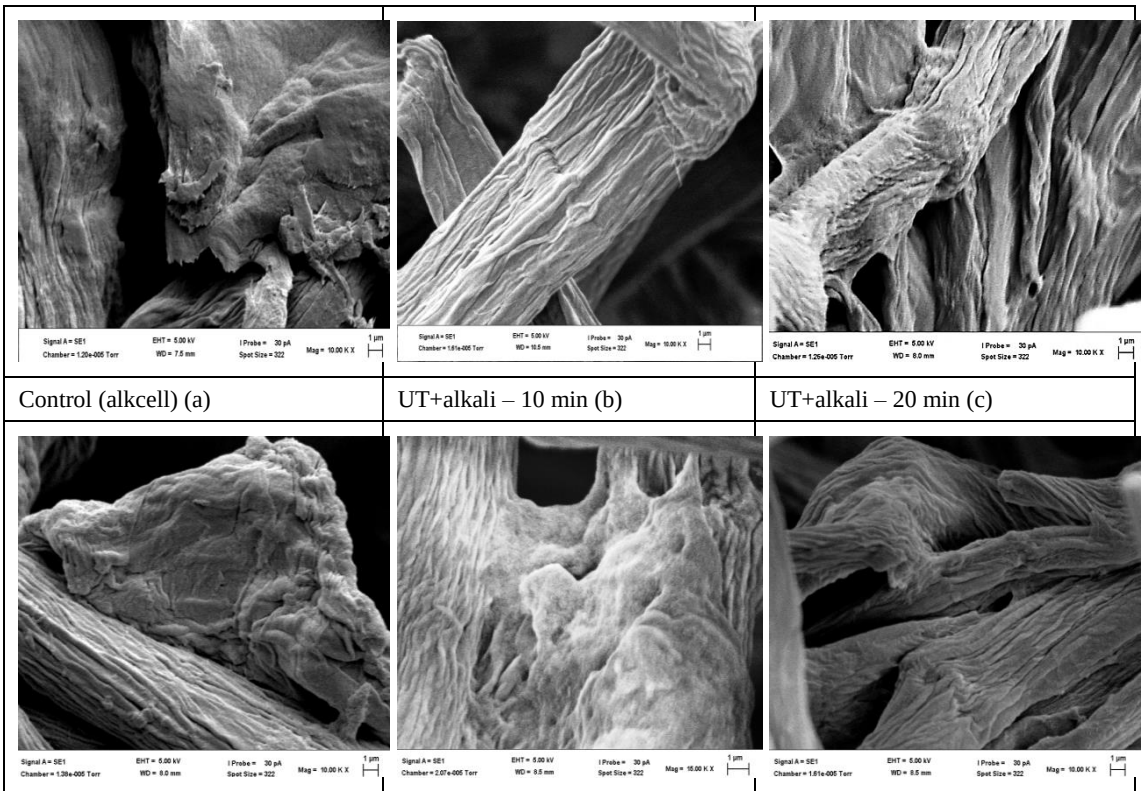

Control (alkcell) (a)	UT+alkali – 10 min (b)	UT+alkali – 20 min (c)
UT+alkali – 30 min (d)	UT+alkali – 45 min (e)	UT+alkali – 60 min (f)

Figure 4.7: SEM images of pulp samples after ultrasound irradiation and treatment with aqueous NaOH solution compared to the control.

4.1.5 Compact Morphological Fibre (MorFi) Analyser results

The MorFi analyser was used to investigate the structural dimensions of the ultrasound irradiated samples and compared to the untreated control samples. The results are shown and discussed below. Table 4.6 displays the fibre distributions of dissolving pulp after ultrasound irradiation compared to the control sample. A slight decrease in fibre lengths for the pretreated pulp fibres is observed in comparison to the control. However, the pretreatment did not have a significant impact on the number of fibres and the average width of the fibres. The number of fibres displayed an increase with increasing ultrasonication time, although the increase did not show a linear relationship trend. The average fibre widths also exhibited an insignificant decrease with increasing ultrasonication time.

Table 4.6: MorFi analysis of pulp samples after ultrasound irradiation compared to the untreated control

Sample ID	***Fibre No.**	***Ave. Length (µm)**	***Ave. Width (µm)**
Control	5016±7.7	659±12.0	13.4±0.2
UT-10min	5055±4.9	627±5.7	13.0±0.3
UT-20min	5234±3.9	621±1.4	13.2±0.2
UT-30min	5089±5.9	616±10.0	13.0±0.1
UT-45min	5257±2.1	624±4.9	13.1±0.3
UT-60min	5175±4.7	603±1.4	13.3±0.5

*Mean calculated from a total of two experimental trials (n = 2)

Figure 4.8 displays optical microscope images of the fibres after ultrasonication. There are no noticeable visual changes regarding the fibre chain lengths and distribution of the fibres appears to be homogeneous after ultrasonication. These observations are to be expected since ultrasound irradiation is not a random process and it causes chain breakage to occur at the centre of a fibre before reaching a levelling-off point where chains do not fragment further (Suslick & Price, 1999; Caruso *et al.*, 2009).

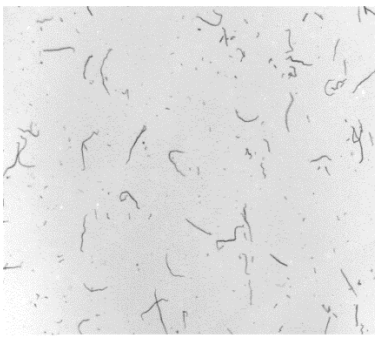	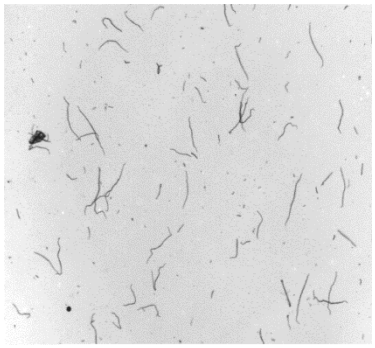	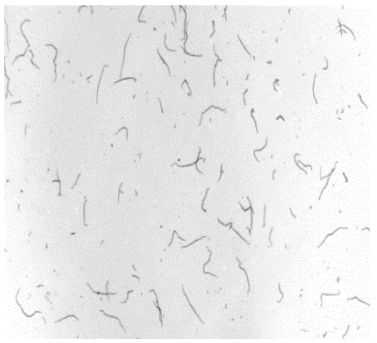
Control	UT-10 min	UT-20 min
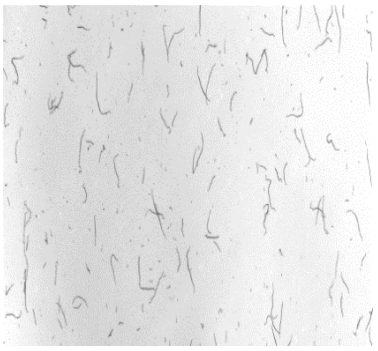	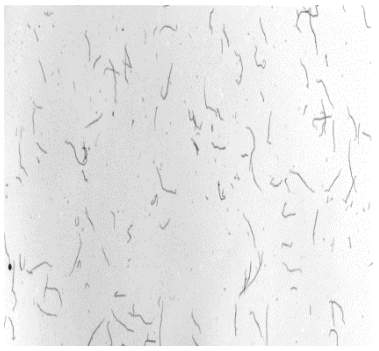	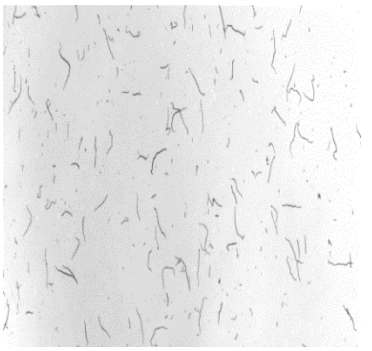
UT-30 min	UT-45 min	UT-60 min

Figure 4.8:Images obtained from the MorFi analyser displaying morphological properties of dissolving pulp samples after ultrasound irradiation.

CHAPTER 5: RESULTS AND DISCUSSIONS – LASER IRRADIATION

5 Introduction

Chapter 5 gives a detailed overview of the results obtained in this study; it is divided into two sections and their respective subsections. Section 5.1 presents structural characterization results for the laser irradiated pulp samples, and section 5.2 outlines the Fock reactivity results and observations.

5.1 Laser irradiation pretreatment

Dissolving pulp samples were irradiated with the carbon dioxide (CO_2) laser that emits at a wavelength of 10.6 μm and the neodymium yttrium aluminium garnet (Nd:YAG) laser emitting at 266 and 355 nm. Irradiation time was set for 15, 30 and 45 minutes. Characterization of the irradiated pulp samples was carried out using various techniques to assess any structural modifications that occurred due to the pretreatment.

5.1.1 Size Exclusion Chromatography Multi-Angle Light Scattering (SEC-MALS) results

The behaviour and chemical reactivity of polymers are strongly influenced by their average weight molar masses (Mw) and molecular weight distribution (MWD) (Bernhard & Oppermann, 2004). When polymers are exposed to radiation treatment, they undergo two main reactions; chain scission and cross-linking, and these reactions ultimately have an impact their final properties (Yacob *et al.*, 2013). The SEC-MALS was used to study the molecular weight of cellulose and its distribution after laser radiation pretreatment.

Figures 5.1 to 5.3 present overlaid chromatograms of the laser irradiated cellulose pulp samples and the untreated control sample. The MWD curves are plots of differential weight fraction (1/log(g/mol)) *versus* molar mass (g/mol), these curves provide a description of the size distribution of the cellulose molecule chains from high to low molar mass regions. The low molar mass region represents degraded short chain glucans (Berggren, 2003). From the obtained MWD data, corresponding parameters Mw, intrinsic viscosity and PDI were acquired and displayed in Table 5.1.

Figure 5.1 shows the MWD of pulp samples that were exposed to Nd:YAG laser radiation at a wavelength of 266 nm for 15, 30 and 45 minutes respectively, the laser density (fluence) was kept in the range of 0.32 – 0.4 W/cm^2. The untreated pulp samples were used as a control, and the results are discussed in comparison to the control samples. A large redistribution of the Mw is observed between the laser irradiated samples and the control sample with increasing pretreatment time from 15 – 45 minutes. Chromatograms of the pretreated samples display a shift in Mw, from a high to a low molar mass region. Moreover, an increase in PDI after irradiation of pulp samples was observed compared to the untreated control (Table 5.1). Since PDI is a measure of the broadness of the MWD of a polymer, an increase in PDI suggests that the pretreatment was able to alter the molecular weight of the cellulose fibres by either degradation or chain scission (Strlič & Kolar, 2003).

The MWD curves of the pretreated samples show a sizeable shift from high to lower Mw values, and an increase in width compared to the narrow curve of the untreated control sample. However, the change between the irradiated samples does not show a significant difference with increasing treatment time. Nonetheless, the marked shift in the distribution of all the test samples suggests that laser irradiation caused degradation of the high molecular weight cellulose chains. A decrease in differential weight fraction is also observed, this suggests that the pretreatment resulted in cleavage of the long molecular chains to short chains. Chain scission leads to a decrease in the degree of polymerization (DP) which is an indirect measure of the viscosity of the polymer (Dupont & Mortha, 2004).

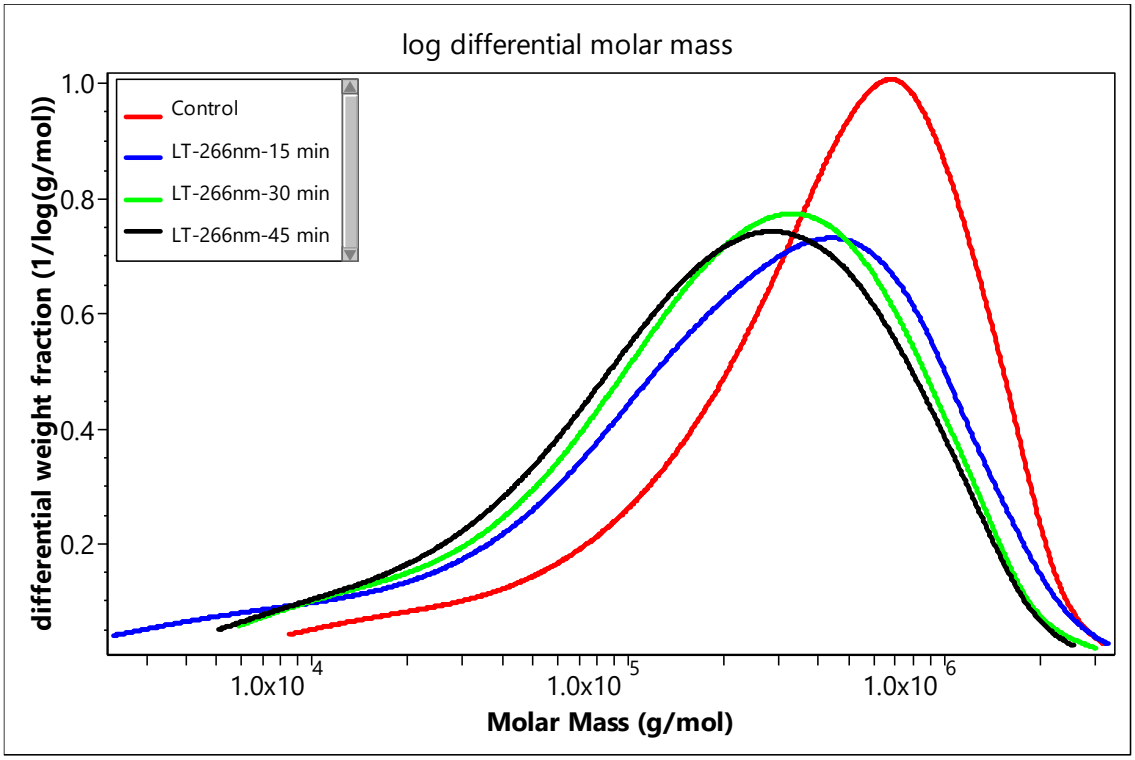

Figure 5.1: SEC-MALS chromatograms of the Nd:YAG laser irradiated samples (λ=266 nm for 15, 30 and 45 minutes) and control sample.

Similar observations are made in Figures 5.2 which displays the MWD of samples that were irradiated with the Nd:YAG laser at a wavelength of 355 nm. A noticeable decrease in Mw is displayed by the shift of the Mw curves to lower Mw regions for all the pretreated samples compared to the control. Figure 5.3 also displays the MWD of samples that were irradiated with the CO_2 laser at a wavelength of 10.6 um and power density in the range of 1.53 – 2.55 W/cm^2. A slight shift from high to lower Mw is observed for all the pretreated samples relative to the untreated control. However, the Mw shift achieved after pretreatment with CO_2 laser was minor compared to what was achieved when the samples were irradiated with Nd:YAG laser at both 266 nm and 355 nm. Overall, the chromatograms in Figures 5.1 -5.3 show that the elution of all the pretreated samples from the column was delayed compared to that of the control sample. The height of the peaks which expresses the differential weight fraction was also decreased. The evaluated laser wavelengths illustrate that optimal MWD shifts occurred when the samples were exposed to the laser for 45 minutes, and more so for the samples pretreated with Nd:YAG laser at 266 nm.

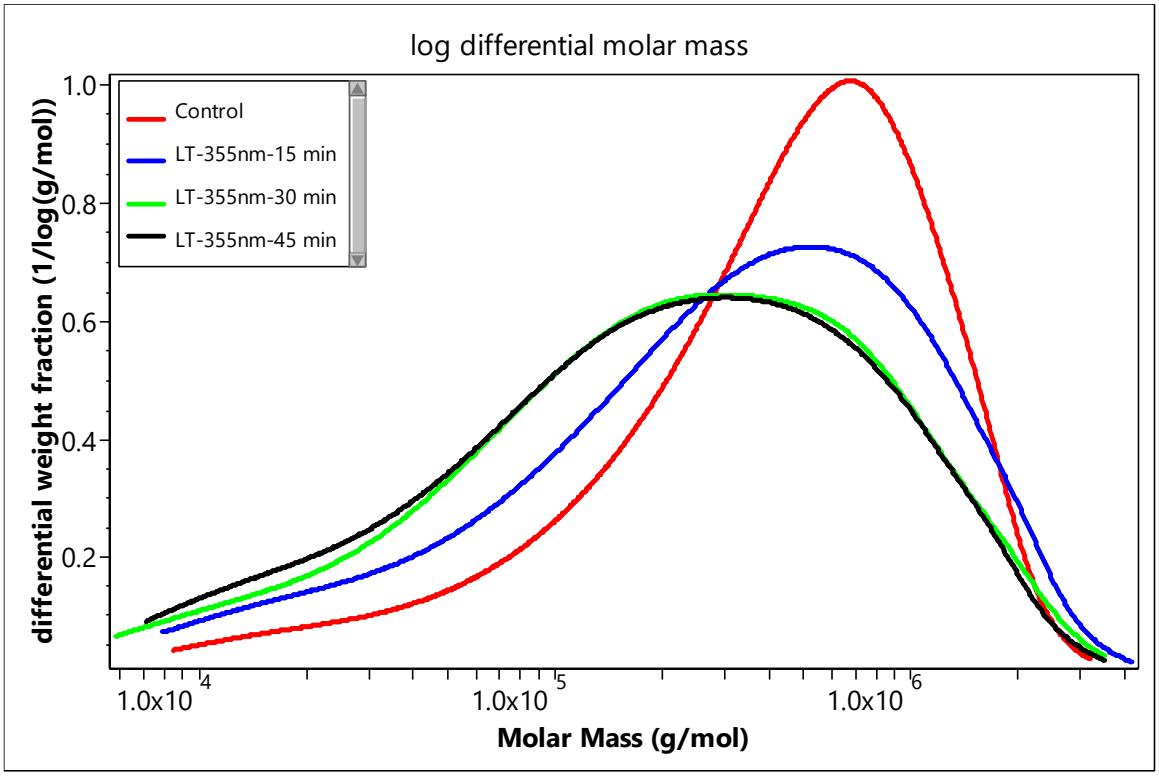

Figure 5.2: SEC-MALS chromatograms of the Nd:YAG laser irradiated samples (λ=355 nm for 15, 30 and 45 minutes) and control sample.

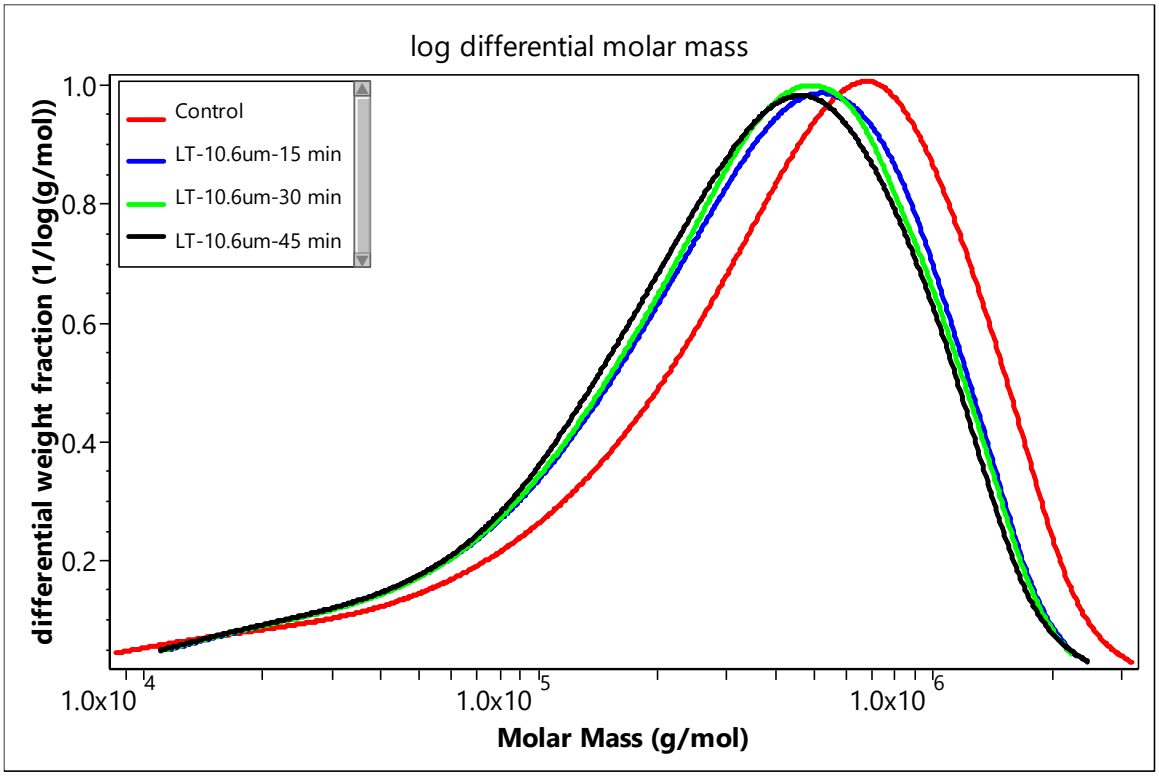

Figure 5.3: SEC-MALS chromatograms of the CO_2 laser irradiated samples (λ=10.6 μm for 15, 30 and 45 minutes) and control sample.

Table 5.1 presents a summary of MWD results that correspond to the changes observed in the chromatograms above (Figures 5.1 - 5.3) after laser irradiation. A linear decrease in both the molecular weight and intrinsic viscosity as a function of time was observed for all the irradiated samples compared to the untreated control sample. A drop in cellulose viscosity and molecular weight has been reported as an important factor that significantly affects the quality of the final product during the production of viscose rayon (Duan *et al.*, 2016). Viscosity is closely linked to polymer chain length; it is an indirect measure of the average degree of polymerization (DP) of cellulose chains, and it gives the extent to which the cellulose fibres were degraded during processing. Moreover, the change in cellulose rigidity due to its strong hydrogen bonds was shown in viscosity (Sjoholm, 2005). Therefore, a decrease in viscosity suggests that the tendency of the cellulose fibril to crystallise was reduced and cellulose accessibility was increased. On the other hand, a weak correlation was established between Polydispersity (PDI) and treatment time. An inconsistent increase in PDI was observed, but there was no linear trend demonstrated between the type of laser used for the pretreatment and the irradiation time.

Table 5.1: SEC-MALS MWD results of the samples irradiated with Nd:YAG laser at λ = 266, 355nm and CO_2 laser at λ = 10.6μm

Wavelength (nm/um)	**Irradiation time/min**	***Mw (x10^5 g/mol)**	***Intrinsic viscosity [η]w (mL/g)**	***PDI (Mw/Mn)**
Control	0	5.78±0.2	1218.0	4.28±0.2
Nd:YAG – 266nm	15	4.76 ±0.7	972.57	5.96±0.1
	30	4.12 ±0.6	1043.8	4.94±0.01
	45	4.03 ±0.4	879.38	4.67±0.3
Nd:YAG – 355nm	15	5.37 ±0.5	1120.1	4.68±0.8
	30	5.06 ±0.7	1130.4	4.04±0.9
	45	4.29 ±0.1	918.32	4.11±0.8
CO_2 – 10.6um	15	5.55 ±0.6	1203.5	3.10±0.4
	30	5.64 ±0.7	1227.9	3.25±0.9
	45	4.56 ±0.1	1141.03	3.03±0.03

*Mean calculated from a total of three experimental trials (n = 3)

Figures 5.4 and 5.5, present the effect of the Nd:YAG (λ = 266 & 355 nm) and CO_2 (λ = 10.6 μm) lasers on the molecular structure of cellulose is compared. Figure 5.4 displays a plot of molecular weight *versus* time for laser irradiated samples compared to the control sample. Percentage change in Mw lies between 17.7% – 30.2% for samples irradiated with Nd:YAG laser at 266 nm. For samples irradiated with Nd:YAG at 355 nm and CO_2 at 10.6 μm, change in Mw were between 7.1% – 25.8% and 2.5% – 10%, respectively. Furthermore, the effect on intrinsic viscosity (Figure 5.5) was also compared between the three different wavelengths. At 266 nm and 355 nm, an intrinsic viscosity decrease of 14% – 28% and 7% – 25% was achieved respectively. Moreover, for the CO_2 laser, a viscosity decline in the range 1% - 20% resulted.

The observed minimal changes in viscosity of CO_2 laser irradiated samples compared to the Nd:YAG laser treated samples at both 266 nm, and 355 nm wavelengths may be due to a more favourable radiation absorption of cellulose in the UV region compared to the IR region. Laser radiation in the UV spectrum has been reported to cause efficient photodegradation of cellulosic material compared to other radiation sources with higher wavelengths (Kolar *et al.*, 2000; Pandey & Vuorinen, 2008; Vargas-Radillo *et al.*, 2013).

A negative linear correlation was observed for both Mw with increasing irradiation time but not with intrinsic viscosity. However, a significant reduction in both Mw and intrinsic viscosity was observed for samples that were irradiated for 45 minutes and the Nd:YAG laser at 266 nm was the most effective compared to the Nd:YAG at 355 nm and the CO_2 laser emitting at 10.6 μm. Overall regression statistics analysis at 95% confidence level showed a significant decrease of the Mw for Nd:YAG laser irradiated samples at wavelengths, 266 nm and 355 nm respectively ($P = 0.05$, $P < 0.05$). A moderate decline was however observed for both intrinsic viscosity and PDI (P-value > 0.05 obtained for pretreatment with both Nd:YAG and CO_2 lasers). Observations from the presented results show that the Nd:YAG laser at both wavelengths was efficient at causing degradation of cellulose compared to the CO_2 laser which had a high power density. Laser radiation wavelength was the main influential parameter that caused the observed cellulose modifications.

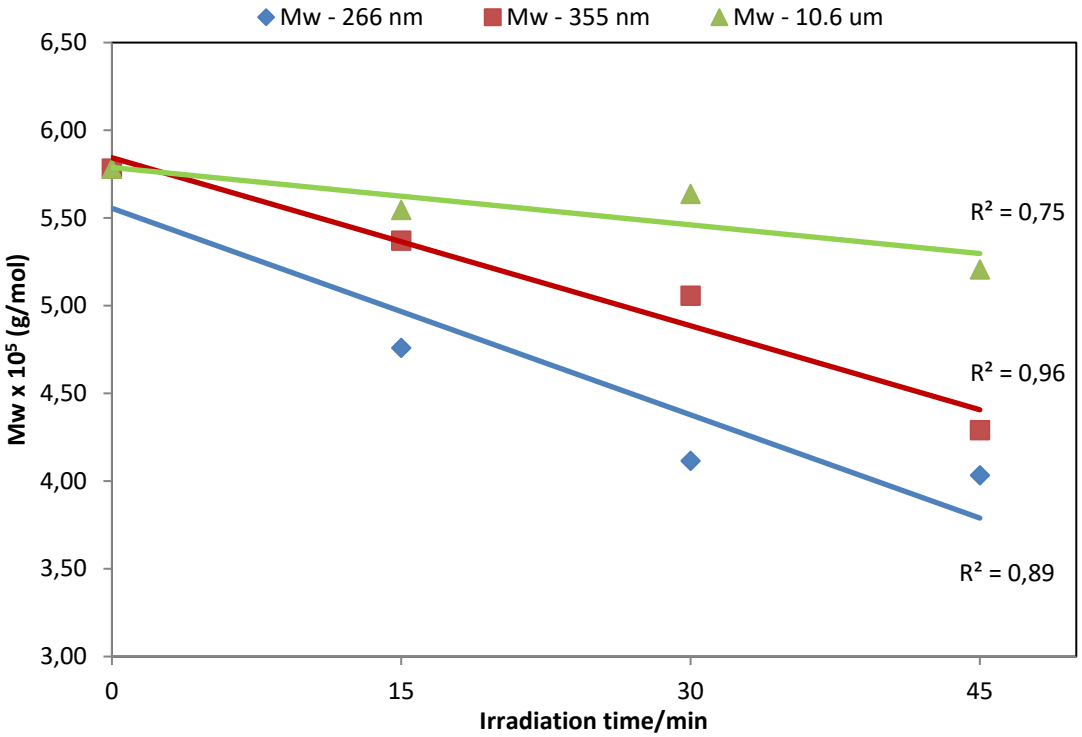

Figure 5.4: Decrease in molecular weight (Mw) of irradiated samples with increasing pretreatment time (15, 30 & 45 minutes).

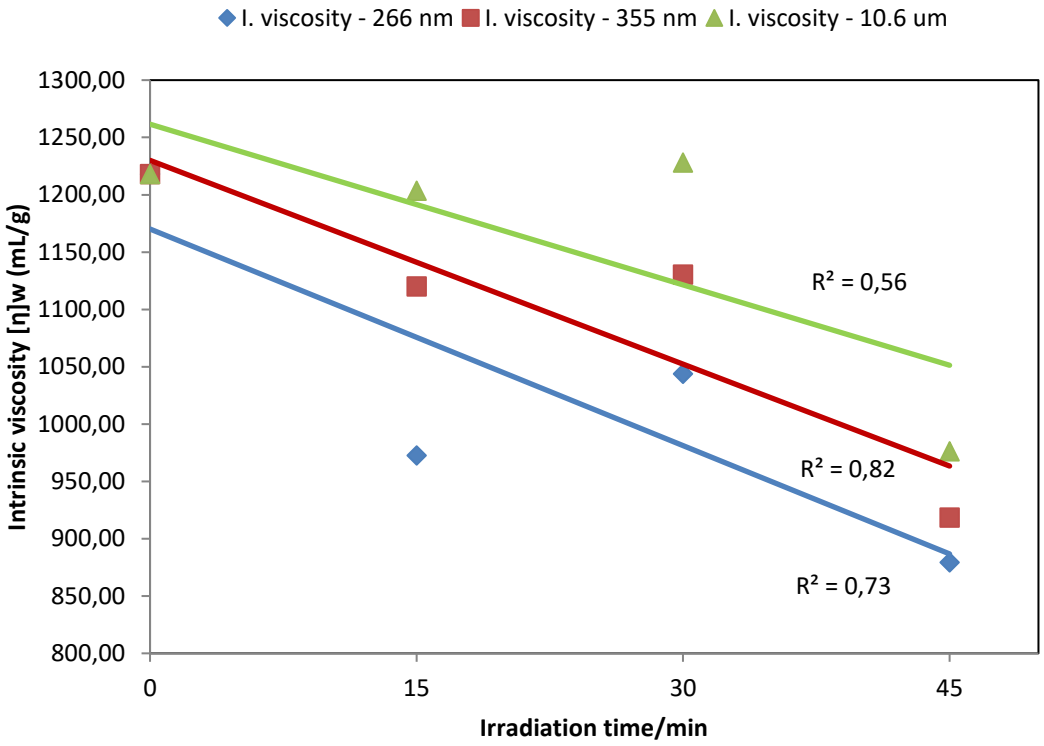

Figure 5.5: Intrinsic viscosity of the laser irradiated samples as a function of time

5.1.2 X-Ray Diffractions (XRD) results

Cellulose crystallinity has a significant influence on cellulose reactivity and processing. XRD is widely used in determining the crystallographic nature and characteristics of cellulose including the crystallinity index (CrI) (Park *et al.*, 2010; French & Cintrón, 2013).

Figures 5.6, 5.7 and 5.8 present superimposed XRD patterns obtained after laser irradiation of dissolving pulp samples compared to the control sample. The diffractograms display typical natural cellulose patterns which consist of three characteristic peaks at approximately two theta (2θ) = 14°, 16°, and 22°-24° which correspond to (101), (1-01) and (002) Miller indices (Park *et al.*, 2010). The high sharp intensity of the peaks defines the crystalline nature of the material, while the intensity value is a measure of the crystalline structure.

After laser irradiation, all the diffraction peaks of the test samples maintained the typical cellulose diffraction pattern even though the width of the peaks increased. They also overlapped with the control sample and shifted towards higher 2θ values. These observed peak shifts and broadening can be ascribed to three factors: instrumental effects, crystallite size, residual stress and strain on the crystal lattice due to the pretreatment (Zhao & Zhang, 2008; Mishra *et al.*, 2015). These factors have been reported to reduce the crystal grain sizes and cause amorphization of crystalline materials after exposure to high pressure and high temperature treatments (Zhao & Zhang, 2008). A decrease in the intensities of the peaks was also observed compared to the control sample. Using these XRD patterns, CrI values for XRD were calculated, and the results are presented in Table 5.2.

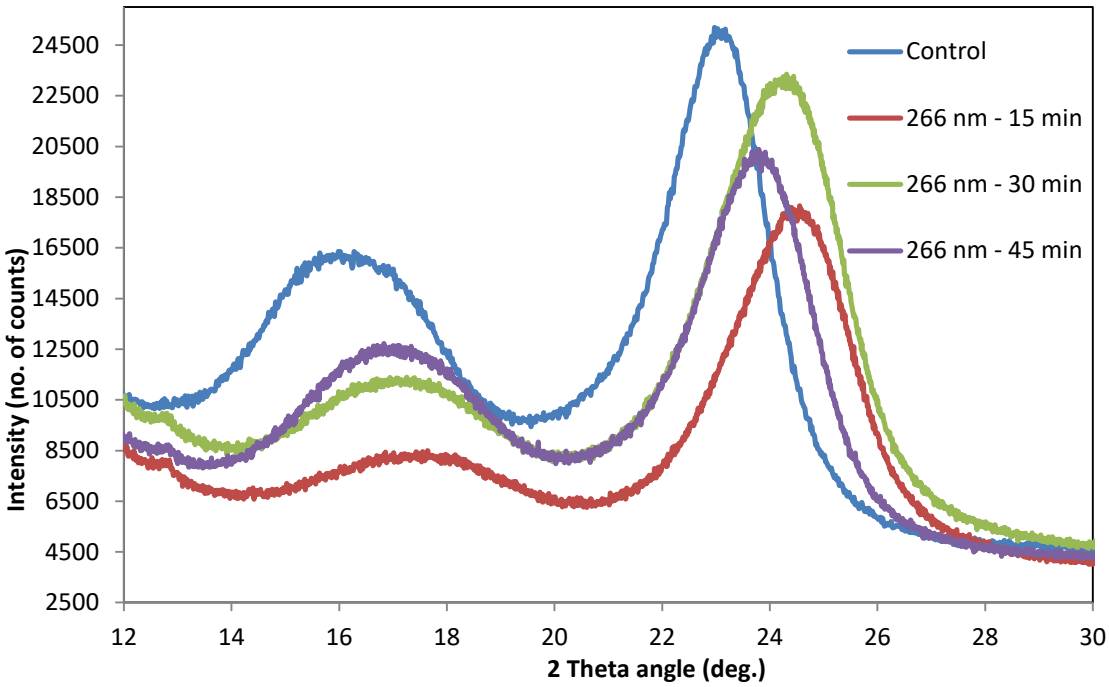

Figure 5.6: XRD pattern of dissolving pulp samples pretreated with the Nd:YAG laser at λ = 266 nm

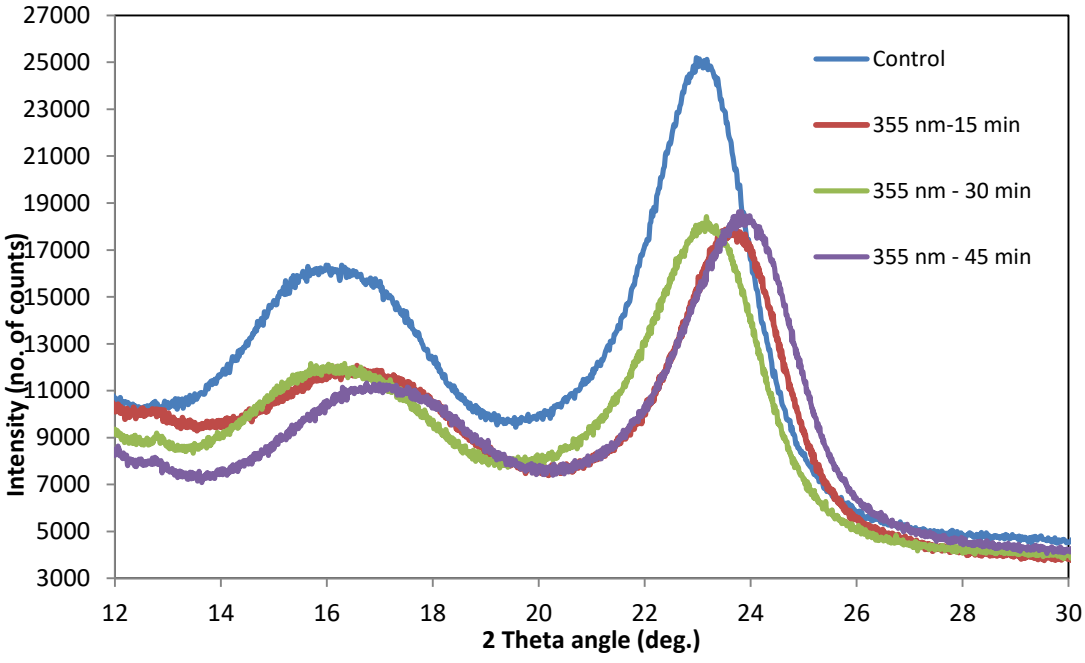

Figure 5.7: XRD pattern of dissolving pulp samples pretreated with the Nd:YAG laser at λ = 355 nm

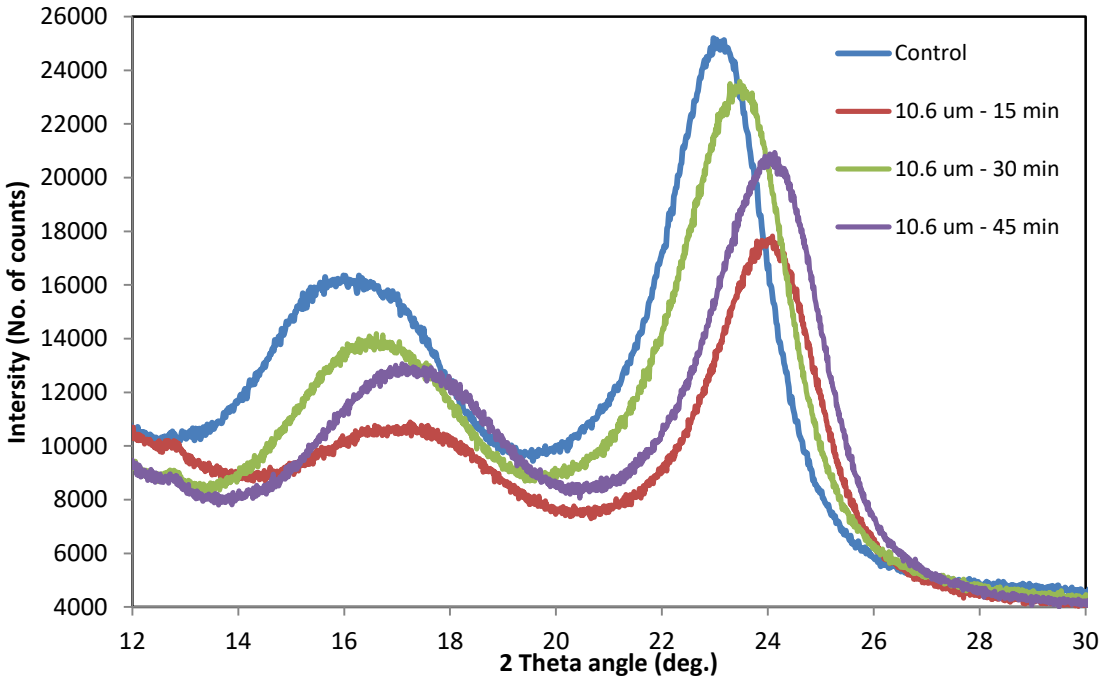

Figure 5.8: Superimposed XRD pattern of dissolving pulp samples pretreated with the CO_2 laser at $\lambda = 10.6$ μm

Table 5.2 displays CrI results calculated from the XRD peak intensities. After laser irradiation, there were minor changes in the CrI values. For samples irradiated with Nd:YAG laser at a wavelength of 266 nm, a slight decrease in CrI from 64.2% to 61.5%, 59.3% and 57.7% with increasing treatment time was observed. Samples that were irradiated with Nd:YAG at 355 nm and CO_2 at 10.6 μm respectively displayed a CrI decrease more than 10%. Compared to the control sample the degree of crystallinity samples treated at 355 nm decreased from 64.2% to 57.7%, 53.5%, and 54.8%, while samples treated at CO_2 decreased from 64.2% to 55.5%, 56.0% and 55.8% with increasing treatment time respectively. The overall CrI decrease between the three wavelengths does not show significant differences as it would otherwise be expected based on the discussed trends of Mw and its distributions in section 5.1.1.

A drop in the intensity and sharpness of the peaks confirms the observed decrease in CrI results. The % decrease recorded in Table 5.2 is presented graphically in Figure 5.9 to show the decline in %CrI as a function of laser irradiation time. A strong linear relationship is observed between the %CrI and treatment time for samples irradiation with Nd:YAG laser at 266nm compared to Nd:YAG laser and CO_2 laser. However, with

increasing treatment time the degree of crystallinity of the three wavelengths decreases. A negative linear correlation (R-value) of 0.99, 0.87 and 0.76 was obtained for Nd:YAG laser at 266nm, 355 nm, and CO_2 laser at 10.6 μm respectively.

Table 5.2: XRD results showing the effect of irradiation time on %CrI

Wavelength (nm/um)	**Time (min)**	**CrI - XRD (%)**
Control	0	64.2 ±4.1
Nd:YAG - 266 nm	15	61.5 ±1.5
	30	59.3 ±6.2
	45	57.7 ±2.0
Nd:YAG - 355 nm	15	57.5 ±1.6
	30	53.5 ±3.4
	45	54.8 ±0.8
CO_2 - 10.6 um	15	55.5 ±1.1
	30	56.0 ±5.1
	45	55.8 ±4.0

*Mean calculated from a total of three experimental trials (n = 3)

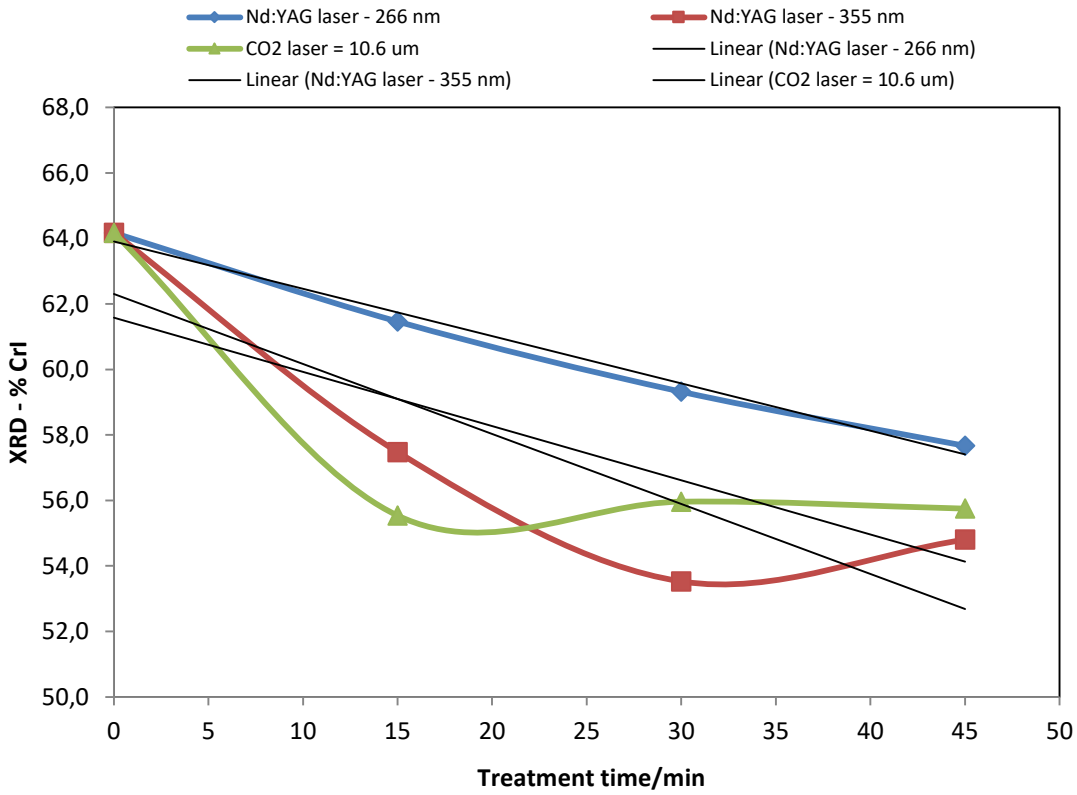

Figure 5.9: Graphical representation of the XRD %CrI results as a function of laser treatment time (0, 15, 30 and 45 minutes).

5.1.3 CP/MAS ^{13}C-Nuclear Magnetic Resonance (CP/MAS ^{13}C-NMR) results

CP/MAS solid-state ^{13}C-NMR spectroscopy is also one of the commonly used techniques for determining the degree of cellulose crystallinity or the crystallinity index (CrI). In this study, the solid state ^{13}C-NMR was used to monitor the ultrastructural changes that occurred on cellulose due to the pretreatment with the Nd:YAG and CO_2 lasers. Figures 5.10 to 5.12 display the region between 81 and 93 ppm which represents the C-4 region of the solid state ^{13}C-NMR spectra of the cellulose samples that were irradiated with Nd:YAG and CO_2 lasers for 15, 30 and 45 minutes. The spectra of the irradiated samples are superimposed together with the control sample. The peak at the resonance of 89 ppm is assigned to the C4 carbon in the crystalline cellulose, and the peak at 84 ppm is assigned to the C4 carbon of the non-crystalline cellulose (Larsson *et al.*, 1999).

The three spectra in Figures 5.10 to 5.12 do not show significant changes in the C4 region peaks that are used to estimate cellulose crystallinity compared to the control sample after pretreatment. Except, for the minor broadening of the peaks at 84 ppm for the samples

irradiated with Nd:YAG at 266 nm for 45 minutes and the one irradiated at 355 nm for 45 minutes. These slight or lack of changes in cellulose crystallinity after pretreatment are however to be expected because both NMR and XRD studies have reported that most of the pretreatment techniques do not have an effect on cellulose crystallinity (Zhao *et al.*, 2007).

Table 5.3 shows the CrI results of cellulose that were calculated by dividing the area of the crystalline peak (from 88 to 90 ppm) by the total area assigned to the peaks in the C-4 region (79 to 90 ppm). The crystallinity index results, on the other hand, display a slight decrease in the crystallinity of irradiated pulp samples, the reduction ranges between 2.0% to 9.1%. After 15 minutes irradiation of the pulp samples with Nd:YAG laser at 266 nm, the CrI decreased from 43.6 ±0.01 to 41.7 ±0.02. For samples treated with the same laser for 30 and 45 minutes respectively, the decrease was from 43.6 ±0.01 to 42.3 ±0.02 and 42.0 ±0.0. Radiation pretreatment of cellulose with shorter wavelength lasers has been reported to cause breakage of cellulose chain bonds and creation of shorter chains (Kaminska *et al.*, 2007).

On the other hand, irradiation of cellulose with higher wavelength lasers has been reported to lead to the formation of undesired intra- and intermolecular cross-links of ether origin which cause the DP to increase (Kolar *et al.*, 2000; Kolar *et al.*, 2003). Similar observations are made for samples that were irradiated with Nd:YAG laser at 355 nm and CO_2 laser at 10.6 μm. These observations correspond to the XRD CrI results presented in section 5.1.2 even though the decrease does not follow an identical pattern. This can be expected because these two techniques have underlying differences in terms of their measurement scales and estimates. The NMR provides sample information based on the physical and chemical environment, whereas XRD is sensitive to long-range order (Terinte *et al.*, 2011; Ahvenainen *et al.*, 2016). A decreasing trend in CrI is observed after laser irradiation (Figure 5.13), although the decrease does not show a linear relationship increasing treatment time for the different wavelengths used in this study (266, 355 nm and 10.6 μm).

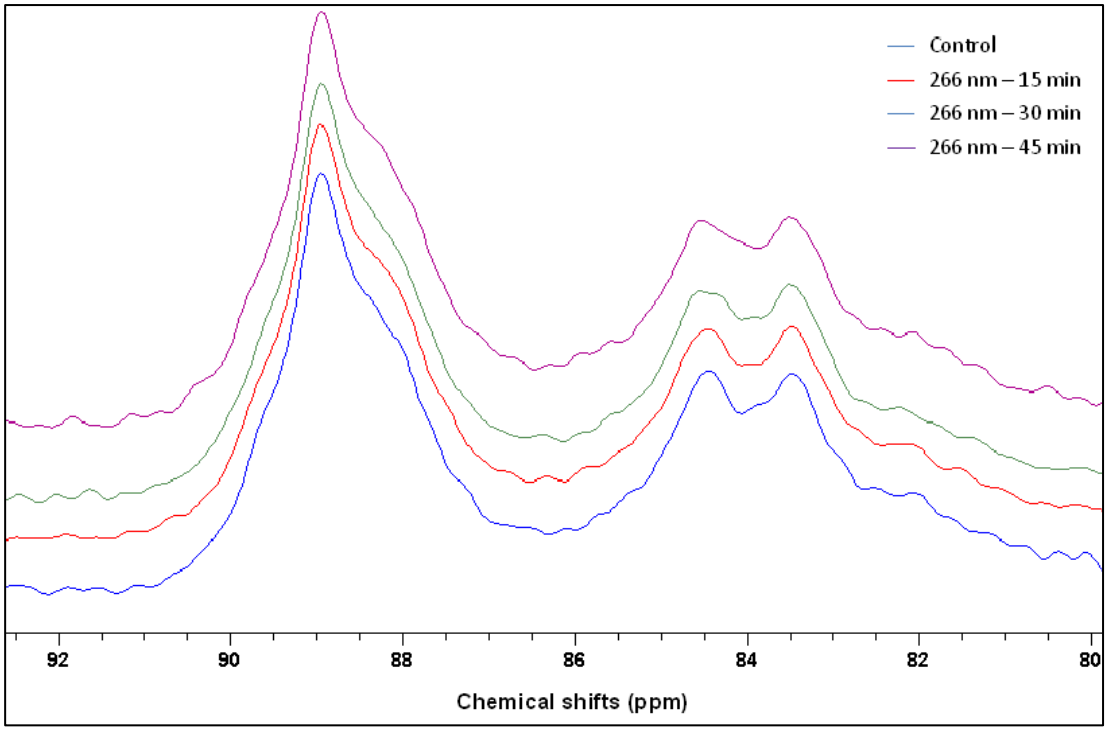

Figure 5.10: C-4 region of the ^{13}C-NMR spectra of the pulp samples irradiated with Nd:YAG laser at λ = 266 nm for 15, 30 and 45 minutes compared to the control

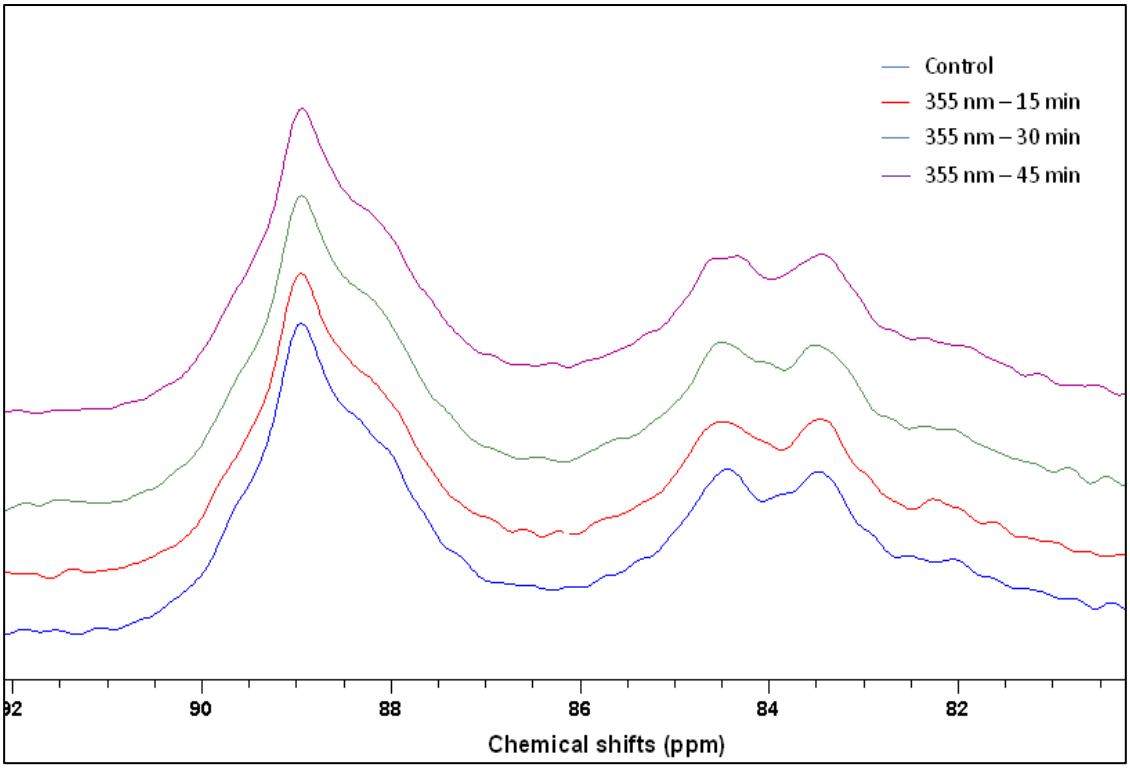

Figure 5.11: C-4 region of the ^{13}C-NMR spectra of pulp samples irradiated with Nd:YAG laser at λ = 355 nm for 15, 30 and 45 minutes compared to the control.

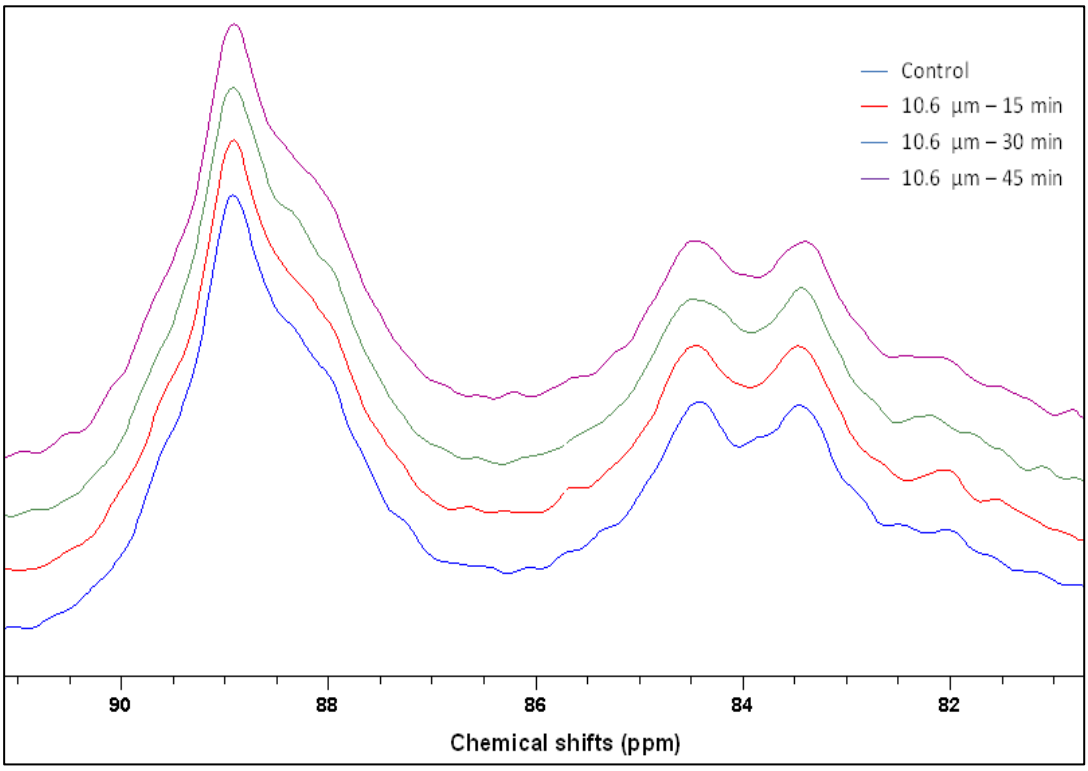

Figure 5.12: C-4 region of the ^{13}C-NMR spectra of the pulp samples irradiated with CO_2 laser at λ = 10.6 µm for 15, 30 and 45 minutes compared to the control

Table 5.3: Calculated CrI results of the Nd:YAG and CO_2 laser irradiated samples

Wavelength (nm/um)	**Time (min)**	**CrI - NMR (%)**
Control	0	43.6 ±0.01
Nd:YAG 266 nm	15	41.7 ±0.02
	30	42.3 ±0.02
	45	42.0 ±0.0
Nd:YAG 355 nm	15	42.9 ±0.01
	30	41.9 ±0.01
	45	42.9 ±0.01
CO_2 10.6 um	15	39.9 ±0.02
	30	40.1 ±0.01
	45	40.0 ±0.01

*Mean calculated from a total of three experimental trials (n = 3)

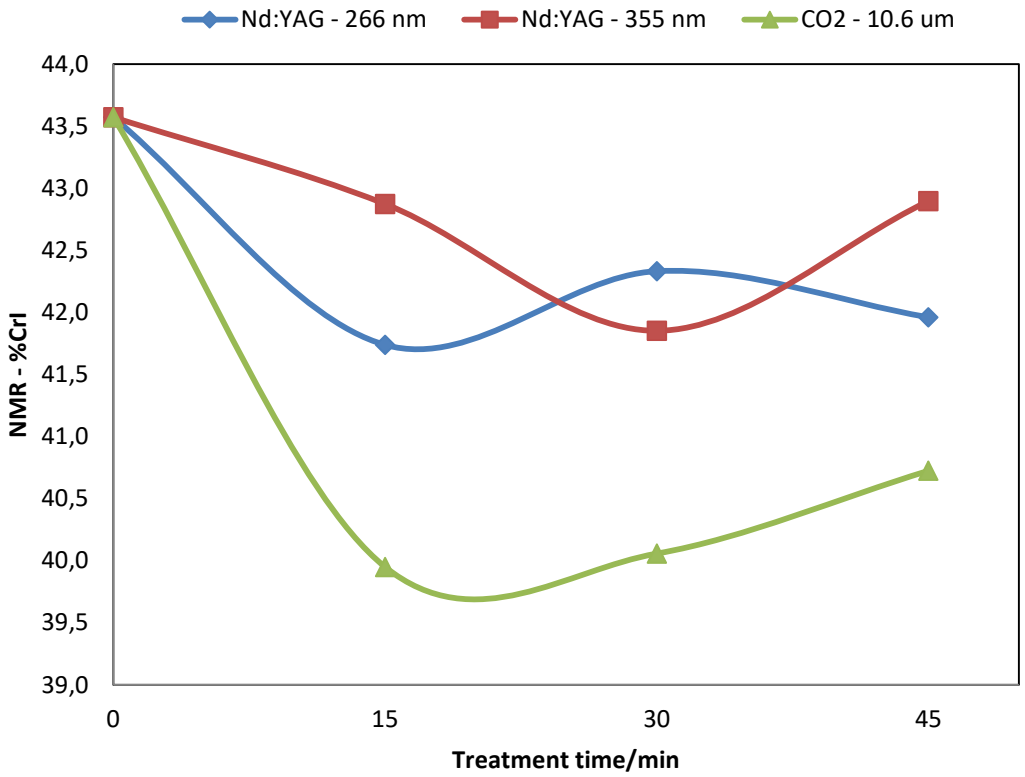

Figure 5.13: Graphical representation of the solid state ^{13}C NMR %CrI results as a function of treatment time (0, 15, 30 and 45 minutes).

5.1.4 Atomic Force Microscopy (AFM) results

The AFM in conjunction with image analysis was used to study the organization of the surface chains of cellulose and to assess topographical changes caused by the pretreatment. The Image Pro Plus (Version 6.0) software with watershed segmentation was used for processing the images and for calculating the lateral fibril aggregate dimensions (LFAD). Figure 5.14 presents AFM 1x1 μm phase images of the S2 cell wall layer of cellulose pulp samples after irradiation with Nd:YAG and CO_2 lasers (treatment time: 15, 30 and 45 minutes).

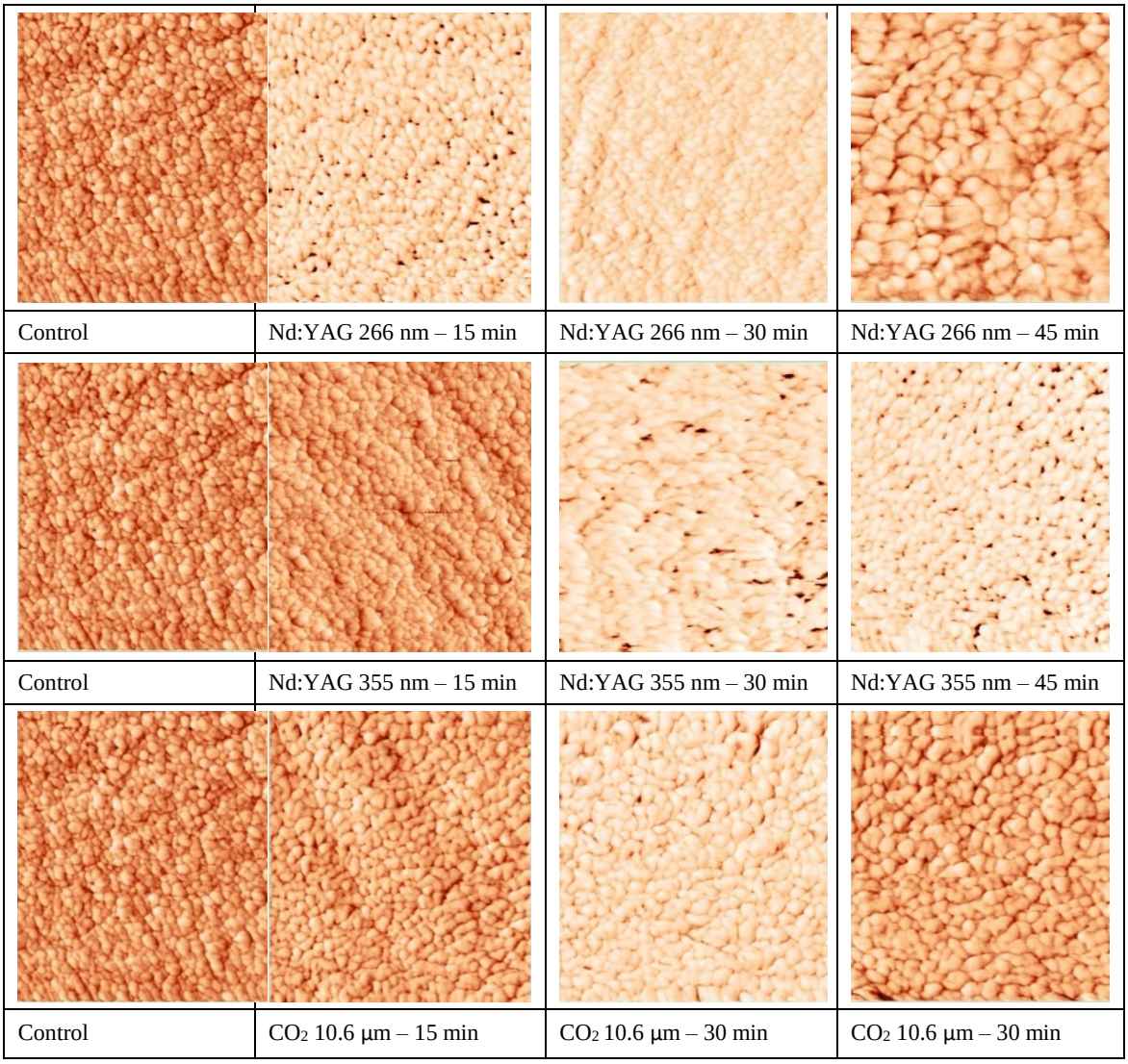

Figure 5.14: 1x1 µm AFM scans of the secondary plant cell wall (S2) layer for the pulp samples irradiated with Nd:YAG and CO_2 lasers and the untreated control sample.

The recorded AFM micrographs of the control sample displayed a dense agglomeration of the cellulose surface fibrils with an even alignment. On the other hand, the micrographs for the cellulose fibrils of the irradiated samples appeared sparse and less aggregated. In particular, more interesting observations were made on the samples that were irradiated with Nd:YAG laser at 266 nm for 15 minutes, and at 355 nm for 30 and 45 minutes. The surface of the samples showed an uneven surface with small holes which appeared as dark areas between the fibrils which may have been created by the pulse effect of the Nd:YAG laser. These findings correspond to what has been reported by (Fahlén & Salmén, 2005) that bright areas on the AFM images represent regions of high stiffness and dark areas represent the less stiff regions between the fibril aggregates. Furthermore, they correspond to what Choi and co-workers observed after pretreatment of natural

cellulose fibres with electron beam radiation. Their study observed that the pretreatment led to the removal of the pectin, wax and the primary layer from the cell wall (Choi *et al.*, 2008). This might have also contributed to the surface roughness and unevenness of the pretreated samples.

Perforation and loosening up of the cellulose fibril aggregates is an indication of increased reaction sites and accessibility for solvents during chemical processing of cellulose. Table 5.4 displays LFAD results for the irradiated sample. A linear decrease in the LFAD from 31.98±2.7 for the control sample to 23.8±4.4 nm was observed for pulp samples that were irradiated with Nd:YAG laser at 266 nm. An overall decrease in LFAD for samples irradiated with Nd:YAG laser at a wavelength of 355 nm and CO_2 laser at 10.6 μm was also observed, but a weak linear relationship was observed between the LFAD decline and the laser pretreatment times.

An inversely proportional relationship between the LFAD and the specific surface area (SSA) has widely been investigated, as well as the effect of these properties on the accessibility and reactivity of cellulose (Chunilall *et al.*, 2012). A decrease in LFAD leads to increased specific surface area; hence an increase in reaction sites and this enhances cellulose reactivity. AFM results presented below depict a decline in LFAD within the molecular cell wall structure.

Table 5.4: Calculated average lateral fibril aggregate dimensions (LFAD) results

Sample ID	Irradiation time/min	LFAD/nm
Control	0	31.98±2.7
Nd:YAG-266 nm	15	25.9±3.2
	30	24.0±3.0
	45	23.8±4.4
Nd:YAG-355 nm	15	24.8±4.1
	30	28.8±2.4
	45	25.4±1.3
CO_2 – 10.6 μm	15	24.9±3.4
	30	28.9±1.2
	45	22.5±0.9

*Mean calculated from a total of three experimental trials (n = 3)

5.1.5 Scanning Electron Microscopy (SEM) results

Cellulose pretreatment with the aim of improving its accessibility and reactivity towards chemical reagents is a significant step in the production of valuable cellulose derivatives (Chen, 2014). SEM analysis was performed on the laser irradiated pulp samples to characterise any surface morphology changes that might have occurred as a result of the laser pretreatment. Figure 5.15 presents SEM images obtained after the pretreatment with Nd:YAG laser at wavelengths of 266 nm and 355 nm, and the CO_2 laser at a wavelength of 10.6 μm.

The surface morphology of the pretreated samples was compared to the morphology of the untreated pulp sample. The untreated pulp samples displayed a smooth, but cracked surface with relatively straight lines and trenches parallel to the direction of the fibre axis. The micrographs for all the irradiated samples, on the other hand, indicated that to some degree, laser irradiation caused damage to the surface of the samples; the surface of the samples appeared rough with trenches and small holes with “sponge” like areas compared to the surface of the control sample.

The pulp samples irradiated with the Nd:YAG laser at a wavelength of 266 nm for 15 minutes showed that the surface of the pulp had cracks and terraces after the pretreatment.

Similar observations were made for samples irradiated with the same laser for 30 and 45 minutes respectively. The surface of the sample treated for 30 minutes showed small holes and fibrillation of the upper layer on the fibril. Pronounced peeling off and fold shapes on the fibre wall surface was also observed in the sample treated for 45 minutes. These modifications can be due to the effects of the radiation energy that have previously been reported such as cross-linking and breakage of the cellulose molecular chains (Martínez-Barrera *et al.*, 2015). These observations correspond to what has previously been reported in the literature that irradiation of cellulose fibres with a laser in the UV range especially at 266 nm affects the morphology of the fibres leading to peeling off of the outer fibre wall (Kaminska *et al.*, 2007).

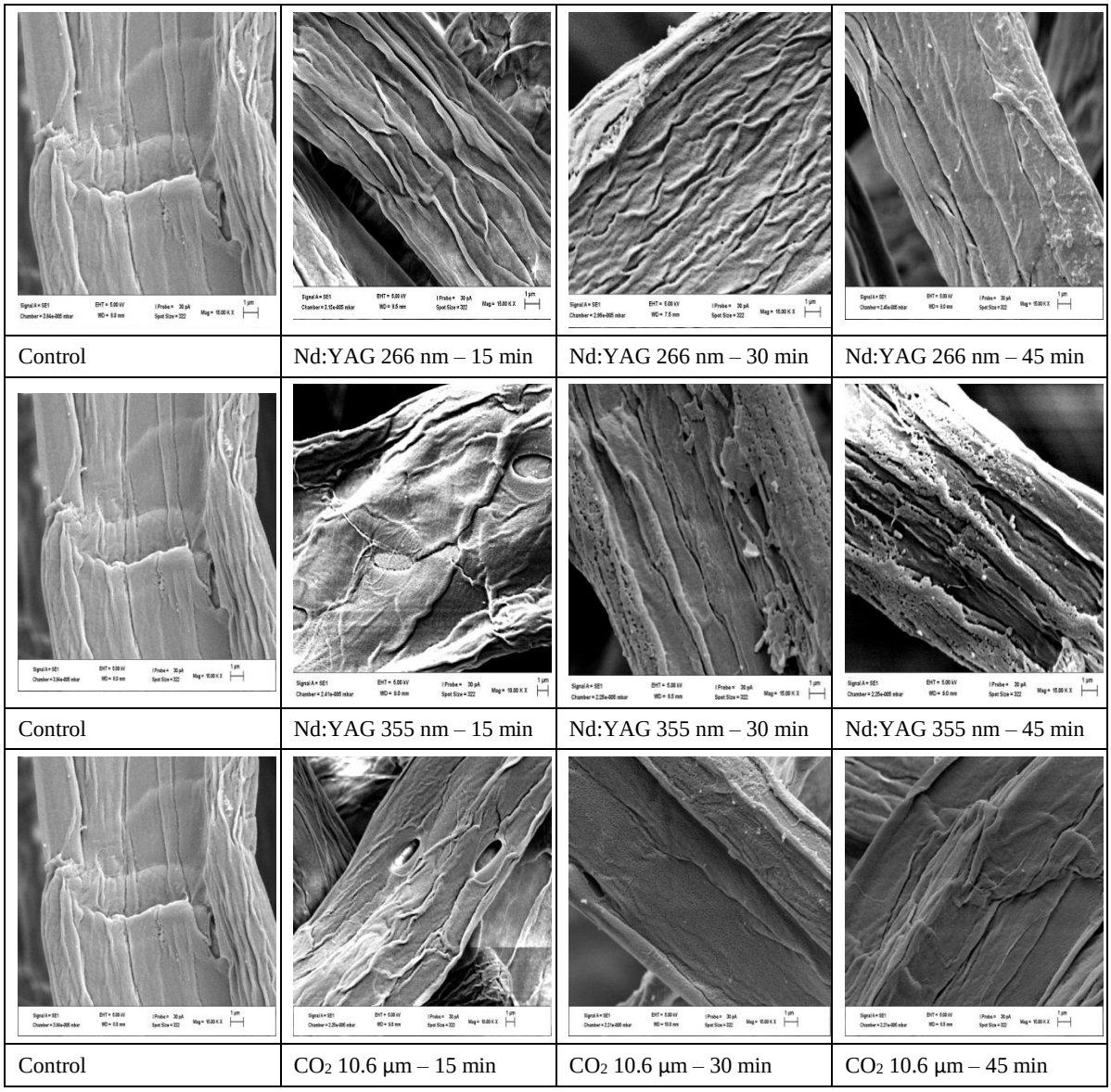

Figure 5.15: SEM images of pulp samples pretreated with laser radiation at three different wavelengths for different treatment times compared to the control.

SEM micrographs of samples irradiated with the Nd:YAG laser at 355 nm also showed that the surface of the cellulose material was disrupted. The surface of the samples irradiated for 30 and 45 minutes demonstrates that laser radiation pretreatment caused perforation and fibrillation of the fibre wall layers. The surface of all the irradiated pulp samples shows cracks and irregular terraces compared to the control sample. The observed cracks and surface pores have been suggested to be a result of dehydration of the pulp due to the thermal energy of the laser released during irradiation (Hung *et al.*, 2016). The surface of samples that were irradiated with a CO_2 laser at 10.6 µm also displayed kinks and a non-homogenous surface with wrinkles and cracks which

corresponds to what Chow and co-workers also reported (Chow *et al.*, 2010). The samples also showed small holes even though they were not pronounced compared to the Nd:YAG laser irradiated samples. These observations are comparable to what has been described by other scholars that lasers with shorter wavelengths such as 266 nm have a more visible effect on the surface of cellulose fibres compared to lasers with longer wavelengths (Kaminska *et al.*, 2007).

During laser irradiation, thermal energy is released from the laser source and absorbed by the cellulose samples; this leads to perforation and degradation of the polymer because of the high temperature (Hung *et al.*, 2016). Formation of pores on the surface of the cellulose exhibit a more open structure which would lead to improved exposure of the hydroxyl groups and increase reaction sites for processing. Ultimately, the disruption of the primary cell wall and exposure of the microfibers leads to the improved application of cellulose in various industries (Jiao & Xiong, 2014; Duan *et al.*, 2016). These observations correspond to those that have been discussed in the AFM images.

5.2 Cellulose reactivity results (Fock test method)

The Fock test is a widely used method for studying the reactivity of dissolving pulp, whereby the pulp is first mercerised with aqueous NaOH solution to form alkali cellulose which is subsequently reacted with carbon disulphide (CS_2) (Tian *et al.*, 2013). High cellulose reactivity is indicative of pulp homogeneity, and this is a major factor for the production of high-quality cellulose derivatives (Ibarra *et al.*, 2010).

In the present study, the effect of laser irradiation on cellulose pulp reactivity was determined by the Fock test, and the results are displayed in Table 5.5 and graphically represented in Figure 5.16. The effect of pretreatment time, laser power density and laser wavelengths on cellulose reactivity are displayed and discussed. Table 5.5 shows recorded Fock reactivity values (%); for the control pulp sample, % reactivity was noted as 44.2%. With increasing laser irradiation time, all samples display an overall linear increase in cellulose reactivity. For samples that were irradiated with Nd:YAG at 266 nm a sharp increase of 60.8%, 60.9%, and 60.9% in cellulose reactivity was achieved at with increasing pretreatment times of 15, 30 and 45 minutes respectively. This increase accounts for more than 35% increase in reactivity compared to the control sample. Fock

test reactivity for samples irradiated with Nd:YAG laser at 355 nm increased from 44.2% to 54.2%, 58.8% and 59.4% at a treatment time of 15, 30 and 45 minutes respectively. The reactivity increase ranged from 22% to 34%. Finally, the samples that were irradiated with a CO_2 laser at 10.6 μm also displayed a linear increase in reactivity from 48.3%, 54.3%, and 61.2% for samples irradiated for 15, 30 and 45 minutes respectively. Longer exposure of the samples to laser radiation did not have much effect on cellulose reactivity. Moreover, the greatest Fock reactivity increase was achieved in samples that were pretreated for 15 minutes with Nd:YAG at a wavelength of 266 nm. This observation can be attributed to what has been reported in the literature that UV laser irradiation can significantly disrupt the structure of cellulose and cause cellulose chains to break into shorter chains compared to lasers in the visible and near-IR ranges (Kaminska *et al.*, 2007; Pandey & Vuorinen, 2008).

The increase in cellulose reactivity was observed with increasing treatment time for all three wavelengths; a noticeable increase was recorded for samples irradiated with Nd:YAG at 266 nm and the CO_2 laser at 10.6 μm for 45 minutes. These observations correspond to previous reports which showed that cellulose activation before chemical processing increased the accessibility and reactivity of cellulose for downstream reactions (Kunze & Fink, 2005). Moreover, these results concur with a study by (Tian *et al.*, 2012) which showed that pretreatment of lignocellulosic biomass with CO_2 laser significantly increased the reactivity and the rate of cellulose saccharification for the production of bioethanol. However, these observations also displayed that laser wavelength was more efficient in cellulose modification than high power density.

Furthermore, this increase in cellulose reactivity is in correspondence with SEC-MALS molecular weight distribution data (Table 5.1) which showed that the pretreatment decreased the Mw and intrinsic viscosity of cellulose. The overall decrease in CrI and surface morphology characterization results also illustrated that laser irradiation pretreatment altered the structure of cellulose. Similar observations have been reported by Ibarra and colleagues when they observed that exposure of cellulose pulps to various enzymatic pretreatments modified the structural properties and behaviour of this polymer (Ibarra *et al.*, 2010).

Table 5.5: Fock test reactivity results for laser irradiated samples

Sample ID	Irradiation time/min	Fock reactivity (%)
Control	0	44.2±1.3
Nd:YAG-266 nm	15	60.8±0.8
	30	60.9±2.2
	45	60.9±1.7
Nd:YAG-355 nm	15	54.2±3.6
	30	58.8±4.0
	45	59.4±2.9
CO_2 – 10.6 µm	15	48.3±0.2
	30	54.3±2.4
	45	61.2±0.8

*Mean calculated from a total of three experimental trials (n = 3)

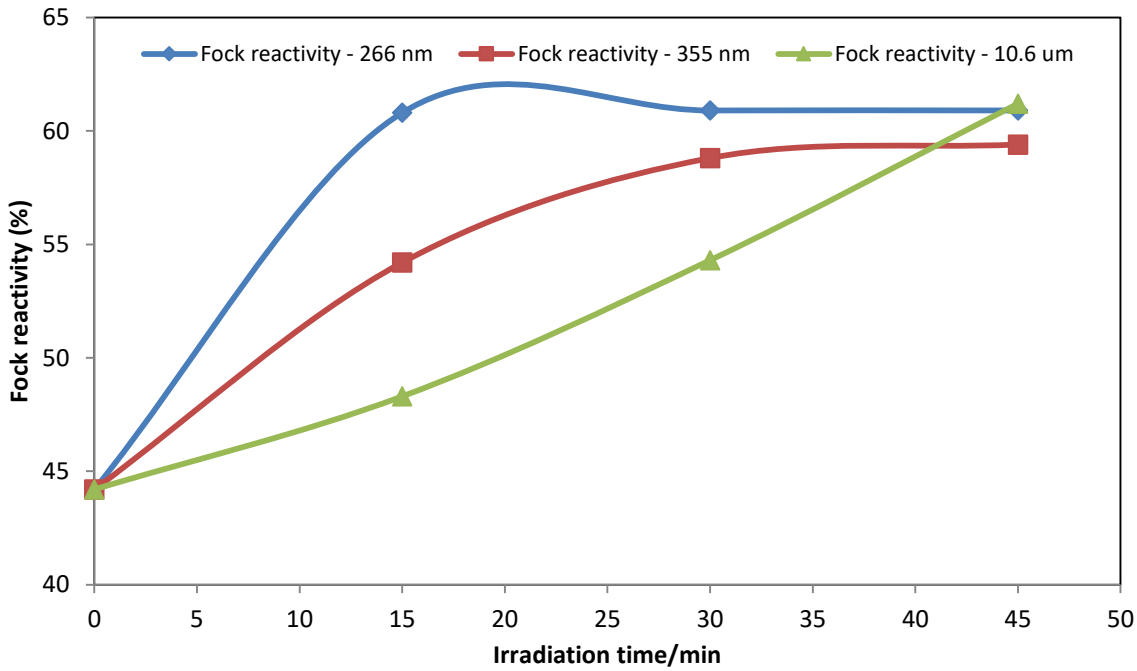

Figure 5.16: A plot of the Fock reactivity of cellulose pulp samples after laser irradiation as a function of treatment time (0, 15, 30 and 45 minutes).

Overall results and observations outlined in this chapter agree with what has been reported by other scholars that cellulose reactivity is greatly influenced by its structural characteristics, mainly; the degree of polymerization (DP) and crystallinity. With laser

irradiation, the average Mw and intrinsic viscosity of cellulose were altered, and this can be attributed to the cellulose chain scission during the pretreatment. This observation is in agreement with a study by Chow *et al.* (2011) which displayed a directly proportional relationship between the % weight loss of cotton and the laser irradiation time. Furthermore, a noticeable decrease in the degree of cellulose crystallinity was observed due to the disruption of the breakdown of the amorphous and crystalline regions of cellulose. This is comparable to what has been argued by several scholars using both ionising and non-ionising radiation technologies (Beardmore *et al.*, 1980; Dlugunovich *et al.*, 2003; Kubovsky & Kacik, 2009; Hsu *et al.*, 2012).

CHAPTER 6 – CONCLUSIONS AND RECOMMENDATIONS FOR FURTHER RESEARCH

6 Introduction

This section gives a comprehensive overview of the major observations, experimental findings and results obtained in this study, and conclusions deduced from them. Furthermore, recommendations for future work are outlined.

6.1 Conclusions

The primary focus of this study was to investigate the effect of ultrasound and laser irradiation on the structure of cellulose in dissolving wood pulp (raw material) and to further establish their impact on the dissolution behaviour and reactivity of this polymer. A variety of analytical instruments and characterization techniques were used to evaluate the influence of these two pretreatment technologies on the structural properties of cellulose. Moreover, observed structural modifications caused by the two methods were compared.

The goal of cellulose pretreatment is to activate cellulose by opening it up and disrupting its highly ordered crystalline structure to increase its chemical accessibility and thus improve its dissolution and reactivity. Therefore, after pretreatment of DWP samples with ultrasound and laser radiation respectively, alkali dissolution and Fock reactivity tests were performed. Alkali dissolution tests and structural characterization of the ultrasound irradiated samples were conducted, and the Fock reactivity tests were carried out on the laser irradiated samples.

A summary of the experimental results and observations that were made from this study is given below:

- SEC-MALS was used to characterise the Mw and MWD of cellulose after ultrasound and laser pretreatments. Results demonstrated that both techniques caused disruption on the molecular structure of cellulose. However, laser irradiated samples displayed more apparent modifications compared to the ultrasound irradiated samples. The effect of the two lasers on cellulose samples was also compared based on their power densities and wavelengths. The

chromatograms obtained from SEC-MALS analysis revealed that samples irradiated with the UV range laser, Nd:YAG experienced a noticeable shift in MWD and a decrease in Mw compared to the samples irradiated to the high wavelength CO_2 laser and the untreated control. Ultrasound irradiation resulted in minor alteration of the Mw and MWD compared to both the laser irradiated and the control samples. Moreover, the decrease in Mw and intrinsic viscosity relative to the untreated control also confirms that laser pretreatment resulted in cellulose chain scission and depolymerization.

- Ultrasonicated samples did not show outstanding alterations in Mw and MWD compared to the laser irradiated samples. Furthermore, after these samples were treated with an alkali solution, they displayed different dissolution behaviour relative to the irradiation time. The observed changes in MWD data did not show trends relative to treatment time.
- XRD results showed that laser irradiation efficiently disrupted the crystalline structure of cellulose compared to ultrasound irradiation pretreatment which displayed minor or no changes. This shift in cellulose crystallinity was demonstrated by the calculated decrease in CrI.
- Ultrasound irradiated samples only displayed significant changes and disruptions on the crystalline structure after the samples were treated with alkali. X-ray diffractograms showed characteristics of cellulose II allomorph; the transformation of native cellulose (cellulose I) to alkali cellulose (cellulose II) was demonstrated by the shift in 2θ peaks and the complete disruption of the high intensity crystallinity peak located at $2\theta = 22°\text{-}24°$ in native cellulose.
- SEM results showed that laser irradiation caused cracks, fibrillation and perforation of the fibre surfaces which may be due to laser thermal energy which is released in the form of heat. AFM results were in agreement with these observations: alterations and small pores in between cellulose fibril aggregates were observed. Moreover, LFAD results were also favourable, slight decreases in LFAD were observed suggesting a possible increase of surface reaction sites.
- Morphological analysis of ultrasonicated samples showed that the pretreatment removed the outer layer of the cellulose fibres and it able disrupted the amorphous regions. These observations concur with the XRD crystallinity results that demonstrated that ultrasonication did not have a significant effect on

cellulose crystallinity. However, when the samples were treated with aqueous NaOH solution after ultrasonication, a complete destruction of the cellulose crystalline structure was observed.

- Structural characterization results have shown that laser irradiation has the potential to cause cellulose degradation, with increasing pretreatment time, an average decrease of more than 10% in Mw, and intrinsic viscosity was obtained for samples that were irradiated with Nd:YAG laser emitting at both 266 nm and 355 nm. The intrinsic viscosity gives an indication of the DP of the irradiated samples. From these observations, it can be concluded that laser pretreatment caused cellulose fibre chains to break and decreased the DP of the polymer. Modified cellulose DP is a favourable condition for increased accessibility and reactivity of this biopolymer.
- Fock test results have shown that % reactivity of cellulose increased significantly after laser irradiation. Relative to the untreated control sample, samples irradiated with Nd:YAG emitting at 266 nm showed a reactivity increase of 35%, at 355 nm an increase of more 22% was achieved. For samples irradiated with a CO_2 laser emitting at 10.6 µm, a linear % increase of more than 35% was obtained with increasing treatment time.
- Laser wavelength and treatment time are parameters that had the greatest impact on the modification of cellulose. The Nd:YAG laser (fluence = 0.32 – 0.4 W/cm^2) is a low power laser compared to the CO_2 laser (fluence = 1.53 – 2.55 W/cm^2), but it was more effective in causing cellulose degradation and ultimately increasing cellulose reactivity from 44.2% to 60.8% within 15 minutes of treatment.
- Overall deductions from this study are that laser irradiation had a significant impact on the structural properties of dissolving pulp compared to ultrasound irradiation, the reactivity of cellulose was increased by more than 20% for all the irradiated samples compared to the control sample. Furthermore, significant structural modifications and % increase in cellulose reactivity were observed in samples pretreated with Nd:YAG laser emitting at 266 nm.

6.2 Recommendations for further research

The main aim and objectives of this study have been achieved. Findings and observations made in this study have demonstrated that laser irradiation is a prospective pretreatment technique that has effect on various structural properties of cellulose. The surface morphology and ultrastructural properties of the cellulose fibres were significantly modified compared to samples exposed to ultrasound irradiation. However, further research of laser radiation pretreatment is necessary in order to improve and develop this method into an effective technique for industrial usage.

Therefore, it would be interesting to investigate the following in future:

- To carry out a computer-based model study of laser radiation pretreatment of cellulose and to compare the simulated results with experimental results with the aim of optimising laser parameters such as the laser power density of the Nd:YAG and CO_2 lasers.
- Structural characterization results obtained in this study have shown that the laser radiation pretreatment can modify the surface properties and structure of cellulose without destroying the samples. Therefore, it would thus be interesting to evaluate the effect of increased treatment time on the structure of cellulose and to explore what effect laser resolution would have on this biopolymer.
- Cellulose pretreatment with high energy radiation techniques has been postulated to improve cellulose accessibility and reactivity, thus leading to a reduction in the amount of chemical reagents required for reactivity tests (i.e. NaOH and CS_2). Therefore, since Fock reactivity test results have shown that laser radiation pretreatment improved cellulose reactivity, it would be interesting to carry out reactivity tests on the pretreatment samples using varying concentrations of the chemical reagents. This will be done to determine whether the improved cellulose accessibility caused by laser irradiation will help to reduce the amount of chemical reagents required for Fock test method.
- To prepare cellulose derivatives (e.g., films and electrospun fibres) from the laser pretreated viscose dope, and examine the quality and properties of the resulting cellulose based products.
- To upscale the laser pretreatment technology and produce electrospun cellulose fibres for practical applications by electrospinning process.

- Finally, an investigation on the technical and economic feasibility on the application of this technique in an industrial mill scale would also be beneficial.

REFERENCES

AHVENAINEN, P., KONTRO, I. and SVEDSTRÖM, K., 2016. Comparison of sample crystallinity determination methods by X-ray diffraction for challenging cellulose I materials. *Cellulose,* **23**(2), pp. 1073-1086.

AIMIN, T., HONGWEI, Z., GANG, C., GUOHUI, X. and WENZHI, L., 2005. Influence of ultrasound treatment on accessibility and regioselective oxidation reactivity of cellulose. *Ultrasonics Sonochemistry,* **12**(6), pp. 467-472.

AKERHOLM, M., 2003. *Ultrastructural Aspect of Pulp Fibers as Studies by Dynamic FT-IR Spectroscopy. PhD Thesis*, Swedish Pulp and Paper Research Institute, Sweden.

ALBERTI, A., BERTINI, S., GASTALDI, G., IANNACCONE, N., MACCIANTELLI, D., TORRI, G. and VISMARA, E., 2005. Electron beam irradiated textile cellulose fibres.: ESR studies and derivatisation with glycidyl methacrylate (GMA). *European Polymer Journal,* **41**(8), pp. 1787-1797.

ALDAEUS, F., LARSSON, K., SRNDOVIC, J.S., KUBAT, M., KARLSTRÖM, K., PECIULYTE, A., OLSSON, L. and LARSSON, P.T., 2015. The supramolecular structure of cellulose-rich wood pulps can be a determinative factor for enzymatic hydrolysability. *Cellulose,* **22**(6), pp. 3991-4002.

ANTTI, G., PENTTI, P. and HANNA, K., 2008. Ultrasonic degradation of aqueous carboxymethylcellulose: effect of viscosity, molecular mass, and concentration. *Ultrasonics Sonochemistry,* **15**(4), pp. 644-648.

ATALLA, R.H., 1990. The structures of cellulose. *Materials Research Society,* **197**, pp. 89-98.

ATALLA, R.H., GAST, J., SINDORF, D., BARTUSKA, V. and MACIEL, G., 1980. Carbon-13 NMR spectra of cellulose polymorphs. *Journal of the American Chemical Society,* **102**(9), pp. 3249-3251.

ATALLA, R.H. and VANDERHART, D.L., 1999. The role of solid state 13C NMR spectroscopy in studies of the nature of native celluloses. *Solid State Nuclear Magnetic Resonance,* **15**(1), pp. 1-19.

ATALLA, R.H. and VANDERHART, D.L., 1984. Native cellulose: a composite of two distinct crystalline forms. *Science (New York, N.Y.),* **223**(4633), pp. 283-285.

AZEREDO, H.M.C.D., 2009. Nanocomposites for food packaging applications. *Food Research International,* **42**(9), pp. 1240-1253.

BADIEI, M., ASIM, N., JAHIM, J.M. and SOPIAN, K., 2014. Comparison of chemical pretreatment methods for cellulosic biomass. *APCBEE Procedia,* **9**, pp. 170-174.

BALAKHNINA, I.A., BRANDT, N.N., CHIKISHEV, A.Y. and REBRIKOVA, N., 2013. Effect of Laser Radiation on 19th Century Paper. *Restaurator,* **33**, pp. 30-44.

BALDACCHINI, G., DI LAZZARO, P., MURRA, D. and FANTI, G., 2008. Coloring linens with excimer lasers to simulate the body image of the Turin Shroud. *Applied Optics,* **47**(9), pp. 1278-1285.

BARATTIN, R. and VOYER, N., 2008. Chemical modifications of AFM tips for the study of molecular recognition events. *Chemical Communications,* (13), pp. 1513-1532.

BASS, M., 1983. Laser materials processing. 3rd edn. North Holland: Elsevier.

BEARDMORE, D.H., FAN, L.T. and LEE, Y., 1980. Gamma-Ray Irradiation as a Pretreatment for the Enzymatic Hydrolysis of Cellulose. *Biotechnology Letters,* **2**(10), pp. 435-438.

BERGGREN, R., 2003. *Cellulose degradation in pulp fibers studied as changes in molar mass distributions. PhD Thesis*, Royal Institute of Technology.

BERNHARD, K. and OPPERMANN, W., 2004. Molar Mass Distributions of cellulose by Analytical Ultracentrifugation. *Lenzinger Berichte,* **83**, pp. 60-63.

BESBES, I., VILAR, M.R. and BOUFI, S., 2011. Nanofibrillated cellulose from alfa, eucalyptus and pine fibres: preparation, characteristics and reinforcing potential. *Carbohydrate Polymers,* **86**(3), pp. 1198-1206.

BHATLA, A. and YAO, Y.L., 2008. LASER SURFACE TREATMENT OF A BIODEGRADABLE POLYMER AT VARYING FLUENCES. *Transactions of NAMRI/SME*, **36**, pp. 25-32.

BHATTACHARYA, A., 2000. Radiation and industrial polymers. *Progress in Polymer Science,* **25**(3), pp. 371-401.

BINNIG, G., QUATE, C.F. and GERBER, C., 1986. Atomic Force Microscope. *Physical Review Letters*, **56**(9), pp. 930-933.

BODHLYERA, O., ZEWOTIR, T., RAMROOP, S. and CHUNILALL, V., 2015. Analysis of the changes in the chemical properties of dissolving pulp during the bleaching process using piecewise linear regression models. *Cellulose Chemistry and Technology,* **49**(3-4), pp. 317-332.

BÖRJESSON, M. and WESTMAN, G., 2015. Crystalline Nanocellulose—Preparation, Modification, and Properties. In: M. POLETTO and L.O.J. ORNAGHI, eds, *Cellulose - Fundamental Aspects and Current Trends.* Gothenburg, Sweden: InTech, pp. 159-191.

BORYSIAK, S. and DOCZEKALSKA, B., 2005. X-ray diffraction study of pine wood treated with NaOH. *Fibres & Textiles in Eastern Europe,* **13**(5), pp. 87-89.

BOUCHARD, J., METHOT, M. and JORDAN, B., 2006. The Effects of Ionizing Radiation on the Cellulose of Woodfree Paper. *Cellulose,* **13**, pp. 601-610.

BOULNOIS, J., 1986. Photophysical processes in recent medical laser developments: a review. *Lasers in Medical Science,* **1**(1), pp. 47-66.

BRAGG, W.L., 1913. The structure of some crystals as indicated by their diffraction of X-rays, *Proceedings of the Royal Society of London A: Mathematical, Physical and Engineering Sciences,* September 1913, The Royal Society pp248-277.

BRODEUR, G., YAU, E., BADAL, K., COLLIER, J., RAMACHANDRAN, K.B. and RAMAKRISHNAN, S., 2011. Chemical and physicochemical pretreatment of lignocellulosic biomass: A review. *Enzyme Research,* pp. 1-17.

BROWN, R.M.J., 1999. Cellulose structure and biosynthesis. *Pure and Applied Chemistry,* **71**(5), pp. 767-775.

BURTON, J.O. and RASCH, R.H., 1931. The determination of the alpha-cellulose content and paper number of copper. *Bureau of Standards Journal of Research,* **6**(4), pp. 603-619.

BYUN, E., KIM, J., SUNG, N., CHOI, J., LIM, S., KIM, K., YOOK, H., BYUN, M. and LEE, J., 2008. Effects of gamma irradiation on the physical and structural properties of beta-glucan. *Radiation Physics and Chemistry,* **77**, pp. 781.

CARLMARK, A., LARSSON, E. and MALMSTRÖM, E., 2012. Grafting of cellulose by ring-opening polymerisation–A review. *European Polymer Journal,* **48**(10), pp. 1646-1659.

CARUSO, M.M., DAVIS, D.A., SHEN, Q., ODOM, S.A., SOTTOS, N.R., WHITE, S.R. and MOORE, J.S., 2009. Mechanically-induced chemical changes in polymeric materials. *Chemical reviews,* **109**(11), pp. 5755-5798.

CHANG, P.I. and ANDERSSON, S.B., 2011. Non-raster scanning in atomic force microscopy for high-speed imaging of biopolymers. *Control Technologies for Emerging Micro and Nanoscale Systems.* Springer, pp. 101-117.

CHAPIRO, A., 2002. XIIth international meeting on radiation processing Avignon 25–30 March 2001 (Polymer irradiation: past–present and future). *Radiation Physics and Chemistry,* **63**(3–6), pp. 207-209.

CHEN, H., 2014. Chapter 4.3: Pretreatment Technology of Natural Lignocelluloses. *Biotechnology of Lignocellulose: Theory and Practice Technology Engineering.* China: Chemical Industry Press, pp. 151-524.

CHEN, Y., WU, Q., HUANG, B., HUANG, M. and AI, X., 2014. Isolation and characteristics of cellulose and nanocellulose from lotus leaf stalk agro-wastes. *BioResources,* **10**(1), pp. 684-696.

CHENG, Q., WANG, S. and HAN, Q., 2010. Novel process for isolating fibrils from cellulose fibers by high-intensity ultrasonication. II. Fibril characterization. *Journal of Applied Polymer Science,* **115**(5), pp. 2756-2762.

CHENG, Q., WANG, S. and RIALS, T.G., 2009. Poly (vinyl alcohol) nanocomposites reinforced with cellulose fibrils isolated by high intensity ultrasonication. *Composites Part A: Applied Science and Manufacturing,* **40**(2), pp. 218-224.

CHEVALIER-BILLOSTA, V., JOSELEAU, J., COCHAUX, A. and RUEL, K., 2007. Tying together the ultrastructural modifications of wood fibre induced by pulping processes with the mechanical properties of paper. *Cellulose,* **14**(2), pp. 141-152.

CHMIELEWSKI, A.G. and HAJI-SAEID, M., 2004. Radiation technologies: past, present and future. *Radiation Physics and Chemistry,* **71**(1–2), pp. 17-21.

CHMIELEWSKI, A.G. HAJI-SAEID, M.et al AHMED, S. 2005. *Progress in radiation processing of polymers*. Available from: <**http://www.sciencedirect.com/science/article/pii/S0168583X0500474X**>.

CHOI, H.Y., HAN, S.O. and LEE, J.S., 2008. Surface morphological, mechanical and thermal characterization of electron beam irradiated fibers. *Applied Surface Science,* **255**(5, Part 1), pp. 2466-2473.

CHOW, Y.L., CHAN, C.K. and AND KAN, C.W., 2010. SEM analysis of CO_2 laser treated cotton grey fabric. In: A. MENDEZ-VILAS and J. DIAZ, eds, *Microscopy: Science, Technology, Applications and Education.* 4 edn. Spain: Formatex Research Centre, pp. 1860-1867.

CHOW, Y., CHAN, C. and KAN, C., 2011. Effect of CO2 laser treatment on cotton surface. *Cellulose,* **18**(6), pp. 1635-1641.

CHRISTOFFERSSON, K.E., 2005. *Dissolving Pulp - Multivariate Characterisation and Analysis of Reaction and Spectroscopic Properties. PhD Thesis*, Umea University.

CHRISTOFFERSSON, K.E., SJÖSTRÖM, M., EDLUND, U., LINDGREN, Å and DOLK, M., 2002. Reactivity of dissolving pulp: characterisation using chemical properties, NMR spectroscopy and multivariate data analysis. *Cellulose,* **9**(2), pp. 159-170.

CHUNILALL, V., 2009. *Structure, Accessibility and 'Reactivity' of Cellulose I as revealed by CP/MAS ^{13}C-NMR Spectroscopy and Atomic Force Microscopy. PhD Thesis*, University of KwaZulu-Natal.

CHUNILALL, V., BUSH, T. and ERASMUS, R., 2012. Investigating the lignocellulosic composition during delignification using confocal Raman spectroscopy, Cross-Polarization Magic Angle Spinning Carbon 13-Nuclear Magnetic Resonance (CP/MAS 13C-NMR) spectroscopy and Atomic Force Microscopy. *Cellulose Chemistry and Technology,* **46**(3-4), pp. 269-276.

CHUNILALL, V., WESLEY-SMITH, J. and BUSH, T., 2006. Cellulose fibril aggregation studies of Eucalyptus dissolving pulps using atomic force microscopy. *Proc. Microsc. Society of South Africa,* **36**(45), pp. 54.

CHUNILALL, V., BUSH, T. and LARSSON, P.T., 2013. Supra-molecular structure and chemical reactivity of cellulose I studied using CP/MAS (sup) 13 C-NMR. In: T. VAN DE VEN and L. GODBOUT, eds, *Cellulose - Fundamental Aspects.* Croatia: Intech Publishing, pp. 69-90.

CHUNILALL, V., BUSH, T., LARSSON, P.T., IVERSEN, T. and KINDNESS, A., 2010. A CP/MAS 13C-NMR study of cellulose fibril aggregation in eucalyptus dissolving pulps during drying and the correlation between aggregate dimensions and chemical reactivity. *Holzforschung,* **64**(6), pp. 693-698.

CIOLACU, D., CIOLACU, F. and POPA, V.I., 2011. Amorphous cellulose—structure and characterization. *Cellulose Chemistry and Technology,* **45**(1), pp. 13-21.

CLELAND, M.R., HERER, A.S., JONGEN, Y., ABS, M., MEISSNER, J. and KERLUKE, D.R., 1999. A Rhodotron Electron Beam Facility for Pre-Treatment of Cellulosic Pulp. *The American Institute of Physics,* **475**, pp. 953-956.

CLELAND, M.R., 2006. Industrial applications of electron accelerators, D. BRANDT, ed. In: *Small Accelerators,* 24th May - 2nd June 2005 2006, CERN Accelerator School pp383-416.

CLELAND, M., PARKS, L. and CHENG, S., 2003. Applications for radiation processing of materials. *Nuclear Instruments and Methods in Physics Research Section B: Beam Interactions with Materials and Atoms,* **208**, pp. 66-73.

CLOUGH, R.L., 2001. High-energy radiation and polymers: A review of commercial processes and emerging applications. *Nuclear Instruments and Methods in Physics Research Section B: Beam Interactions with Materials and Atoms,* **185**(1–4), pp. 8-33.

CONNER, A.H., 1995. Size exclusion chromatography of cellulose and cellulose derivatives. *Chromatographic Science Series,* **69**, pp. 331-352.

COPOLOVICI, D. and SÎRGHIE, C., 2013. Structural Investigation by Atomic Force Microscopy. *Scientific Bulletin of ESCORENA,* **8**, pp. 23-29.

CZAJA, W., KRYSTYNOWICZ, A., BIELECKI, S. and BROWN, R.M., 2006. Microbial cellulose—the natural power to heal wounds. *Biomaterials,* **27**(2), pp. 145-151.

DAHLAN, K.Z.H.M., 2001. 18 RADIATION SCIENCES. In: G.O. PHILLIPS and A. NATHER, eds, *The Scientific Basis of Tissue Transplantation.* Singapore: World Scientific, pp. 309-341.

DEE SNELL, F., 1926. Rayon by the viscose process. *Journal of Chemical Technology and Biotechnology,* **45**(50), pp. 925-926.

DLUGUNOVICH, V.A., ZHBANKOV, R., ZHDANOVSKII, V.A., NASENNIK, L., PUHNAREVICH, S. and FIRSOV, S., 2003. Changes in IR spectra of polysaccharides induced by CW CO2-laser radiation, M. PLUTA and M. SZYJER, eds. In: *Lightmetry 2002: Metrology and Testing Techniques using Light.* 7th April 2003, International Society for Optical Engineering pp98-102.

DONALDSON, L., 2007. Cellulose microfibril aggregates and their size variation with cell wall type. *Wood Science and Technology,* **41**(5), pp. 443-460.

DUAN, C., VERMA, S.K., LI, J., MA, X. and NI, Y., 2016. Viscosity control and reactivity improvements of cellulose fibers by cellulase treatment. *Cellulose,* **23**(1), pp. 269-276.

DUBEY, K.A., PUJARI, P.K., RAMNANI, S.P., KADAM, R.M. and SABHARWAL, S., 2004. Microstructural studies of electron beam-irradiated cellulose pulp. *Radiation Physics and Chemistry,* **69**(5), pp. 395-400.

DUPONT, A. and MORTHA, G., 2004. Comparative evaluation of size-exclusion chromatography and viscometry for the characterisation of cellulose. *Journal of Chromatography A,* **1026**(1–2), pp. 129-141.

DURBAK, I., 1993. *Dissolving Pulp Industry - Market Trends.* FPL-GTR-77. Madison, WI, USA: Department of Agriculture, Forest Service.

DUTTA MAJUMDAR, J. and MANNA, I., 2011. Laser material processing. *International materials reviews,* **56**(5-6), pp. 341-388.

EL-DESSOUKY, H.M., 2014. Novel surface treatments for high perfomance textiles. In: C. LAWRENCE, ed, *High performance textiles and their applications.* Ed edn. Cambridge, UK: Woodhead Publishing, pp. 70-90.

ELECTROPAEDIA, 2005-last update, electromagnetic radiation and radio waves (natural and man-made miracles) [Homepage of Woodbank Communications Ltd.], [Online]. Available: **http://www.mpoweruk.com/radio.htm** [03/04, 2017].

ENGSTROM, A., EK, M. and HENRIKSSON, G., 2006. Improved accessibility and reactivity of dissolving pulp for the viscose process: Pretreatment with monocomponent endoglucanase. *Biomacromolecules,* **7**(6), pp. 2027-2031.

EPA, 2012. *Radiation: Facts, Risks and Realities.* EPA-4-2-K-10-008. United States: United States Environmental Protection Agency.

ERIKSSON, H., 2014. *Cellulose Reactivity- difference between Sulfite and PHK dissolving pulps. MSc Dissertation*, Umea University.

ERSHOV, B. and KLIMENTOV, A., 1984. The radiation chemistry of cellulose. *Russian Chemical Reviews,* **53**(12), pp. 1195-1207.

ESA, F., TASIRIN, S.M. and RAHMAN, N.A., 2014. Overview of Bacterial Cellulose Production and Application. *Agriculture and Agricultural Science Procedia,* **2**, pp. 113-119.

EVANS, R., NEWMAN, R.H., ROICK, U.C., SUCKLING, I.D. and WALLIS, A.F., 1995. Changes in cellulose crystallinity during kraft pulping. Comparison of infrared, X-ray diffraction and solid-state NMR results. *Holzforschung-International Journal of the Biology, Chemistry, Physics and Technology of Wood,* **49**(6), pp. 498-504.

FAHLÉN, J. and SALMÉN, L., 2005. Pore and matrix distribution in the fiber wall revealed by atomic force microscopy and image analysis. *Biomacromolecules,* **6**(1), pp. 433-438.

FAHLÉN, J. and SALMÉN, L., 2003. Cross-sectional structure of the secondary wall of wood fibers as affected by processing. *Journal of Materials Science,* **38**(1), pp. 119-126.

FAHLÉN, J. and SALMÉN, L., 2002. On the lamellar structure of the tracheid cell wall. *Plant Biology,* **4**(03), pp. 339-345.

FANG, Z., LIU, K., CHEN, F., ZHANG, L. and GUO, Z., 2014. Cationic Surfactant-assisted microwave-NaOH pretreatment for enhancing enzymatic hydrolysis and fermentable sugar yield from peanut shells. *BioResources,* **9**(1), pp. 1290-1302.

FESTUCCI-BUSELLI, R.A., OTONI, W.C. and JOSHI, C.P., 2007. Structure, organization, and functions of cellulose synthase complexes in higher plants. *Brazilian Journal of Plant Physiology,* **19**(1), pp. 1-13.

FOCK, W., 1959. A modified method for determining the reactivity of viscose-grade dissolving pulps. *Papier,* **13**, pp. 92-95.

FOSTON, M.B., HUBBELL, C.A. and RAGAUSKAS, A.J., 2011. Cellulose isolation methodology for NMR analysis of cellulose ultrastructure. *Materials,* **4**(11), pp. 1985-2002.

FRENCH, A.D. and CINTRÓN, M.S., 2013. Cellulose polymorphy, crystallite size, and the Segal crystallinity index. *Cellulose,* **20**(1), pp. 583-588.

FRONE, A., PANAITESCU, D., DONESCU, D., SPATARU, R., C., TRUSCA, R. and SOMOGHI, R., 2011. Preparation and characterization of PVA composites with cellulose nanofibers obtained by ultrasonication. *Bioresources,* **6**(1), pp. 487-512.

FUNES, D., 30 May 2013, 2013-last update, 3.2 carbohydrates [Homepage of Biomedicine Blog], [Online]. Available: **http://www.davidfunesbiomed.eu/2015_10_01_archive.html** [October/12, 2016].

GABHANE, J., WILLIAM, S.P., VAIDYA, A.N., ANAND, D. and WATE, S., 2014. Pretreatment of garden biomass by alkali-assisted ultrasonication: effects on enzymatic hydrolysis and ultrastructural changes. *Journal of Environmental Health Science and Engineering,* **12**(76), pp. 1-6.

GABORIEAU, M. and CASTIGNOLLES, P., 2011. Size-exclusion chromatography (SEC) of branched polymers and polysaccharides. *Analytical and Bioanalytical Chemistry,* **399**(4), pp. 1413-1423.

GARCIA-LOPERA, R., CODONER, A., BANO, M.C., ABAD, C. and CAMPOS, A., 2005. Size-exclusion chromatographic determination of polymer molar mass averages using a fractal calibration. *Journal of Chromatographic Science,* **43**(5), pp. 226-234.

GARDNER, K. and BLACKWELL, J., 1974. The hydrogen bonding in native cellulose. *Biochimica et Biophysica Acta (BBA)-General Subjects,* **343**(1), pp. 232-237.

GEHMAYR, V., SCHILD, G. and SIXTA, H., 2011. A precise study on the feasibility of enzyme treatments of a kraft pulp for viscose application. *Cellulose,* **18**(2), pp. 479-491.

GIESSIBL, F.J., 2003. Advances in Atomic Force Microscopy. *Reviews of Modern Physics,* **75**(3), pp. 949-983.

GOODWIN, D., PICOUT, D., ROSS-MURPHY, S., HOLLAND, S., MARTINI, L. and LAWRENCE, M., 2011. Ultrasonic degradation for molecular weight reduction of pharmaceutical cellulose ethers. *Carbohydrate Polymers,* **83**(2), pp. 843-851.

GUEVEN, O., 2004. An overview of current developments in applied radiation chemistry of polymers, O. GUEVEN, ed. In: *Advances in radiation chemistry of polymers,* 13 - 17 September 2003 2004, International Atomic Energy Agency (IAEA) pp33-39.

GÜMÜSKAYA, E., USTA, M. and KIRCI, H., 2003. The effects of various pulping conditions on crystalline structure of cellulose in cotton linters. *Polymer Degradation and Stability,* **81**(3), pp. 559-564.

H.P.S. 2010. *Food Irradiation.* Health Physics Society Specialists in Radiation Safety. Available from: <**http://hps.org/documents/food_irradiation_fact_sheet.pdf**>.

HALLAC, B.B. and RAGAUSKAS, A.J., 2011. Analyzing cellulose degree of polymerization and its relevancy to cellulosic ethanol. *Biofuels, Bioproducts and Biorefining,* **5**(2), pp. 215-225.

HALLER, P., BEYER, E., WIEDEMANN, G., PANZNER, M., WUST, H. and NAVI, P., 2001. Experimental study of the effect of a laser beam on the morphology of wood surfaces, *First International Conference of the European Society for Wood Mechanics, 19Á21 April, Lausanne, Switzerland,* 19-21 April 2001, pp1-10.

HARMSEN, P., HUIJGEN, W., BERMUDEZ, L. and BAKKER, R., 2010. *Literature review of physical and chemical pretreatment processes for lignocellulosic biomass.* ECN-E--10-013. Netherlands: Wageningen UR Food & Biobased Research.

HATAKKA, A.I., 1984. *Biological Pretreatment of Lignocellulose for Enzymatic Hydrolysis of Cellulose.* Helsinki: Department of Microbiology, University of Helsinki.

HEINZE, T. and KOSCHELLA, A., 2005. Solvents applied in the field of cellulose chemistry: a mini review. *Polímeros,* **15**(2), pp. 84-90.

HENNIGES, U., OKUBAYASHI, S., ROSENAU, T. and POTTHAST, A., 2012. Irradiation of Cellulosic Pulps: Understanding its impact on cellulose oxidation. *Biomacromolecules,* **13**, pp. 4171-4178.

HENNIGES, U., HASANI, M., POTTHAST, A., WESTMAN, G. and ROSENAU, T., 2013. Electron Beam Irradiation of Cellulosic Materials-Opportunities and Limitations. *Materials (1996-1944),* **6**(6), pp. 1584-1598.

HENRIKSSON, G., CHRISTIERNIN, M. and AGNEMO, R., 2005. Monocomponent endoglucanase treatment increases the reactivity of softwood sulphite dissolving pulp. *Journal of Industrial Microbiology and Biotechnology,* **32**, pp. 211-214.

HENRY, D., EBY, N., GOODGE, J. and MOGK, D., 10 November 2016, 2012-last update, X-ray reflection in accordance with bragg's law [Homepage of Science Education Resource Centre], [Online]. Available: **http://serc.carleton.edu/research_education/geochemsheets/BraggsLaw.html** [January/08, 2017].

HIRN, U. and BAUER, W., 2006. A review of image analysis based methods to evaluate fiber properties. *Lenzinger Berichte,* **86**(1), pp. 96-105.

HON, D.N.-., 1994. Cellulose: A random walk along its historical path. *Cellulose,* **1**, pp. 1.

HORN, H., BEIL, S., WESNER, D.A., WEICHENHAIN, R. and KREUTZ, E.W., 1999. Excimer laser pretreatment and metallization of polymers. *Nuclear Instruments and Methods in Physics Research Section B: Beam Interactions with Materials and Atoms,* **151**(1–4), pp. 279-284.

HSU, S., TAN, H. and YAO, Y.L., 2012. Effect of excimer laser irradiation on crystallinity and chemical bonding of biodegradable polymer. *Polymer Degradation and Stability,* **97**(1), pp. 88-97.

HU, H., ZHANG, Y., LIU, X., HUANG, Z., CHEN, Y., YANG, M., QIN, X. and FENG, Z., 2014. Structural changes and enhanced accessibility of natural cellulose pretreated by mechanical activation. *Polymer Bulletin,* **71**(2), pp. 453-464.

HULT, E., LARSSON, P.T. and IVERSEN, T., 2000. A comparative CP/MAS 13C-NMR study of cellulose structure in spruce wood and kraft pulp. *Cellulose,* **7**(1), pp. 35-55.

HUNG, O., CHAN, C., KAN, C. and YUEN, C.M., 2016. Microscopic study of the surface morphology of CO_2 laser-treated cotton and cotton/polyester blended fabric. *Textile Research Journal,* **87**(9), pp. 1107-1120.

IBARRA, D., KÖPCKE, V. and EK, M., 2010. Behavior of different monocomponent endoglucanases on the accessibility and reactivity of dissolving-grade pulps for viscose process. *Enzyme and Microbial Technology,* **47**(7), pp. 355-362.

ILLER, E., STUPIŃSKA, H. and STAROSTKA, P., 2007. Properties of cellulose derivatives produced from radiation—Modified cellulose pulps. *Radiation Physics and Chemistry,* **76**(7), pp. 1189-1194.

ILLER, E., KUKIEŁKA, A., STUPIŃSKA, H. and MIKOŁAJCZYK, W., 2002. Electron-beam stimulation of the reactivity of cellulose pulps for production of derivatives. *Radiation Physics and Chemistry,* **63**(3), pp. 253-257.

IMAMURA, R., UENO, T. and MURAKAMI, K., 1972. Depolymerization of Cellulose by electron beam irradiation. *Bulletin of the Institute for Chemical Research,* **50**(1), pp. 51-63.

IOELOVICH, M., 2009. Accessibility and crystallinity of cellulose. *BioResources,* **4**(3), pp. 1168-1177.

IQBAL, H.M.N., KYAZZE, G. and KESHAVARZ, T., 2013. Advances in the valorization of lignocellulosic materials by biotechnology: An overview. *Bioresources.com,* **8**(2), pp. 3157-3176.

IRFAN, M., GULSHER, M., ABBAS, S., SYED, Q., NADEEM, M. and BAIG, S., 2011. Effect of various pretreatment conditions on enzymatic saccharification. *Songklanakarin Journal of Science & Technology,* **33**(4), pp. 397-404.

ISOGAI, A. and ATALLA, R., 1998. Dissolution of cellulose in aqueous NaOH solutions. *Cellulose,* **5**(4), pp. 309-319.

JAHAN, M.S., AHSAN, L., NOORI, A. and QUAIYYUM, M.A., 2008. Process for the Production of Dissolving Pulp from Trema Orientalis (Nalita) by Prehydrolysis Kraft and Soda-Ethylendiamine (EDA) Process. *BioResources,* **3**(3), pp. 816-828.

JAHAN, M.S. and RAHMAN, M.M., 2012. A Biorefinery Initiative in Producing Dissolving Pulp from Dhaincha (Sesbania Aculeata) - A Short-Rotation Crop. *Cellulose Chemistry and Technology,* **46**(5-6), pp. 375-380.

JARVIS, M.C., 2000. Interconversion of the I_A and I_B Crystalline Forms of Cellulose by bending. *Carbohydrate Research,* **325**, pp. 150-154.

JI, X., LIU, S., WANG, Q., YANG, G., CHEN, J. and FANG, G., 2015. Wet Oxidation Pretreatment of Wood Pulp Waste for Enhancing Enzymatic Saccharification. *BioResources,* **10**(2), pp. 2177-2184.

JIAO, C. and XIONG, J., 2014. Accessibility and morphology of cellulose fibres treated with sodium hydroxide. *Bioresources.com,* **9**(4), pp. 6504-6513.

JOHN, M.J. and ANANDJIWALA, R.D., 2008. Recent developments in chemical modification and characterization of natural fiber-reinforced composites. *Polymer Composites,* **29**(2), pp. 187-207.

JOSEFSSON, T., LENNHOLM, H. and GELLERSTEDT, G., 2001. Changes in cellulose supramolecular structure and molecular weight distribution during steam explosion of aspen wood. *Cellulose,* **8**(4), pp. 289-296.

JU, X., BOWDEN, M., BROWN, E.E. and ZHANG, X., 2015. An improved X-ray diffraction method for cellulose crystallinity measurement. *Carbohydrate Polymers,* **123**, pp. 476-481.

KACZMAREK, H., OŁDAK, D., MALANOWSKI, P. and CHABERSKA, H., 2005. Effect of short wavelength UV-irradiation on ageing of polypropylene/cellulose compositions. *Polymer Degradation and Stability,* **88**(2), pp. 189-198.

KAMINSKA, A., SAWCZAK, M., KOMAR, K. and ŚLIWIŃSKI, G., 2007. Application of the laser ablation for conservation of historical paper documents. *Applied Surface Science,* **253**(19), pp. 7860-7864.

KAN, C., YUEN, C. and CHENG, C., 2010. Technical study of the effect of CO2 laser surface engraving on the colour properties of denim fabric. *Coloration Technology,* **126**(6), pp. 365-371.

KAN, C., 2014. CO2 laser treatment as a clean process for treating denim fabric. *Journal of Cleaner Production,* **66**, pp. 624-631.

KANG, K.E., JEONG, G. and PARK, D., 2013. Rapeseed-straw enzymatic digestibility enhancement by sodium hydroxide treatment under ultrasound irradiation. *Bioprocess and Biosystems Engineering,* **36**(8), pp. 1019-1029.

KARIMI, M., JENKINS, B. and STROEVE, P., 2014. Ultrasound irradiation in the production of ethanol from biomass. *Renewable and Sustainable Energy Reviews,* **40**, pp. 400-421.

KASAAI, M.R., 2013. Input power-mechanism relationship for ultrasonic irradiation: food and polymer applications. *Natural Science,* **5**(8A2), pp. 14-22.

KASSIM, M.A., KHALIL, H.P.S., SERRI, N.A., SYAKIR, M.I., SRI APRILA, N.A. and DUNGANI, R., 2016. Irradiation Pretreatment of Tropical Biomass and Biofiber for Biofuel Production. In: W.A. MONTEIRO, ed, *Radiation Effects of Materials.* InTech, pp. 329-356.

KHAN, M.A., HAQUE, N., AL-KAFI, A., ALAM, M.N. and ABEDIN, M.Z., 2006. Jute reinforced polymer composite by gamma radiation: effect of surface treatment with UV radiation. *Polymer-Plastics Technology and Engineering,* **45**(5), pp. 607-613.

KLEMM, D., SCHMAUDER, H.P. and HEINZE, T., 2005. Cellulose. *Biopolymers Online.* 6 edn. Wuppertal, Germany: pp. 275-287.

KOLAR, J., STRLIC, M. and MARINCEK, M., 2002. IR pulsed laser light interaction with soiled cellulose and paper. *Applied Physics A Materials Science & Processing,* **75**(6), pp. 673-676.

KOLAR, J., STRLIC, M., PENTZIEN, S. and KAUTEK, W., 2000. Near-UV, visible and IR pulsed laser light interaction with cellulose. *APPLIED PHYSICS A MATERIALS SCIENCE AND PROCESSING,* **71**(1), pp. 87-90.

KOLAR, J. STRLIČ, M. MÜLLER-HESS, D. GRUBER, A. TROSCHKE, K. PENTZIEN, S.et al KAUTEK, W. 2003. *Laser cleaning of paper using Nd:YAG laser running at 532 nm.* Available from: <**http://www.sciencedirect.com/science/article/pii/S1296207402011962**>.

KOLLMAN, F.F.P. and CÔTÉ, W.A., 1968. Principles of wood science and technology: solid wood. 1 edn. New York, New York, USA.: Allen & Unwin.

KONG, K. and EICHHORN, S., 2005. The influence of hydrogen bonding on the deformation micromechanics of cellulose fibers. *Journal of Macromolecular Science, Part B: Physics,* **44**(6), pp. 1123-1136.

KONTTURI, E., TAMMELIN, T. and ÖSTERBERG, M., 2006. Cellulose—model films and the fundamental approach. *Chemical Society Reviews,* **35**(12), pp. 1287-1304.

KOPCKE, V., 2010. *Conversion of wood and non-wood paper grade pulps to dissolving-grade pulps. PhD Thesis.* Stockholm: Royal Institute of Technology.

KOYAMA, M., HELBERT, W., IMAI, T., SUGIYAMA, J. and HENRISSAT, B., 1997. Parallel-up structure evidences the molecular directionality during biosynthesis of bacterial cellulose. *Proceedings of the National Academy of Sciences of the United States of America,* **94**(17), pp. 9091-9095.

KRAFT, G. and SCHELOSKY, N., 2000. *Irradiation of dissolving pulp by electon beams.* 79. Austria: Lenzing AG.

KREUTZ, E.W. FRERICHS, H. STRICKER, J.et al WESNER, D.A. 1995. *Processing of polymer surfaces by laser radiation.* Available from: <**http://www.sciencedirect.com/science/article/pii/0168583X95005390**>.

KUBOVSKY, I. and KACIK, F., 2009. FTIR study of Maple wood changes due to CO_2 laser irradiation. *Cellulose Chemistry and Technology,* **43**(7-8), pp. 235.

KULICKE, W.-., CLASEN, C. and LOHMAN, C., 2005. Characterization of Water-Soluble Cellulose Derivatives in Terms of the Molar Mass and Particle Size as well as Their Distribution. *Macromolecular Symposia,* **223**(1), pp. 151-174.

KUMAR, P., BARRETT, D.M., DELWICHE, M.J. and STROEVE, P., 2009. Methods for pretreatment of lignocellulosic biomass for efficient hydrolysis and biofuel production. *Industrial & Engineering Chemistry Research,* **48**(8), pp. 3713-3729.

KUNZE, J. and FINK, H., 2005. Structural changes and activation of cellulose by caustic soda solution with urea. *Macromolecular Symposia,* **223**(1), pp. 175-188.

KWIATKOWSKA, B., BENNETT, J., AKUNNA, J., WALKER, G.M. and BREMNER, D.H., 2011. Stimulation of bioprocesses by ultrasound. *Biotechnology Advances,* **29**(6), pp. 768-780.

LARSSON, P.T., HULT, E., WICKHOLM, K., PETTERSSON, E. and IVERSEN, T., 1999. CP/MAS 13C-NMR spectroscopy applied to structure and interaction studies on cellulose I. *Solid State Nuclear Magnetic Resonance,* **15**(1), pp. 31-40.

LARSSON, P.T., WICKHOLM, K. and IVERSEN, T., 1997. A CP/MAS13C NMR investigation of molecular ordering in celluloses. *Carbohydrate Research,* **302**(1–2), pp. 19-25.

LAVOINE, N., DESLOGES, I., DUFRESNE, A. and BRAS, J., 2012. Microfibrillated cellulose–Its barrier properties and applications in cellulosic materials: A review. *Carbohydrate Polymers,* **90**(2), pp. 735-764.

LENZING, 2017-last update, fibers - viscose and modal fiber production [Homepage of Lenzing AG Group], [Online]. Available: **http://www.lenzing.com/en/fibers/viscose-and-modal-fiber-production.html** [May/11, 2017].

LI, J., ZHANG, X., ZHANG, M., XIU, H. and HE, H., 2015. Ultrasonic enhance acid hydrolysis selectivity of cellulose with HCl-FeCl3 as catalyst. *Carbohydrate Polymers,* **117**, pp. 917-922.

LIDARIS, 2016-last update, laser peak fluence, intensity and peak power [Homepage of LIDARIS LTD.], [Online]. Available: **http://lidaris.com/glossary-2/fluence/** [03/04, 2017].

LIU, C., REN, J., XU, F., LIU, J., SUN, J. and SUN, R., 2006. Isolation and characterization of cellulose obtained from ultrasonic irradiated sugarcane bagasse. *Journal of Agricultural and Food Chemistry,* **54**(16), pp. 5742-5748.

LIU, Y., SHI, L., CHENG, D. and HE, Z., 2016. Dissolving Pulp Market and Technologies: Chinese Prospective-A Mini-Review. *BioResources,* **11**(3), pp. 7902-7916.

LOOW, Y., WU, T.Y., YANG, G.H., JAHIM, J.M., TEOH, W.H. and MOHAMMAD, A.W., 2016. Role of energy irradiation in aiding pretreatment of lignocellulosic biomass for improving reducing sugar recovery. *Cellulose,* **23**(5), pp. 2761-2789.

LOS ALAMOS SCIENCE, 1995. A brief history of radiation. *Los Alamos Science,* (23), pp. 116-123.

LUO, J., FANG, Z. and SMITH JR., R.L., 2014. Ultrasound-enhanced conversion of biomass to biofuels. *Progress in Energy and Combustion Science,* **41**, pp. 56-93.

MA, S., XUE, X., YU, S. and WANG, Z., 2012. High-intensity ultrasound irradiated modification of sugarcane bagasse cellulose in an ionic liquid. *Industrial Crops and Products,* **35**(1), pp. 135-139.

MARTÍNEZ-BARRERA, G., ÁVILA CÓRDOBA, L.I., MARTÍNEZ-LÓPEZ, M., HERRERA-SOSA, E.S., VIGUERAS-SANTIAGO, E., BARRERA-DÍAZ, C.E., UREÑA-NUÑEZ, F. and GONZÁLEZ RIVAS, N., 2015. Gamma Radiation as a

Recycling Tool for Waste Materials Used in Concrete. In: M. NENOI, ed, *Evolution of Ionizing Radiation Research.* InTech, pp. 259-279.

MARTINI, S., 2013. Sonocrystallization of fats. *Sonocrystallization of Fats.* Springer, pp. 41-62.

MAURYA, D.P., SINGLA, A. and NEGI, S., 2015. An overview of key pretreatment processes for biological conversion of lignocellulosic biomass to bioethanol. *3 Biotech,* **5**(5), pp. 597-609.

MAZZOCCOLI, J.P., 2010. *Ultrasonication of Polysaccharide Materials,* Case Western Reserve University.

MEDRONHO, B. and LINDMAN, B., 2015. Brief overview on cellulose dissolution/regeneration interactions and mechanisms. *Advances in Colloid and Interface Science,* **222**(0), pp. 502-508.

MELÉNDEZ-ORTIZ, H.I., VARCA, G.H., LUGÃO, A.B. and BUCIO, E., 2015. Smart polymers and coatings obtained by ionizing radiation: synthesis and biomedical applications. *Open Journal of Polymer Chemistry,* **5**(03), pp. 17.

MIAO, Q., TIAN, C., CHEN, L., HUANG, L., ZHENG, L. and NI, Y., 2015. Combined mechanical and enzymatic treatments for improving the Fock reactivity of hardwood kraft-based dissolving pulp. *Cellulose,* **22**(1), pp. 803-809.

MILLERT, M., BARKER, A.J. and SATTER, L.D., 1975. Pretreatments to enhance chemical, enzymatic and microbiological attack of cellulosic materials. *Biotechnology and Bioengineering Symposium,* (5), pp. 193-219.

MISHRA, S., ROY, H., LOHAR, A., SAMANTA, S., TIWARI, S. and DUTTA, K., 2015. A comparative assessment of crystallite size and lattice strain in differently cast A356 aluminium alloy, *IOP Conference Series: Materials Science and Engineering,* 2015, IOP Publishing pp012001.

MONTAZER, M., CHIZARIFARD, G. and HARIFI, T., 2014. CO2 laser irradiation of raw and bleached cotton fabrics, with focus on water and dye absorbency. *Coloration Technology,* **130**(1), pp. 13-20.

MONTAZER, M., TAHERI, S.J. and HARIFI, T., 2012. Effect of laser CO2 irradiation on various properties of polyester fabric: focus on dyeing. *Journal of Applied Polymer Science,* **124**(1), pp. 342-348.

MORGAN, P., 2005. Carbon fibers and their composites. 1 edn. Boca Rotan: CRC press.

MOSIER, N., WYMAN, C., DALE, B., ELANDER, R., LEE, Y.Y., HOLTZAPPLE, M. and LADISCH, M., 2005. Features of promising technologies for pretreatment of lignocellulosic biomass. *Bioresource Technology,* **96**(6), pp. 673-686.

NECHYPORCHUK, O., 2015. *Cellulose nanofibers for the production of bionanocomposites. PhD Thesis*, Université Grenoble Alpes.

NELSON, R. and OLIVER, D.W., 1971. Study of cellulose structure and its relation to reactivity. *Journal of Polymer Science Part: Polymer Symposia,* **36**(1), pp. 305-320.

NG, K., 2003. Non-ionizing radiations–sources, biological effects, emissions and exposures, K. NG, ed. In: *Proceedings of the international conference on non-ionizing radiation at UNITEN (ICNIR2003),* 20th - 22nd October 2003, Electromagnetic Fields and our Health pp1-16.

NIEMINEN, S., HEIKKINEN, J. and RÄTY, J., 2013. Laser transillumination imaging for determining wood defects and grain angle. *Measurement Science and Technology,* **24**(12), pp. 1-7.

NISHIYAMA, Y., LANGAN, P. and CHANZY, H., 2002. Crystal structure and hydrogen-bonding system in cellulose Iβ from synchrotron X-ray and neutron fiber diffraction. *Journal of the American Chemical Society,* **124**(31), pp. 9074-9082.

OBERHOFER, M., 1984. *Non-Ionizing Radiation Dosimetry.* EUR 9110 EN. Luxembourg: Commission of the European Communities.

OBERLERCHNER, J.T., ROSENAU, T. and POTTHAST, A., 2015. Overview of methods for the direct molar mass determination of cellulose. *Molecules,* **20**(6), pp. 10313-10341.

OFORI-BOATENG, C. and LEE, K.T., 2014. Ultrasonic-assisted simultaneous saccharification and fermentation of pretreated oil palm fronds for sustainable bioethanol production. *Fuel,* **119**, pp. 285-291.

OGURA, T., DATE, Y. and KIKUCHI, J., 2013. Differences in cellulosic supramolecular structure of compositionally similar rice straw affect biomass metabolism by paddy soil microbiota. *PLoS One,* **8**(6), pp. e66919.

OGUTU, F.O., MU, T., ELAHI, R., ZHANG, M. and SUN, H., 2015. Ultrasonic Modification of Selected Polysaccharides-Review. *Journal of Food Processing & Technology,* **6**(5), pp. 1-8.

OLSSON, C. and WESTMAN, G., 2013. Direct dissolution of cellulose: Background, means and applications. In: T. VAN DE VEN and L. GODBOUT, eds, *Cellulose - Fundamental Aspects.* Croatia: InTech, pp. 143-178.

OSTBERG, L., HAKANSSON, H. and GERMGARD, U., 2012. Some aspects of the reactivity of pulp intended for high-viscosity viscose. *BioResources,* **7**(1), pp. 743-755.

O'SULLIVAN, A.C., 1997. Cellulose: the structure slowly unravels. *Cellulose,* **4**(3), pp. 173-207.

OUBANI, H., ABBAS, A. and HARRIS, A., 2006. *Investigation on the mechanical pretreatment of cellulose by high intensity ultrasound and ball milling.* Sydney, Australia: The University of Sydney.

OUDIANI, A.E., CHAABOUNI, Y., MSAHLI, S. and SAKLI, F., 2011. Crystal transition from cellulose I to cellulose II in NaOH treated Agave americana L. fibre. *Carbohydrate Polymers,* **86**(3), pp. 1221-1229.

ÖZTÜRK, H.B., POTTHAST, A., ROSENAU, T., ABU-ROUS, M., MACNAUGHTAN, B., SCHUSTER, K.C., MITCHELL, J.R. and BECHTOLD, T., 2009. Changes in the intra-and inter-fibrillar structure of lyocell (TENCEL®) fibers caused by NaOH treatment. *Cellulose,* **16**(1), pp. 37-52.

PANDEY, K.K. and VUORINEN, T., 2008. Comparative study of photodegradation of wood by a UV laser and a xenon light source. *Polymer Degradation and Stability,* **93**(12), pp. 2138-2146.

PARK, S., BAKER, J.O., HIMMEL, M.E., PARILLA, P.A. and JOHNSON, D.K., 2010. Cellulose crystallinity index: measurement techniques and their impact on interpreting cellulase perfomance. *Biotechnology for Biofuels,* **3**, pp. 1-10.

PECIULYTE, A., KARLSTRÖM, K., LARSSON, P.T. and OLSSON, L., 2015. Impact of the supramolecular structure of cellulose on the efficiency of enzymatic hydrolysis. *Biotechnology for Biofuels,* **8**(1), pp. 1-13.

PENG, F., BIAN, J., PENG, P., ZHANG, X. and SUN, R., 2013. Physico-chemical characterisation of cellulose from the Broussonetia papyrifera Bark and Stem, and Eucommia ulmoides Over stem. *Pulp Production and Processing: From papermaking to High-Tech Products.* Shawbury, Shropshire, UK: Smithers Rapra Technology Ltd, pp. 199-216.

PICK, R.M. and COLVARD, M.D., 1993. Current status of lasers in soft tissue dental surgery. *Journal of Periodontology,* **64**(7), pp. 589-602.

POLETTO, M., HEITOR, L. and ZATTERA, A.J., 2014. Native Cellulose: Structure, Characterization and Thermal Properties. *Materials,* **7**(9), pp. 6105-6119.

PÖNNI, R., VUORINEN, T. and KONTTURI, E., 2012. Proposed nano-scale coalescence of cellulose in chemical pulp fibers during technical treatments. *BioResources,* **7**(4), pp. 6077-6108.

PURI, V.P., 1984. Effect of crystallinity and degree of polymerization of cellulose on enzymatic saccharification. *Biotechnology and Bioengineering,* **26**(10), pp. 1219-1222.

QUIROZ-CASTANEDA, R.E. and FOLCH-MALLOL, J.L., 2013. Hydrolysis of Biomass Mediated by Cellulases for the Production of Sugars. *Sustainable Degradation of Lignocellulosic Biomass-Application and Commercialization.* Cuernavaca: Biotechnology Research Centre, University of Morelos, pp. 119-154.

QUIROZ-CASTAÑEDA, R.E. and FOLCH-MALLOL, J.L., 2013. Hydrolysis of biomass mediated by cellulases for the production of sugars. *Sustainable degradation of lignocellulosic biomass techniques, applications and commercialization.InTech,* pp. 119-155.

RAFSANJANI, A., STIEFEL, M., JEFIMOVS, K., MOKSO, R., DEROME, D. and CARMELIET, J., 2014. Hygroscopic swelling and shrinkage of latewood cell wall micropillars reveal ultrastructural anisotropy. *Journal of the Royal Society, Interface / the Royal Society*, **11**(95), pp. 20140126.

RAHKAMO, L., SIIKA-AHO, M., VEHVILÄINEN, M., DOLK, M., VIIKARI, L., NOUSIAINEN, P. and BUCHERT, J., 1996. Modification of hardwood dissolving pulp with purifiedTrichoderma reesei cellulases. *Cellulose,* **3**(1), pp. 153-163.

RAJAGOPAL, S. and STEPANIK, T., 1996. Status of electron processing technology in the viscose industry, *Lenzing International Conference: Imagine the Future of Viscose Technology,* June 1996, Lenzing International Conference pp12-14.

RAO, V., 2009. Radiation processing of polymers. In: S. THOMAS and W. YANG, eds, *Advances in Polymer Processing: From Macro-To Nano-Scales.* 1 edn. Cambridge: Woodhead Publishing Ltd., pp. 402-437.

REHMAN, M.S.U., KIM, I., CHISTI, Y. and HAN, J., 2013. Use of ultrasound in the production of bioethanol from lignocellulosic biomass. *EEST Part A: Energy Science Research,* **30**(2), pp. 1391-1410.

REPORTLINKER, 2014. *Global and China Dissolving Pulp Industry Report, 2013-2016.* China: ReportLinker.

ROGOŠIĆ, M., MENCER, H.J. and GOMZI, Z., 1996. Polydispersity index and molecular weight distributions of polymers. *European polymer journal,* **32**(11), pp. 1337-1344.

ROJAS, J., 2013. Effect of Polymorphism on the Particle and Compaction Properties of Microcrystalline Cellulose. *Cellulose - Medical, Pharmaceutical and Electrical Applications.* InTech, pp. 27-46.

ROSA, A.D., MINES, A.D., BANZON, R. and SIMBUL-NUGUID, Z., 1983. Radiation pretreatment of cellulose for energy production. *Radiation Physics and Chemistry (1977),* **22**(3-5), pp. 861-867.

RUDOLPH, P., LIGTERINK, F.J., PEDERSOLI JR., J.L., VAN BOMMEL, M., BOS, J., AZIZ, H.A., HAVERMANS, J.B.G.A., SCHOLTEN, H., SCHIPPER, D. and KAUTEK, W., 2004. Characterization of laser-treated paper. *Applied Physics A Materials Science & Processing,* **79**, pp. 181-186.

SAFANAMA, D.S., MARASHI, P., ZOLFAGHARI HESARI, A., FIROOZI, S., ABOUTALEBI, S.H. and JALILZADEH, S., 2012. Elastic Modulus Measurement of Nanocomposite Materials by Atomic Force Microscopy, *International Journal of Modern Physics: Conference Series,* 2012, World Scientific pp502-509.

SAID-GALIEV, E.E. and NIKITIN, L.N., 1993. Modification of Polymers and Composites with CO2 Laser Radiation. A Review. *Russian Academy of Sciences*, **6**, pp. 723-734.

SAINI, A., AGGARWAL, N.K., SHARMA, A. and YADAV, A., 2015. Prospects for Irradiation in Cellulosic Ethanol Production. *Biotechnology Research International*, **2015**, pp. 1-13.

SAPPI, 2014. *Dissolving Wood Pulp.* Document no. SCA-27. Revision no. 2, Sappi.

SARRAZIN, P., BENEVENTI, D., CHAUSSY, D., VURTH, L. and STEPHAN, O., 2009. Adsorption of cationic photoluminescent nanoparticles on softwood cellulose fibres: effects of particles stabilization and fibres' beating. *Colloids and Surfaces A: Physicochemical and Engineering Aspects*, **334**(1), pp. 80-86.

SASAKI, K.M., AOKI, A., ICHINOSE, S., YOSHINO, T., YAMADA, S. and ISHIKAWA, I., 2002. Scanning electron microscopy and Fourier transformed infrared spectroscopy analysis of bone removal using Er: YAG and CO2 lasers. *Journal of Periodontology*, **73**(6), pp. 643-652.

SAVALANI, M., HAO, L. and HARRIS, R.A., 2006. Evaluation of CO2 and Nd: YAG lasers for the selective laser sintering of HAPEX®. *Proceedings of the Institution of Mechanical Engineers, Part B: Journal of Engineering Manufacture*, **220**(2), pp. 171-182.

SCHULT, T., HJERDE, T., OPTUN, O.I., KLEPPE, P.J. and MOE, S., 2002. Characterization of cellulose by SEC-MALLS. *Cellulose*, **9**(2), pp. 149-158.

SEGAL, L., CREELY, J., MARTIN JR, A. and CONRAD, C., 1959. An empirical method for estimating the degree of crystallinity of native cellulose using the X-ray diffractometer. *Textile Research Journal*, **29**(10), pp. 786-794.

SHAHIDI, S. and WIENER, J., 2016. Radiation Effects in Textile Materials. In: W.A. MONTEIRO, ed, *Radiation Effects in Materials.* InTech, pp. 309-328.

SHAIKH, T., CHAUDHARI, S. and VARMA, A., 2012. Viscose Rayon: A legendary development in the manmade textile. *Engineering Research and Applications (IJERA)*, **2**(5), pp. 675-680.

SHEN, L., WORRELL, E. and PATEL, M.K., 2010. Environmental impact assessment of man-made cellulose fibres. *Resources, Conservation and Recycling*, **55**(2), pp. 260-274.

SHOKRI, J. and ADIBKIA, K., 2013. Application of cellulose and cellulose derivatives in pharmaceutical industries. In: T. VAN DE VEN and L. GODBOUT, eds, *Cellulose - Medical, Pharmaceutical and Electronic Applications.* Rijeka, Croatia: InTech, Rijeka, Croatia, pp. 47-66.

SIDIRAS, D.K. and SALAPA, I.S., 2015. Organosolv pretreatment as a major step of lignocellulose biomass refining, N. ABATZOGLOU, ed. In: *Biorefinery I: Chemicals*

and Materials From Thermo-Chemical Biomass Conversion and Related Process, September 27 - October 2, 2015, Engineering Conferences International - ECI Digital Archives pp1-9.

SILVA, A.A., 1995. *Molecular weight distribution analysis of wood pulp cellulose by size exclusion chromatography*, Oregon State University.

SINGH, S.C., ZENG, H., GUO, C. and CAI, W., 2012. Lasers: fundamentals, types, and operations. In: S.C. SINGH, H. ZENG, C. GUO and W. CAI, eds, *Nanomaterials: Processing and Characterization with Lasers.* Weinheim, Germany.: Wiley Online Library, pp. 1-34.

SIQUEIRA, G., BRAS, J. and DUFRESNE, A., 2010. Cellulosic bionanocomposites: A review of preparation, properties and applications. *Polymers,* **2**(4), pp. 728-765.

SIQUERA, G., BRAS, J. and DUFRESNE, A., 2010. Cellulosic bionanocomposites: A Review of preparation properties and applications. *Polymers,* **2**, pp. 728-765.

SIXTA, H., HARMS, H., DAPIA, S., PARAJO, J.C., PULS, J., SAAKE, B. and FINK, H.P., 2004. Evaluation of new organosolv dissolving pulps. Part I: Preparation analytical characterization and viscose processability. *Cellulose,* **11**, pp. 73-83.

SIXTA, H., IAKOVLEV, M., TESTOVA, L., ROSELLI, A., HUMMEL, M., BORREGA, M., VAN HEININGEN, A., FROSCHAUER, C. and SCHOTTENBERGER, H., 2013. Novel concepts of dissolving pulp production. *Cellulose,* **20**, pp. 1547-1561.

SIXTA, H., 2006. Pulp properties and applications. In: H. SIXTA, ed, *Handbook of pulp.* Volume 1 edn. Verlag: Wiley Online Library, pp. 1009-1067.

SJOHOLM, E., 2005. Chapter 12: Size Exclusion Chromatography of Cellulose and Cellulose Derivatives. In: C. WU, ed, *Handbook of Size Exclusion Chromatography and Related Techniques: Revised and Expanded.* 2nd edn. USA: CRC Press, pp. 316-358.

SLINEY, D.H., 2001. Nonionizing Radiation: Lasers. *Patty's Industrial Hygiene.* John Wiley & Sons, Inc., pp. 1379-1400.

SOMERVILLE, C., 2006. Cellulose synthesis in higher plants. *Annual Review of Cell and Developmental Biology,* **22**, pp. 53-78.

SRIBALA, G., CHENNURU, R., MAHAPATRA, S. and VINU, R., 2016. Effect of alkaline ultrasonic pretreatment on crystalline morphology and enzymatic hydrolysis of cellulose. *Cellulose,* **23**(3), pp. 1725-1740.

STAROSTINA, N. and WEST, P., 2006. Atomic Force Microscopy in the Characterisation of Drug Nanoparticles. *Innovations in Pharmaceutical Technology,* pp. 74-77.

STEPANIK, T., RAJAGOPAL, S., EWING, D. and WHITEHOUSE, R., 1998. Electron-processing technology: A promising application for the viscose industry. *Radiation Physics and Chemistry,* **52**(1), pp. 505-509.

STEPANIK, T.M., EWING, D.E. and WHITEHOUSE, R., 2000. Electron treatment of wood pulp for the viscose process. *Radiation Physics and Chemistry,* **57**(3-6), pp. 377-379.

STRLIČ, M. and KOLAR, J., 2003. Size exclusion chromatography of cellulose in LiCl/N,N-dimethylacetamide. *Journal of Biochemical and Biophysical Methods,* **56**(1–3), pp. 265-279.

STRUNK, P., 2012. *Characterization of cellulose pulps and the influence of their properties on the process and production of viscose and cellulose ethers,* Umea University.

SUMARI, S., ROESYADI, A. and SUMARNO, S., 2013. Effects of ultrasound on the morphology, particle size, crystallinity, and crystallite size of cellulose. *Scientific Study & Research.Chemistry & Chemical Engineering, Biotechnology, Food Industry,* **14**(4), pp. 229.

SUN, F. and SUN, Q., 2015. Current Trends in Lignocellulosic Analysis with Chromatography. *Annals of Chromatography and Separation Techniques,* **1**(2), pp. 1-8.

SUN, Y., LIN, L., DENG, H., LI, J., HE, B., SUN, R. and OUYANG, P., 2008. Structural changes of bamboo cellulose in formic acid. *BioResources,* **3**(2), pp. 297.

SUN, Y. and CHENG, J., 2002. Hydrolysis of lignocellulosic materials for ethanol production: a review. *Bioresource Technology,* **83**(1), pp. 1-11.

SUSLICK, K.S. and PRICE, G.J., 1999. Applications of ultrasound to materials chemistry. *Annual Review of Materials Science,* **29**(1), pp. 295-326.

SZABÓ, L., SORIA, A., FORSSTRÖM, J., KERÄNEN, J.T. and HYTÖNEN, E., 2009. A world model of the pulp and paper industry: Demand, energy consumption and emission scenarios to 2030. *Environmental Science & Policy,* **12**(3), pp. 257-269.

TABET, T.A. and AZIZ, F.A., 2013. Cellulose microfibril angle in wood and its dynamic mechanical significance. *Cellulose-Fundamental Aspects,* **10**, pp. 51105.

TAHERZADEH, M.J. and KARIMI, K., 2008. Pretreatment of lignocellulosic wastes to improve ethanol and biogas production: a review. *International Journal of Molecular Sciences,* **9**(9), pp. 1621-1651.

TAKACS, E., WOJNAROVITS, L., FOLDVARY, C., HARGITTAI, P., BORSA, J. and SAJO, I., 2000. Effect of combined gamma-irradiation and alkali treatment on cotton-cellulose. *Radiation Physics and Chemistry,* **57**, pp. 399-403.

TAKACS, E., WOJNAROVITS, L., FÖLDVÁRY, C., BORSA, J. and SAJO, I., 2001. Radiation activation of cotton-cellulose prior to alkali treatment. *Research on chemical intermediates,* **27**(7), pp. 837-845.

TAKÁCS, E., WOJNÁROVITS, L., BORSA, J., FÖLDVÁRY, C., HARGITTAI, P. and ZÖLD, O., 1999. Effect of γ-irradiation on cotton-cellulose. *Radiation Physics and Chemistry,* **55**(5–6), pp. 663-666.

TEE, T.P. 2003. *Short notes on laser radiation.* **http://www.ciba.nus.edu.sg/safety/laser_safety_notes.pdf** edn. Centre for Radiation Protection: Health Sciences Authority.

TERAS, T. and JOKINEN, P., 02/11/2010, 2010-last update, dissolving pulp - the great come-back [Homepage of Paper Advance], [Online]. Available: **http://www.paperadvance.com/sciences-a-innovations/sciences/176-dissolving-pulp-the-great-come-back.html** [13/04, 2017].

TERINTE, N., IBBETT, R. and SCHUSTER, K.C., 2011. Overview on native cellulose and microcrystalline cellulose I structure studied by X-ray diffraction (WAXD): Comparison between measurement techniques. *Lenzinger Berichte,* **89**, pp. 118-131.

TIAN, C., ZHENG, L., MIAO, Q., CAO, C. and NI, Y., 2014. Improving the reactivity of kraft-based dissolving pulp for viscose rayon production by mechanical treatments. *Cellulose,* **21**, pp. 3647-3654.

TIAN, C., ZHENG, L., MIAO, Q., NASH, C., CAO, C. and NI, Y., 2013. Improvement in the Fock test for determining the reactivity of dissolving pulp. *Tappi Journal,* **12**(11), pp. 21-26.

TIAN, S., WANG, Z., FAN, Z. and ZUO, L., 2012. Comparison of ultrasonic and CO2 laser pretreatment methods on enzyme digestibility of corn stover. *International journal of molecular sciences,* **13**(4), pp. 4141-4152.

TIAN, S., WANG, Z., FAN, Z. and ZUO, L., 2011. Optimization of CO2 laser-based pretreatment of corn stover using response surface methodology. *Bioresource technology,* **102**(22), pp. 10493-10497.

TILLER, J.R., SCHILLING, R.S.F. and MORRIS, J.N., 1968. Occupational toxic factor in mortality from coronary heart disease. *British Medical Journal,* **4**, pp. 407-411.

TRATHNIGG, B., 2000. Size-exclusion chromatography of polymers. In: R.A. MEYERS, ed, *Encyclopedia of Analytical Chemistry.* Chichester: John Wiley & Sons, Ltd., pp. 8008-8034.

U.S.NRC, 28/06/2013, 2013-last update, uses of radiation [Homepage of U.S.NRC], [Online]. Available: **http://www.nrc.gov/about-nrc/radiation/around-us/uses-radiation.html** [01/31, 2014].

URQUHART, A., 1958. The Reactivity of Cellulose1. *Textile Research Journal,* **28**(2), pp. 159-169.

VARGAS-RADILLO, J.J., RUIZ-LÓPEZ, M.A., RODRÍGUEZ-MACÍAS, R., BARRIENTOS-RAMÍREZ, L., MANRÍQUEZ-GONZÁLEZ, R., NAVARRO-ARZATE, F., SALCEDO-PÉREZ, E. and TORAL, F.A.L., 2013. Fermentable Sugars from Lupinus rotundiflorus by Cumulative Pretreatments Using UV Light, Freezing, and Boiling in Alkaline Medium, Followed by Enzymatic Hydrolysis. *BioResources,* **8**(3), pp. 4016-4028.

VIGLIANI, E.C., 1954. Carbon disulphide poisoning in viscose rayon factories. *British Journal of Industrial Medicine,* **11**(4), pp. 235-244.

WADA, M., NISHIYAMA, Y., CHANZY, H., FORSYTH, T. and LANGAN, P., 2008. The structure of celluloses. *Powder Diffraction,* **23**(02), pp. 92-95.

WANG, S. and CHENG, Q., 2009. A novel process to isolate fibrils from cellulose fibers by High-Intensity Ultrasonication, Part 1: Process optimization. *Journal of Applied Polymer Science,* **113**(2), pp. 1270-1275.

WANG, Y., 2008. *Cellulose fiber dissolution in sodium hydroxide solution at low temperature: Dissolution kinetics and solubility improvement*, Georgia Institute of Technology.

WANG, Y. and DENG, Y., 2009. The kinetics of cellulose dissolution in sodium hydroxide solution at low temperatures. *Biotechnology and Bioengineering,* **102**(5), pp. 1398-1405.

WANG, H., PANG, B., WU, K., KONG, F., LI, B. and MU, X., 2014. Two stages of treatments for upgrading bleached softwood paper grade pulp to dissolving pulp for viscose production. *Biochemical engineering journal,* **82**(0), pp. 183-187.

WEIGHTMAN, D.A. FISCHER, H.K.et al MOBIUS, H. 2007. *Pulp reactivity enhancement.* United States: US20090321025 A1. Available from: <**http://www.google.com/patents/US20090321025**>.

WEISSLER, A., 1950. Depolymerization by ultrasonic irradiation: the role of cavitation. *Journal of Applied Physics,* **21**(2), pp. 171-173.

WERTZ, J. and BEDUE, O., 2013. Pretreatments of lignocellulosic biomass. In: J. WERTZ and O. BEDUE, eds, *Lignocellulose Biorefineries.* Lausanne, Switzerland: EPFL Press, pp. 299-349.

WICKHOLM, K., LARSSON, P.T. and IVERSEN, T., 1998. Assignment of non-crystalline forms in cellulose I by CP/MAS 13C NMR spectroscopy. *Carbohydrate Research,* **312**(3), pp. 123-129.

WILKENING, G.M., 1991. Nonionizing Radiation. In: G.D. CLAYTON and F.E. CLAYTON, eds, *Patty's Industrial Hygiene and Toxicology.* 4th edn. New York: John Wiley & Sons, Inc., pp. 657-742.

WILKES, A.G., 2001. The viscose process. In: C. WOODINGS, ed, *Regenerated cellulose fibres.* 1st edn. Boca Raton: Woodhead Publishing, pp. 37-61.

WOJNÁROVITS, L., 2011. Radiation chemistry. *Handbook of Nuclear Chemistry.* Springer, pp. 1263-1331.

WONG, S., KASAPIS, S. and HUANG, D., 2012. Molecular weight and crystallinity alteration of cellulose via prolonged ultrasound fragmentation. *Food Hydrocolloids,* **26**(2), pp. 365-369.

WONG, S., KASAPIS, S. and TAN, Y.M., 2009. Bacterial and plant cellulose modification using ultrasound irradiation. *Carbohydrate Polymers,* **77**(2), pp. 280-287.

XIAO, R. CHEN, X. WANG, F.et al YU, G. 2010. *Pyrolysis pretreatment of biomass for entrained-flow gasification.* Available from: <**http://www.sciencedirect.com/science/article/pii/S0306261909002591**>.

XING, M., YAO, S., ZHOU, S., ZHAO, Q., LIN, J. and PU, J., 2010. The influence of ultrasonic treatment on the bleaching of CMP revealed by surface and chemical structural analyses. *BioResources,* **5**(3), pp. 1353-1365.

YACOB, N., TALIP, N., MAHMUD, M., SANI, N., AKMA, N. and SAMSUDDIN, N.A.F., 2013. Determination of viscosity-average molecular weight of chitosan using intrinsic viscosity measurement. *Journal of Nuclear and Related Technologies,* **10**(1), pp. 39-44.

YE, D. and FARRIOL, X., 2005. Improving accessibility and reactivity of celluloses of annual plants for the synthesis of methylcellulose. *Cellulose,* **12**(5), pp. 507-515.

ZHANG, D., 2014. Lightweight Materials from Biofibers and Biopolymers. *Lightweight Materials from Biopolymers and Biofibers.* 1st edn. Washington, DC, USA: ACS Publications, pp. 1-20.

ZHANG, L., RUAN, D. and GAO, S., 2002. Dissolultion and regeneration of cellulose in NaOH/Thiourea aqueous solution. *Journal of Polymer Science: Part B: Polymer Physics,* **40**, pp. 1521-1529.

ZHAO, Y. and ZHANG, J., 2008. Microstrain and grain-size analysis from diffraction peak width and graphical derivation of high-pressure thermomechanics. *Journal of Applied Crystallography,* **41**(6), pp. 1095-1108.

ZHAO, H., KWAK, J.H., CONRAD ZHANG, Z., BROWN, H.M., AREY, B.W. and HOLLADAY, J.E., 2007. Studying cellulose fiber structure by SEM, XRD, NMR and acid hydrolysis. *Carbohydrate Polymers,* **68**(2), pp. 235-241.

ZHOU, J. and ZHANG, L., 2000. Solubility of cellulose in NaOH/urea aqueous solution. *Polymer Journal,* **32**(10), pp. 866-870.

ZUCKERSTATTER, G., SCHILD, G., WOLLBOLDT, P., RODER, T., WEBER, H.K. and SIXTA, H., 2009. The elucidation of cellulose supramolecular structure by ^{13}C CP-MAS NMR. *Lenzinger Berichte,* **87**, pp. 38-46.